January 1987

Engineering Treatment of Hazardous Wastewaters Utilizing Dye-sensitized Photooxidation

Betty-Ann Naeger

R. Ryan Dupont

William M. Moore

Engineering Treatment of Hazardous Wastewaters Utilizing Dye-sensitized Photooxidation

Betty-Ann Naeger
R. Ryan Dupont
William M. Moore

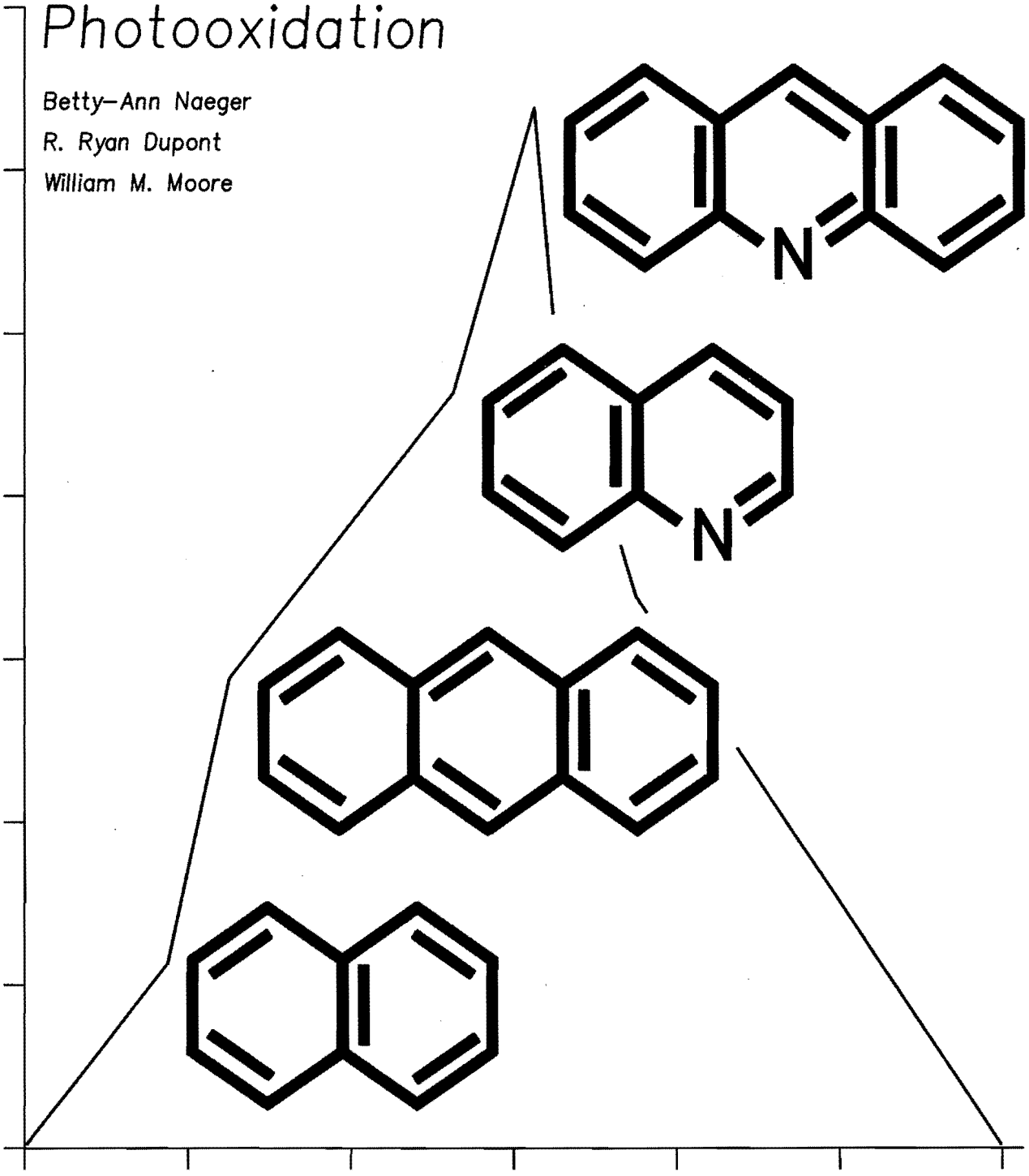

Utah Water Research Laboratory
Utah State University
Logan, Utah 84322-8200

November 1987

WATER QUALITY SERIES
UWRL/Q-87/01

ENGINEERING TREATMENT OF HAZARDOUS WASTEWATERS UTILIZING DYE-SENSITIZED PHOTOOXIDATION

Betty-Ann Naeger, R. Ryan Dupont, and William M. Moore

WATER QUALITY SERIES
UWRL/Q-87/01

Utah Water Research Laboratory
Utah State University
Logan, UT 84322-8200

November 1987

ABSTRACT

Studies were conducted to determine the applicability of photooxidation for the degradation of selected hazardous and refractory organic compounds. These photochemical oxidation reactions occur through the transfer of energy from electronically excited sensitizer molecules which attain excited states by absorbing visible light energy.

Optimum conditions for photooxidation were established based on sensitizer concentration and reaction pH for four polynuclear aromatic pollutants.

The rate of photooxidation was found to be independent of the initial substrate concentration for methylene blue-sensitized reactions, and dependent on substrate concentration for solutions without a sensitizing dye. Photolysis of substrate mixtures established acridine and anthracene as photochemically active substrates.

Photochemical reaction data suggest predictable trends in substrate reactivity based on pKa values of both sensitizer and substrate, initial substrate concentration and light absorbance characteristics.

The photoproducts formed during the photolysis of acridine were found to be more toxic than the parent compound. These reaction products appear to be stable and warrant further study.

TABLE OF CONTENTS

TABLE OF CONTENTS (Continued)

LIST OF FIGURES

LIST OF FIGURES (Continued)

LIST OF TABLES

LIST OF TABLES (Continued)

LIST OF TABLES (Continued)

LIST OF TABLES (Continued)

INTRODUCTION

The unpredictability of the international energy market and the potential of global energy shortages in the next few decades have convinced most national energy planners of the long-term need to develop major new energy sources. One means of supplementing domestic oil and gas deposits is with synthetic fuels derived from fossil fuel sources. The largest untapped fossil fuel resource in the United States is the oil bearing shale in the Green River Formation located in Colorado, Utah, and Wyoming. This area contains one of the largest deposits of hydrocarbons in the world and is projected to be a potential source of more than two trillion barrels of shale oil (Yen 1978).

When energy resources are extracted, processed, converted, and utilized, the related impacts to human health and the environment often require new and increasingly more efficient pollution control methods. New synthetic fuel processes, including oil extraction from shale, are expected to have unique air, water and solid waste control requirements.

The Department of Energy has established a research, development and demonstration (RD&D) program for encouraging the development of this country's oil shale resource (Hartstein and Harney 1981). The aim of the Oil Shale RD&D Program is to stimulate the commercial development of shale oil by eliminating technical and environmental barriers to its production. Among the key environmental needs that were outlined, development of efficient oil shale wastewater treatment systems was strongly stressed.

Development of oil shale resources will require large quantities of water, estimated by Fox et al. (1980) to be from 78 to 278 gallons per barrel oil, depending on the retort technology utilized. In addition to the high industrial demand for water, the Green River Formation is located in a water deficient area, much of the limited groundwater and surface water is moderately to highly saline (Israelsen et al. 1980), and water rights are difficult to obtain. Present plans call for the siting of many shale oil production facilities along major western rivers which are to be used as a water source and wastewater sink.

The rate of oil shale production may be limited by water availability (Maase 1980, Maase and Adams 1983) and it may be imperative that the large volumes of wastewater produced during production be treated for reuse within the plant. The wastewater may be a valuable resource for the arid regions if effective and economical treatment methods are found. The shale oil industry, to be economically competitive with the other fuel industries, requires low cost water pollution control technologies, capable of supplementing conventional treatment methods, in order to substantially reduce or eliminate contaminants in oil shale processing wastewaters.

Conventional biological and chemical pollution control technologies will sufficiently handle the biological and inorganic pollutants produced. However, numerous researchers (Fox et al. 1980, Mercer 1980, and Klieve et al. 1981) have shown biological treatment by activated sludge to be ineffective in sufficiently reducing total organic carbon for reuse or discharge. Treatment processes, including activated carbon, solvent

extraction, ion exchange, reverse osmosis, air stripping and coagulation, have major technical and/or economic limitations. Photooxidation of hazardous organic wastewater may be a cost-effective process capable of degrading trace organic compounds since sunlight needed to drive the decomposition reaction is available at no cost.

Photooxidation reactions can be divided into two types: direct and indirect. Direct photolysis occurs when the chemical itself absorbs light energy and undergoes reaction from its excited state. Organic compounds absorb light energy primarily in the UV region. Since little of the energy of UV wavelength reaches the earth's surface, direct photolysis is not a common decomposition pathway for most organic pollutants.

In the sensitized, or indirect, photolysis process, another chemical species, called a sensitizing molecule, absorbs the light energy emitted in the visible region where there is an abundant supply reaching the earth's surface. The sensitizing molecule becomes electronically excited to a new unstable energy level. Excited sensitizing molecules, or triplet sensitizers, return to ground state by transferring energy to molecular oxygen or organic substrates present in the system. If dissolved oxygen is present in even trace amounts, a triplet sensitizer will selectively transfer its energy to oxygen due to its low energy requirement in forming singlet oxygen (Foote 1958). Singlet oxygen is a highly reactive species capable of quickly oxidizing substrate molecules.

While few research studies have investigated photochemical treatment methods specifically applicable to oil shale retort wastewaters, several researchers have observed successful photodegradation of refractory organic compounds similar to those found in retort water. Spikes and Straight (1967) reported that many organic compounds including alcohols, nitrogen heterocycles, organic acids, olefins, benzenoids, phenols,and aromatic compounds, are susceptible to photodecomposition. Watts (1983) along with Sargent and Sanks (1974, 1976) have shown dye-sensitized photooxidation to be an effective treatment method for degrading biorefractory pesticides and aromatic compounds, respectively.

OBJECTIVES

The objective of this research was to investigate the use of dye-sensitized photooxidation as a potential treatment method for removal of organic compounds from retort wastewaters rendering these waters suitable for subsequent biological treatment, reuse and/or discharge.

A literature search provided information regarding the most abundant, recalcitrant and/or toxic compounds on which to concentrate research efforts. Four chemicals were chosen for investigation based on the following criteria:

1. existence in retort wastewater,
2. recalcitrance to conventional biological treatment,
3. proven toxic, mutagenic or carcinogenic activity, and/or
4. included on the USEPA Consent Decree, Priority Pollutant List (U.S. EPA 1976).

Two polynuclear aromatic hydrocarbons, (PNAs), anthracene and naphthalene, and their nitrogen heterocyclic analogs, quinoline and acridine, were selected. These four compounds are classified in Table 1, based on the criteria for selection. Pertinent physical characteristics of the compounds are shown in Table 2.

Specific objectives included:

1) Analysis of dye-sensitized photooxidation as a treatment method to completely degrade, decrease the toxicity of, or increase the biodegradability of selected hazardous compounds identified in oil shale production wastewaters. The effect of pH, dye concentration, and initial substrate concentration on photodecomposition reaction rates was used as criteria in determining optimum photooxidation conditions.

2) Evaluation of the toxicity of parent compounds and the photodegradation products to determine whether dye-sensitized photooxidation treatment reduces toxicity prior to biological treatment or discharge.

3) Development of a chemical actinometer, closely simulating actual experimental conditions, suitable for use in monitoring light intensity during sensitized photodecomposition experiments.

Table 1. Characteristics of selected polycyclic aromatic hydrocarbons meeting criteria for this study.

Compound Criteria	Anthracene	Naphthalene	Quinoline	Acridine
Retort water	X	X	X	X
Polynuclear aromatic hydrocarbon	X	X		
Nitrogen heterocycle			X	X
EPA priority pollutant[a]	X	X		
Suspected carcinogen/ mutagen[a,b]	X	X	X	X
Environmental levels: Toxicity based permissible concentration				
Based on health effects (mg/l)[c]	2.0	0.69	0.14	0.8
Based on ecological effects (mg/l)[c]		0.05	0.5	0.25

[a]-U.S. EPA (1976)
[b]-Pelroy and Petersen (1979)
[c]-Kingsbury et al. (1979)

Table 2. Physical characteristics of selected polycyclic aromatic hydrocarbons.

Physical Characteristics	Anthracene	Naphthalene	Quinoline	Acridine
Structure	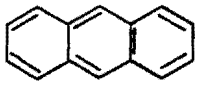	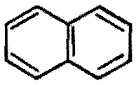	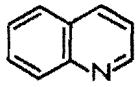	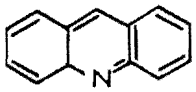
Formula	$C_{14}H_{10}$	$C_{10}H_8$	C_9H_7N	$C_{13}H_9N$
Molecular weight	178	128	129	179
Melting point, °C	216	88	-15	111
Boiling point, °C	340	218	238	345
Aqueous solubility, mg/l	.07	30		

LITERATURE REVIEW

Shale Oil

Organic rich sedimentary rock, referred to as oil shale, was originally deposited over 50 million years ago as sediment in inland lakes. As a result of a complex geologic history, these sediments have been converted into marlstones, rich in solid hydrocarbons. The organic fraction of oil shale was not subjected to the same geologic conditions that yielded petroleum, tar sands, and coal (Yen 1978). In shale oil, chemical bonds between individual organic molecules transformed the original organic matter into solid hydrocarbons known as kerogen, a high molecular weight polymer consisting primarily of heterocyclic molecules with smaller quantities of aliphatic and aromatic compounds (Fox 1980). During oil shale retorting, kerogen is thermally broken down to release shale oil.

The process of extracting oil from shale is not new. The early Indians referred to the "rock that burns," and private retorting of eastern U.S. shale took place in numerous small plants in the mid-1800s (Maase 1980). By the early 1900s nearly 200 claims had been staked in the western United States for oil shale mining (Nowacki 1981).

Oil shale occurs throughout the world on every continent and in at least 30 of the United States. The world's richest reserves occur in the 25,000 square mile Eocene Age Green River Formation of Colorado, eastern Utah and southern Wyoming (U.S. DOI 1973). Deposits of known resources are estimated to contain an equivalent of 2.0 trillion barrels of crude oil in the Green River Formation alone (Yen 1978). Six hundred billion barrels of oil equivalent are contained within high grade deposits, capable of producing 25 to 100 gallons of shale oil per ton of shale. The U.S. Department of the Interior has estimated that 80 billion barrels of this reserve are recoverable by present mining technology. This total is approximately twice the present domestic crude oil reserve in the United States exclusive of Alaska, and represents 75 percent of the oil the United States has produced since the Civil War (Pfeffer 1974).

Three basic methods of processing shale oil have been tested at pilot scale facilities: surface retorting, in-situ, and modified in-situ retorting. Surface retorting processes (Figure 1) involve mining the oil shale with conventional techniques, crushing and retorting the material in surface operations, and disposing of the spent shale residue. Spent shale solids pose a major disposal problem. Redente et al. (1981) estimate that although the mass of the shale oil is reduced 12 to 15 percent during retorting, its volume will increase by as much as 30 percent.

The second method of extracting oil involves retorting the oil shale in place (in-situ) and is not as technically advanced as surface retort operations. In-situ retorting offers a number of advantages over surface retort processes. It eliminates the necessity of disposing of large quantities of spent shale; and it may be used where the shale is deeply buried, where it occurs in relatively thin layers of rich and lean shale, or where conventional mining methods cannot be applied (Yen 1978).

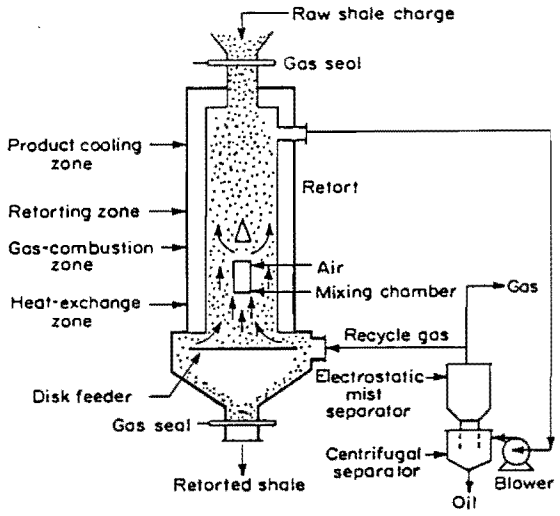

GAS-COMBUSTION RETORT

Recycle gas is mixed with air and burned within the retort. Gases flow upward and shale moves downward.

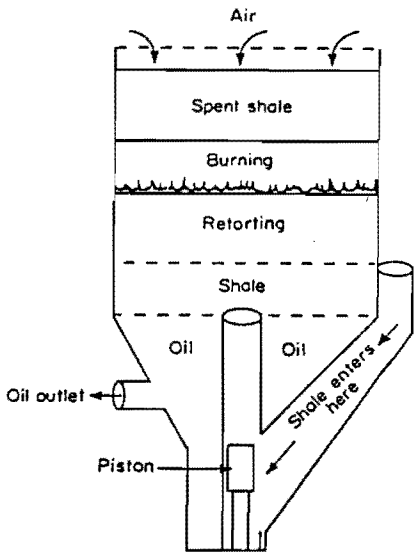

UNION OIL RETORT

Shale is introduced near bottom of retort and forced upward. Air enters at the top and flows downward.

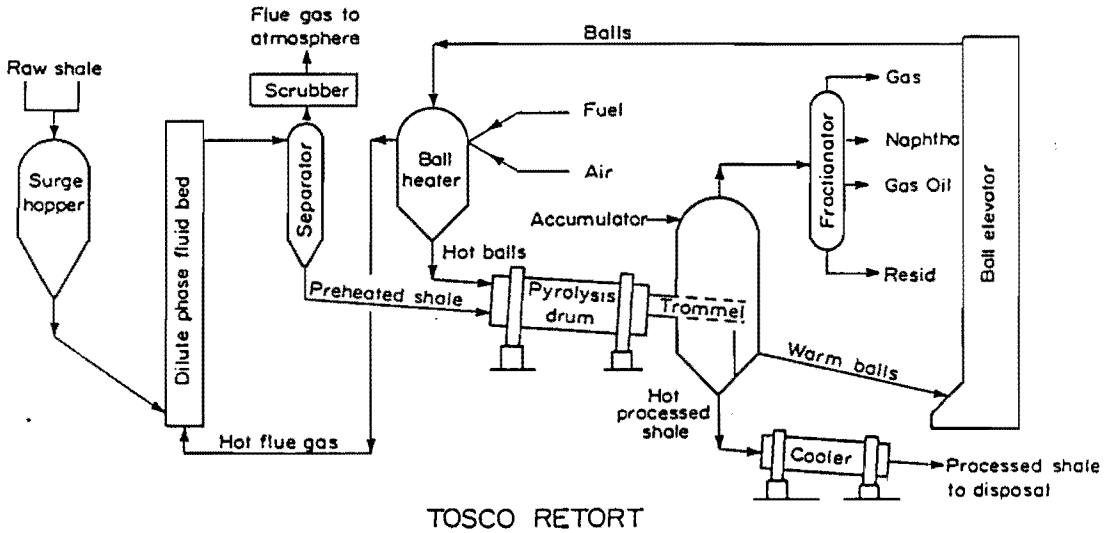

TOSCO RETORT

Ceramic balls transfer heat to shale. No combustion takes place in retort.

Figure 1. Schematic representation of three surface oil shale retorting processes (U.S. DOI 1973).

One application of the in-situ approach, known as true in-situ retorting, is shown in Figure 2. This process consists of drilling a predetermined pattern of wells in a rectangular shale section. If naturally occurring permeability is low, permeability is increased by fracturing the shale with explosives (Nowacki 1981) or by excessive hydraulic injections (Pfeffer 1974). The overburden is left intact. The fractured shale section is ignited at one end, air is injected through ignition wells to support combustion, and shale is retorted with a horizontally moving combustion front, converting the organic matter to oil (Dinneen 1974). The oil, water and gas produced is recovered from other wells in the section. In a true in-situ process all the retorting is done underground.

A modified in-situ process entails mining some of the oil shale to create a permeable combustion zone for in-situ retorting with the mined shale retorted above ground.

Retort Wastewater

The main wastewater streams generated from oil shale processing include mine drainage, gas condensate, and retort water. No mining/retorting can begin until the water table is lowered below the level of the mining/retorting operation. The quality and volume of mine drainage water is extremely site specific and depends upon the type of mining, rate of mine expansion, and the permeability and porosity of the material in which the mine is located. Generally, mine drainage water contains high levels of total dissolved solids, boron, and fluorides (Nowacki 1980). The developers in the Piceance Creek basin of the Green River Formation, employing modified in-situ retorting techniques, anticipate 2.4 to 6.8 barrels of water per barrel of oil produced to be extracted as mine drainage water (Hicks et al. 1980).

Gas condensate is the waste stream generated from air pollution devices used to treat process off-gas streams. Gas condensate is characterized by high levels of ammonia, CO_2, alkalinity and dissolved organics (Hicks et al. 1980), while inorganic salt content is negligible.

Retort water is formed when water vapor condenses in cool, rubblized shale ahead of the flame front during pyrolysis, and is collected with the recovered oil. Depending on the process, up to 22 barrels of retort water will be generated per barrel of oil produced. The volume may be higher if groundwater intrusion occurs (Fox et al. 1980). Retort water leaches large quantities of inorganic salts and dissolved organics from the shale oil. The organic content may reach 4 percent while inorganic species at concentrations of as much as 5 percent are typical (Fox et al. 1980). Organic concentrations can range up to 4,000 mg/l as TOC (Fruchter and Wilkerson 1980). Concentrations of chemical constituents in retort water are compared in Table 3 for direct heating and indirect heating surface retorting, true in-situ, and modified in-situ with above ground retorting. The wide range of concentrations reflect the differences in retorting processes and the degree of groundwater infiltration. While mine drainage may potentially be the largest wastewater stream produced, retort water may be the most complex and difficult to treat (Klieve et al. 1981).

With the breakdown of the kerogen in the oil shale, polynuclear aromatic (PNA) compounds, polycyclic aromatic amines, various heterocycles and other carcinogenic compounds are distributed between the shale retort water and the spent shale (Jones et al. 1982). The principal inorganic components of retort water are ammonium, sodium and bicarbonate ions (Fox et al. 1980). These materials can interfere with other treatment processes, via toxicity to biological systems and scaling in gas

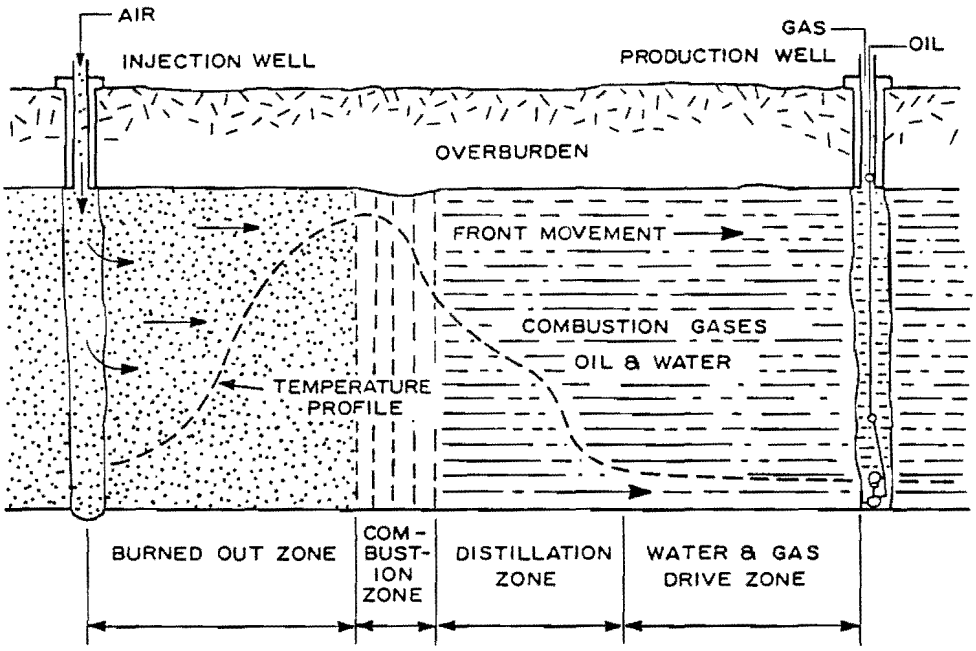

(a)

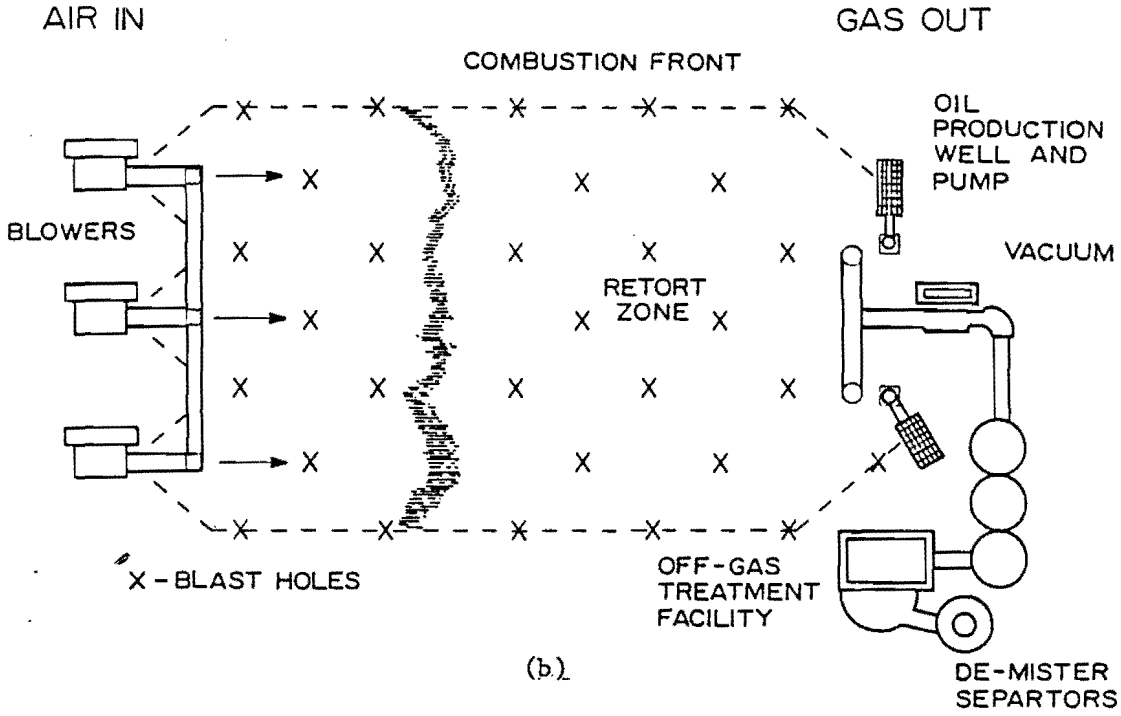

(b)

Figure 2. Schematic representation of an in-situ oil shale retorting process, a) vertical cross section; b) plan-view (Nowacki 1981).

Table 3. Water quality of oil shale retort wastewater (Nowacki 1981).

	Above Ground Indirect	Above Ground Direct	True In-situ	Modified In-situ
Conductivity, mhos/cm	120,000	16,000	49,600	82,250
pH, units	8.4	8.8	8.7	8.1
Oil & grease, mg/l	964	392	-	1,432
Phenol, mg/l	8.7	8.2	-	8.0
Chemical oxygen demand, mg/l	86,400	7,700	28,000	15,536
Total organic carbon, mg/l	19,290	15,000	-	12,300
Inorganic carbon, mg/l	-	1,600	-	-
Total dissolved solids, mg/l	160,000	1,856	13,700	1,002
Volatile dissolved solids, mg/l	159,700	1,810	-	-
Total suspended solids, mg/l	70	1	-	50
Chlorides, mg/l	70,000	2,300	5,000	53
Sulfate, mg/l	5,500	29	1,600	376
Fluorides, mg/l	5	3.1	31	5.1
Cyanide, mg/l	> 0.1	11.8	-	0.19
Total nitrogen, mg/l	33,600	5,100	-	30,300
Ammonia, mg/l	31,700	3,388	18,200	38,000
Nitrates, mg/l	580	138	33	-
Nitrites, mg/l	0.1	0.3	-	-
Total alkalinity as $CaCO_3$, mg/l	35,200	12,800	-	92,343
Arsenic, g/l	< 5	0.19	5.9	0.52
Mercury, g/l	< 0.1	< 0.1	0.1	< 0.002
Total sulfides, as S, mg/l	< 0.5	1,354	14	915
Trace elements, mg/l				
Aluminum	2.4	0.36	0.11	-
Antimony	<0.9	-	0.009	-
Barium	<0.3	-	0.012	-
Boron	1.2	0.18	5.2	-
Cadmium	<0.9	-	-	-
Calcium	18	2.5	0.6	-
Chromium	0.3	0.02	0.011	-
Copper	9	0.07	0.008	-
Iron	9	1.1	77	-
Lead	3	-	0.12	-
Magnesium	30	2.5	3.2	-
Manganese	1.2	0.03	0.042	-
Nickel	0.2	0.04	1.1	-
Potassium	3	0.36	8	-
Sodium	30	2.5	210	-
Tin	<0.3	0.14	8.9	-
Zinc	<1.2	-	0.26	-

strippers, and consequently, require removal (Hicks et al. 1980).

The general plan developed by the oil shale industry is for zero or near-zero discharge of wastewater from retorting facilities. Because of the high levels of organics, inorganics, oils, ammonia and alkalinity in retort waters, pretreatment for the removal of some or all of these constituents is required prior to full-scale treatment and/or water reuse. Approximately 50 percent of the organic carbon in retort water is amenable to bioxidation; the remaining organic compounds are recalcitrant. These compounds are predominantly non-polar solutes such as polycyclic aromatic hydrocarbons, and nitrogen and oxygen heterocycles (Jones et al. 1982). Due to the carcinogenic or mutagenic characteristics of these refractory compounds they may pose a potential danger to human health and the environment.

Retort water is generally used for spent shale disposal and dust control and it is anticipated that oil-water separation and steam stripping of ammonia, along with the removal of trace organics, will be required prior to reuse in full-scale facilities (Nowacki 1980).

Raphaelian and Harrison (1981) characterized the organic fraction of retort water from an in-situ process. Results indicate that nitrogen heterocycles are among the most abundant organic species present. Within the nitrogen heterocyclic class, the quinolines in the basic fraction of retort water represent the largest group (Santodonato and Howard 1981), and many nitrogen heterocycles including quinolines have exhibited carcinogenic activity (Coomes 1979). Rao et al. (1979, 1981) have shown in-situ product water and in-situ groundwater from a simulated modified in-situ retort to be mutagenic.

Polynuclear Aromatic Hydrocarbons

There has been growing concern regarding the possible harmful effects to man and other organisms from organic chemicals released into the environment from both natural and man-made sources. Polynuclear aromatic compounds represent one of the largest groups of carcinogens causing concern (Lee et al. 1981).

PNA compounds consist of two or more fused benzene rings in linear, angular or cluster arrangements. Substitution of carbon in the benzene ring with nitrogen, sulfur, oxygen or other elements creates heterocyclic aromatic compounds.

Physical and chemical characteristics of PNA compounds vary with the molecular weight of the compound. The lowest molecular weight member, naphthalene ($C_{10}H_8$, MW 128), consists of two fused benzene rings. One of the largest hydrocarbons commonly studied is coronene ($C_{24}H_{12}$, MW 300) (Neff 1979). Within this range exists a large number of PNA compounds which differ in ring number, structure and chemical activity.

The majority of the PNA's are formed during the incomplete combustion of organic matter at high temperatures. Several mechanisms have been proposed for the formation of PNA's by pyrolysis and pyrosynthesis (Schmeltz and Hoffmann 1976, Crittenden and Long 1976). In pyrolysis, complex organic molecules, exposed to elevated temperatures, are partially broken, yielding lower molecular weight, unstable free radicals. Pyrosynthesis of PNA's then proceeds by rapid combination of these free radical fragments containing one or more carbons, to form larger relatively stable aromatic hydrocarbons.

In general, all organic compounds containing carbon and hydrogen may serve as precursors to PNA's. Where oxygen, nitrogen or sulfur is present in the starting material, oxygen-, nitrogen-, or sulfur-heterocyclic analogs can be expected (Lee et al. 1981).

The yield and molecular weight distribution of the PNA's formed

during combustion depend on the pyrolysis temperature and duration of the exposure (Lee et al. 1976, Lee and Hites 1976) and the chemical composition of the starting organic matter.

During pyrolysis of oil shale, in which kerogen acts as the starting material, a large number of PNA compounds, polycyclic aromatic primary amines, various heterocycles and other carcinogenic compounds are formed and distributed between the shale oil, the retort water and the spent shale. The PNA's and their heterocycles are of critical environmental and health concerns because of: 1) chronic health effects (carcinogenicity), 2) microbial recalcitrance, 3) high bioaccumulation potential, and 4) low removal efficiencies in traditional wastewater treatment processes (Fox et al. 1980).

PNA compounds have received additional attention recently due to the existence of many PNAs in the EPA Priority Pollutant Consent Decree (U.S. EPA 1976). Tabek et al. (1981) examined the biodegradability of PNA compounds along with other organic compounds listed as priority pollutants. The PNAs demonstrated varied rates of biodegradation with different acclimation periods depending on the test compound and the dose of substrate. Tricyclic aromatic hydrocarbons were found more susceptible to biodegradation than the tetracyclic and higher polycyclic hydrocarbons.

Kochevar et al. (1982) have demonstrated that some PNA compounds commonly found in coal tar exhibit phototoxic potential. The degree of erythema produced in guinea pig skin after exposure to the compound and UV-A radiation (320-400 nm) was taken as the measure of phototoxicity. Pyrene, anthracene and fluoranthene were strongly phototoxic. Acridine was phototoxic, but to a lesser degree. These compounds absorbed available light more effectively than other PNA compounds and showed a correlation between relative light absorption and phototoxicity. Among the heterocyclic compounds tested, acridine absorbed UV-A light more effectively than the other heterocyclic compounds and was the only heterocycle found to be phototoxic.

Although the presence of nitrogen heterocycles in the environment has been known for many years, the biological effects of these compounds have not been as intensively investigated as have the polynuclear aromatic hydrocarbons. Several decades ago researchers demonstrated that several naturally occurring nitrogen heterocycles were carcinogenic to mice (Santodonato and Howard 1981), leading to the present concern over their potential human health significance. In recent studies in bacteria, acridine has been demonstrated to cause photodynamic damage to both DNA and cell membranes (Wagner et al. 1980, Snipes et al. 1979).

The basic fraction of many environmental samples usually contains a number of nitrogen heterocycles. Pelroy and Petersen (1979) demonstrated that the basic fraction of shale oil was more mutagenic than any of the other fractions (acidic, neutral, tar, PNA, crude oil) tested. Quinoline and acridine are considered bases possessing these mutagenic characteristics. Concentrations of 0.5 mg/l to 1.0 mg/l of quinoline in water may cause tainting of fish flesh (Kingsbury et al. 1979). Acridine has been shown to be toxic to fish at 5.0 mg/l levels (Kingsbury et al. 1979). Permissible environmental concentrations for the test compounds, based on ecological and health effects, are contained in Table 1.

Treatment Options

Conventional processes

The oil shale industry is still struggling to fully develop and at present no active oil shale mines are operating on a commercial scale. If and when commercialization begins, a

variety of retorting processes may be used, each creating unique environmental problems. Since full scale designs have not been completed, environmental concerns can be considered and incorporated into process design from the early stages of development.

The need for treatment options for the removal of the refractory, and often times hazardous, organic compounds in oil shale retort water has been identified, and various physical and chemical treatment options have been investigated. Many of the options investigated, such as wet air oxidation, ion exchange, reverse osmosis, or excess permanganate treatment, are highly capital and/or operationally cost intensive. Others, such as solvent extraction, coagulation and steam stripping, do not provide adequate removal of the residual organic fraction in the retort water.

Biological treatment is widely used as a cost effective means of removing biodegradable organic materials from municipal and industrial wastewaters. Malaney et al. (1967), Hicks et al. (1980), and Harrison et al. (1975) have shown that many refractory and/or carcinogenic compounds found in industrial waste streams cannot be effectively removed by means of conventional biological treatment.

Successful treatment of oil shale wastewater will require the application of numerous physical/chemical and biological unit processes. A particular process may be extremely effective for the removal of specific classes of compounds, however, when applied to a mixture such as retort water, it may be able to remove only a fraction of the pollutants. Complete treatment will require a combination of methods used in series or parallel applications.

Dye-sensitized photooxidation

Fundamentals. The importance of photochemical transformation in the atmosphere is well documented (Altschuller and Bufalini 1971, Leighton 1961), but comparatively little is known about photodegradation of pollutants in water where other competing processes such as biodegradation and hydrolysis occur (Zepp and Cline 1977). In a water system, biodegradation is often the major pathway for elimination of organic compounds. When the system includes refractory species however, biodegradation is too slow to be effective and photodegradation may become the most important pathway for these compounds.

Light, a form of electromagnetic radiation, has a dual nature, exhibiting properties of both waves and particles. The quantum theory introduces a relationship between the wave and quanta nature of light (Smith 1971). Light is a form of energy and the individual particles, or quanta, possess energy that depends on the wavelength of light, with more energy supplied by light quanta as the wavelength of light decreases (Plimmer 1971). In keeping with the theory of duality of light, photochemists use a particular wavelength in calculating relevant extinction coefficients and count quanta in determining the efficiency of a photochemical reaction (McLaren and Shugar 1964).

The first law of photochemistry, known as the Grotthus-Draper law, states that only light which is absorbed by a system can induce a chemical reaction. As a molecule absorbs light, it receives energy in the form of discrete units called photons or quanta. The second law of photochemistry, the Stark-Einstein law, involving the particle nature of light, states that one quantum of light is absorbed per molecule of absorbing and reacting substance that disappears. Since changes in single molecules of reactants are not ordinarily observed, a more tangible quantity, the einstein, is used in discussing photochemical reactions; an einstein is one mole of quanta (McLaren and Shugar 1964).

Absorption of light can cause oxidation reactions which would otherwise not occur. Chemical reactions are not restricted to the molecule absorbing energy, as excitation energy may be transferred in a number of ways to the species that ultimately undergoes chemical change. An almost unlimited number of photooxidation reactions are possible and these can be broken down into two types: direct and indirect. Direct photolysis occurs when the chemical molecule itself absorbs light and undergoes reaction from its excited state. Indirect photolysis occurs when another chemical species, called a sensitizer molecule, absorbs light energy and then transfers this energy from its excited state to another chemical which undergoes reaction (Mabey et al. 1982).

Absorption of light energy, primarily in the ultraviolet (UV) region, is a common characteristic of most organic pollutants. Transformations of organic pollutants by direct photolysis depend then upon absorption of energy in the UV spectrum. This direct photolysis reaction is generally an inefficient environmental process since light transmittance in the atmosphere in the UV and visible region decreases with the decreasing wavelength. Essentially no light is transmitted to the earth's surface at wavelengths less than 295 nanometers (Zepp and Cline 1977).

In the sensitized photolysis process, however, sensitizing molecules absorb light in the visible region where there is a wealth of energy reaching the earth's surface. The electronically excited sensitizing molecule or triplet sensitizer is usually unstable at this new level of energy and by a deactivation process, it reverts to a lower, less energetic, stable state. Triplet sensitizers return to ground state by transferring energy to molecular oxygen or organic substrates which are nonabsorbing in this same visible wavelength region. For energy transfer to another molecule to occur, the energy gap between ground state and the first excited state of that molecule must be less than the absorbed energy of the triplet sensitizer, which is on the order of 40 kilocalories/mole (kcal/mole) for common sensitizing organic dyes. Most organic molecules require more energy to be excited than is available from a triplet sensitizer. Oxygen however, is unusual because its ground state is a triplet and the energy gap between ground state and the first excited state, which is a singlet, is unusually low (22 kcal/mole). Thus if dissolved oxygen is present in even trace amounts, a triplet sensitizer will selectively transfer its energy to oxygen (Foote 1968, Sargent and Sanks 1976).

Singlet oxygen is a strong oxidizing agent with an average half-life of 2 μ seconds (Kearns 1971), capable of quickly oxidizing photosensitive substrate molecules. Foote (1968) and Pitts et al. (1963) suggest that the two singlet oxygen species most likely involved in photooxidation reactions are singlet delta oxygen ($^1\Delta$ g), and singlet sigma oxygen, ($^1\Sigma_g^+$). Kearns et al. (1967a) have suggested that high energy sensitizers with triplet state energy of formation, E_t, greater than 37 kcal, the energy of $^1\Sigma_g^+$, should produce $^1\Sigma_g^+$ oxygen as the primary product of energy transfer, whereas sensitizers with E_t less than 37 kcal should produce only $^1\Delta$g oxygen which has an energy of formation of 22 kcal. Figure 3 depicts the electronic states and configurations of molecular oxygen.

The $^1\Delta$g oxygen state is long lived and survives at least 10^8 collisions with methanol in the vapor phase, whereas the $^1\Sigma_g^+$ state survives no more than ten collisions under the same conditions (Foote 1968).

Porter and Wilkinson (1961) found that, as the triplet state energy of the sensitizer approaches the triplet state energy of the acceptor, the energy transfer probability is significantly

State	Occupancy of highest orbitals	Energy	Lifetime in solution
$^1\Sigma_g^+$	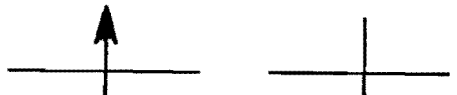	37 kcal	10^{-9} to 10^{-12} sec
$^1\Delta g$	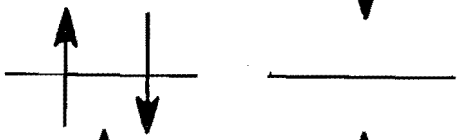	22 kcal	10^{-3} to 10^{-6} sec
$^3\Sigma_g^-$		ground state	

Figure 3. Molecular oxygen states and their electronic configuration (Foote 1968).

reduced. When oxygen is the acceptor, Kearns et al. (1967b) predicted the ratio of $^1\Sigma_g^+$ to $^1\Delta g$ oxygen to decrease to zero as E_t of the sensitizer approaches 37 kcal. This study concluded that the two singlet oxygen species exhibit different reactivities, and that observed variations in reaction product distribution as a function of sensitizer used results from a variation in the relative amounts of $^1\Sigma_g^+$ and $^1\Delta g$ oxygen generated.

The transfer of energy from the excited triplet sensitizer to the reactants in the system may proceed by two routes, one in which the interaction is with the substrate and one in which the primary interaction of the sensitizer triplet is with oxygen (Foote 1968). The former involves energy transfer from the excited triplet sensitizer (S*) to the organic matter (OM) in the system to generate reactive, short lived radical intermediates which dissociate into oxidation products:

$$S + h\nu \rightarrow S^* \quad (1)$$

$$S^* + OM \rightarrow \text{transient species} + S \quad (2)$$

$$\text{transient species} \rightarrow \text{oxidation products} \quad (3)$$

This reaction mechanism is termed Type I and may include hydrogen abstraction, electron abstraction, alkyl radical generation and hydroxide radical generation as intermediate mechanisms (Heelis et al. 1981). A requirement for energy transfer is that the acceptor have a triplet energy lower than that of the sensitizer; triplet energies of sensitizing dyes are very low (on the order of 40 kcal) compared to most organic compounds so this condition is seldom satisfied.

The second process, termed Type II involves energy transfer to molecular oxygen and results in excitation of molecular oxygen to singlet oxygen, where $^1\Delta g\ O_2$ in Equations 4 and 5 represent either species of singlet oxygen since both species may be formed in varying amounts and are capable of reacting with organic matter (Acher and Rosenthal 1977):

$$S + h\nu \rightarrow S^* \quad (1)$$

$$S^* + {}^3\Sigma_g\ O_2 \rightarrow S + {}^1\Delta g\ O_2 \quad (4)$$

$$^1\Delta g\ O_2 + OM \rightarrow \text{oxidation products} \quad (5)$$

Which of the two reaction types predominates and the efficiency of each path depends on the oxygen and substrate concentrations, the rates of reaction of sensitizing triplet with substrate and with oxygen, the rate of triplet decay, reaction pH, and other physicochemical factors (Sargent and Sanks 1974). Foote (1968) found that even traces of oxygen will likely inhibit Type I reactions.

Engineering applications. Much scientific research has been conducted on dye-sensitized photooxidation, however engineering application of the photolysis process to water and wastewater treatment has received little attention. Spikes and Straight (1967) reported that many organic compounds including alcohols, nitrogen heterocycles, organic acids, olefins, benzenoids, phenols and aromatic compounds undergo sensitized photooxidation in natural systems. According to Foote (1968) many organic compounds are capable of absorbing light to initiate these photochemical reactions. Some will sensitize only very specific reactions, while others will sensitize the photooxidation of many substrates. Investigations by Sargent and Sanks (1974 and 1976) indicate that common dyes such as methylene blue, toluidine blue, rose bengal and neutral red are effective non-specific sensitizers.

Gurnani et al. (1966) observed the sensitized photodegradation of the amino acid, tryptophan, in an effort to understand the mechanism of its oxidation. Seven chromatographically separable products were formed when an

aqueous solution of tryptophan was exposed to light at pH 9 in the presence of methylene blue and oxygen. In the absence of methylene blue and/or oxygen, some of these same products were detected, though in much smaller quantities. Exposure of tryptophan to UV light did not result in the formation of any of the products obtained with visible light.

The products formed during sensitized photolysis of cholest-4-en-3B-ol have been studied in considerable detail to gain insight into the singlet oxygen mechanism. Only two products are formed during this photooxidation; epoxy ketone and enone (Kearns et al. 1967a and 1967b), however, the product distribution ratio varied depending on the nature of the sensitizer. This result is linked to the relative amounts of $^1\Sigma_g^+$ and $^1\Delta g$ oxygen generated.

One of the earlier engineering applications of photochemical processes was performed by Bulla and Edgerley (1968) who examined design and operating parameters in the UV photolysis of three chlorinated hydrocarbons: aldrin, dieldrin, and endrin. Kinetic rate equations were used to describe the effect of design parameters. A first order rate law was applicable to retention time, light intensity, and depth of reactive solution. Temperature had no significant effect on the rates measured. Bioassay tests indicated that aldrin degradation products were less toxic than aldrin itself.

First order reaction rate equations were applied to studies by Young et al. (1971) when examining the effects of solvent polarity in dye-sensitized photooxidation. Three solvent systems studied were methanol, n-butyl alcohol, and tert-butyl alcohol. The reaction rates varied due to the change in the lifetime of singlet oxygen in the different systems, related to the viscosity of the solvent.

Engineering design parameters for the treatment of refractory organics were determined by Sargent and Sanks (1974) using cresol and methylene blue as substrate and sensitizer, respectively. Design parameters examined included optimum pH, substrate concentration, dye concentration, effect of dye bleaching, and kinetic rate constants for both anaerobic and aerobic reactions. They found that the photolysis of cresol occurs as much as 2.8 times faster in aerobic systems than in anaerobic systems, again suggesting the importance of singlet oxygen to effective photolytic reactions. A first order rate equation described, with reasonable accuracy, the rate at which cresol was photooxidized. The reaction mechanism is probably not first order, however, but a complex function of substrate concentration, dye concentration, and oxygen concentration, as well as temperature, pH, and light intensity.

The pH dependence of singlet oxygen production in aqueous solutions was studied by Bonneau et al. (1975). Thiazine dyes were utilized as photosensitizers to investigate the yield of singlet oxygen as a function of pH. Both laser flash photolysis and continuous irradiation were used. The production of singlet oxygen by the thiazine dye, methylene blue, was very sensitive to changes in pH in the range of 5 to 9. Based on observed photooxidation rates for methylene blue in aerated solutions, the production of singlet oxygen was approximately 5 times more efficient in basic than in acidic medium.

Cresol and phenol were tested for sensitivity to dye-sensitized photooxidation by Sargent and Sanks (1976). Dyes used as sensitizers included rhodamine 6G, sodium phthalocyanine, 2,7-dichlorofluorescein, neutral red, methylene blue, rose bengal, malachite green, hematoporphyrin-D and acridine orange. Tungsten lamps were used as the light source. Results indicated that singlet oxygen was the mechanism of

oxidation and that methylene blue and rose bengal were the most effective sensitizers studied. The authors concluded that the reaction of singlet oxygen with refractory aromatic heterocyclic compounds gives products tractable to biological oxidation, but the reaction products were not tested for biodegradability.

Acher and Rosenthal (1977) investigating the applicability of dye-sensitized photolysis for the treatment of domestic sewage found that the chemical oxygen demand (COD) could be reduced up to 67 percent and total disinfection was achieved upon photolysis with methylene blue. Experiments were conducted in natural and artificial light, and methylene blue was determined to be the optimum sensitizer at a concentration of 12 mg/l.

Natural water was used in experiments by Zepp et al. (1977) to examine the steady state concentration of singlet oxygen. The highest rates occurred in highly colored water, rich in fulvic acid. Since most organic rich natural waters contain large concentrations of fulvic acid, the authors concluded that photochemical generation of singlet oxygen is a widespread phenomenon in the aquatic environment.

Rates of direct photolysis of two pesticides, carbaryl and trifluralin in pure naturally occurring river water were investigated and modeled by Zepp and Cline (1977) under natural sunlight conditions. Half-lives were calculated as a function of season, latitude, time of day, depth of water bodies and ozone layer thickness. Experimental verification of the computed half-lives was presented.

Using the appearance of stable nitroxide radicals from the photolysis of amine 2,2,6,6-tetramethyl-4-piperidone, as an indication of reaction rates, Houba-Herin et al. (1982) studied the production of singlet oxygen with irradiation of several dyes in aqueous solution at pH 9. Rose bengal, methylene blue and eosin dyes were better singlet oxygen producers by a factor of at least 9 than thiopyronine, proflavine and acridine yellow. Singlet oxygen production was not observed with 9-aminocaridine, acridine orange, quinacrine and ethidium bromide.

Watts (1983) developed rational engineering criteria for the design of dye-sensitized photooxidation lagoons for selected pesticides. Engineering application parameters investigated included optimum pH, maximum lagoon depth, mixing effects, aeration requirements and optimum methylene blue concentrations. Rate constants were also determined for varying treatment conditions including natural sunlight photolysis and artificial light reactions.

Actinometry

Estimation of the rate constants for photolysis of a specific chemical in naturally occurring waters, based upon laboratory data, requires information regarding the absorption spectrum of the chemical, the quantum yield, or efficiency, of the process and the intensity of the light as a function of wavelength (Dulin and Mill 1982). Chemical actinometry is the usual method for determining the quantum yield of photoreactions as well as the light intensity of the given photosystem.

A chemical actinometer system consists of a photochemical reaction possessing a known and accurately reproducible quantum yield. Ideally, the quantum yield of the system should be independent of light intensity over the wavelength range of interest. By establishing reaction quantum yield and light intensity, the kinetic data derived from photolysis under one set of light conditions can be applied to a wide range of light conditions utilizing the photochemical reaction equation indicated below (Dulin and Mill 1982):

$$\phi_{rxn} = \frac{\Sigma I_\lambda \varepsilon_\lambda{}^a}{\Sigma I_\lambda \varepsilon_\lambda{}^c} \frac{K^c}{K^a} \phi_a \qquad (6)$$

where:

ϕ_{rxn} = reaction quantum yield for the chemical, moles/einstein

K^c = initial rate constant for photoreaction of the chemical, mole/sec

K^a = initial rate constant for photoreaction of the actinometer, mole/sec

$\Sigma I_\lambda \varepsilon_\lambda{}^a$ = summation of the product of the light intensity and extinction coefficient of each wavelength of the actinometer, day^{-1}

$\Sigma I_\lambda \varepsilon_\lambda{}^c$ = summation of the product of light intensity and extinction coefficient of each wavelength of the chemical day^{-1}

ϕ_a = quantum yield for the actinometer, mole/einstein

Several criteria for chemical and spectral properties that should be given high priority when selecting actinometers include: 1) a quantum yield that is temperature and wavelength independent, 2) a quantum yield that is independent of the concentration of the actinometer, 3) photolysis products that do not interfere with photolysis, either chemically or spectrally, 4) the ability to be readily analyzed by conventional methods, 5) stability in water, 6) stability in the dark, and 7) moderate solubility and non-volatility in water (Dulin and Mill 1982).

An actinometry procedure described by Hatchard and Parker (1956) utilizing potassium ferrioxalate is regarded as the classic liquid phase chemical actinometer for photochemical research (Calvert and Pitts 1966). It is extremely sensitive over a wide range of wavelengths and is simple to use. When sulfuric acid solutions of $K_3Fe(C_2O_4)^3$ are irradiated in the range of 250 to 577 nm, simultaneous reduction of iron to the ferrous state and oxidation of oxalate occur. The quantum yields of Fe^{2+} formation have been accurately determined, and are independent of wavelength from 250 to 577 nm. The reaction is independent of reactant and product concentrations, incident light intensity and reaction temperature.

Although not as commonly used as the ferrioxalate system, other chemical actinometer systems appear to be useful for environmental photochemical studies. Dulin and Mill (1982) developed two actinometers for intensity measurements from 300 to 370 nm, suitable for natural sunlight experiments. Both systems, p-nitroanisole-pyridine and p-nitroacetophenone-pyridine, have quantum yields invariant of wavelength. Neither are volatile from water nor readily sorbed, and each is easily analyzed by high performance liquid chromatography.

An actinometer for the visible wavelength range, 400 to 580 nm, was presented by Brauer et al. (1982). The photooxidation of heterocoerdianthrone in toluene to an endoperoxide with visible light can be evaluated using UV and visible spectroscopy.

An actinometer system should, however, closely simulate the experimental conditions in the photochemical research. In this study, the usable wavelength region was outside the range for the effective utilization of the ferrioxalate system. An alternate system was required which would monitor light intensity for the wavelength region 570 to 700 nm where the sensitizer, methylene blue, absorbs most strongly.

Bellin and Yankus (1968) found that the amino acid, L-tryptophan, was susceptible to sensitized photodegradation by methylene blue. To maintain a reaction quantum yield of 1.0, Bonneau et al. (1975) discovered that an aqueous solution of tryptophan and methylene blue must be buffered to a pH greater than 8. The utilization of a methylene blue-tryptophan actinometer system would closely parallel the actual photolysis conditions, utilizing the same reaction geometry and light emitting apparatus and consequently was adopted for use in this study.

The quantum yield, ϕ, is a means of quantifying the efficiency of a photochemical reaction and is one of the most useful and fundamental quantities in the study of photochemical mechanisms. Its magnitude provides important information regarding the nature of photooxidation reaction. Small quantum yields ($\phi << 1$) indicate that processes such as deactivation, quenching, fluorescence or other processes that lead to no net chemical change are competing with the photooxidation reaction (Calvert and Pitts 1966). Large quantum yields ($\phi >> 1$) indicate that mechanisms operating in a chain reaction are occurring.

The second law of photochemistry, the Stark-Einstein law, states that one molecule is activated for each photon absorbed in a system. After a molecule absorbs a photon, it is unstable and will undergo a variety of competing primary processes, such as chemical reaction, light emission, energy transfer, or physical deactivation, to return to a stable state. The fraction of photons absorbed is called the primary quantum yield for the process. A corollary of the Stark-Einstein law is that the sum of the primary quantum yields of all the processes that deactivates the excited molecule equals unity (Mousseron-Canet and Mani 1972). This does not apply to the overall reaction quantum yield, ϕ_{rxn}, which may be much larger than unity and for certain chain reactions it may be as high as 10^4 to 10^6 (Turro 1978). It is essential, therefore, to identify the type of quantum yield in discussion. The quantum yield, ϕ_{rxn}, is defined by Calvert and Pitts (1966) as:

$$\phi_{rxn} = \frac{\text{Moles of molecules reacting}}{\text{Moles of photons absorbed}} \qquad (7)$$

By selecting a chemical actinometer with a photoreaction which is sensitized by the same dye used in the photolysis experiment, Equation 6 simplifies to:

$$\phi_{rxn} = \frac{K^c}{K^a} (\phi_a) \qquad (8)$$

and was used for the calculation of the overall reaction quantum yields in this study.

Spikes and Straight (1967) reported that quantum yield is not a function of light intensity so the quantum yield of reaction calculated from laboratory photolysis data using Equation 8 may then be used to predict the rate of disappearance of the pollutant, k^c, in the environment under natural sunlight conditions.

MATERIALS AND METHODS

Photolysis Bench

Photooxidation experiments were performed using artificial constant light provided by Duro Test Vitalite™ lamps, which are 91 percent corrected to the quality of natural sunlight. Radiation impinging upon test solutions was routinely measured using a chemical actinometer and a Lambda-185 Radiometer. A radiometer integrates the light output over the entire visible spectrum and an overall intensity output is recorded. The Lambda-185 Radiometer recorded an average intensity of 48 W/m^2 throughout the experiment. Of greater importance to sensitized photolysis experiments is the incident light intensity in the wavelength region of maximum absorbance of the sensitizing dye. The chemical actinometer monitored the energy output for the maximum absorbing wavelengths, 570 nm to 700 nm for methylene blue.

Radiation as a function of wavelength emitted by the Duro Test Vitalite™ lamps was measured for the visible light spectrum by an Optronic 742 spectroradiometer (Figure 4). The spectroradiometer was also used to measure radiation as a function of wavelength of natural sunlight in July during the solar noon period in Logan, Utah (latitude, 42° N). A comparison of the percent of total light intensity emitted at each wavelength in natural light and under the experimental lights is shown in Figure 5. The sensitizing dye, methylene blue, exhibits its maximum absorbance at 665 nm. The percent of the total light intensity emitted at 665 nm was the same for both the artificial light source and natural sunlight making experimental and expected natural sunlight induced reaction results comparable.

The photobench consisted of 10 pairs of 8 foot lamps placed across a 3 foot wide bench. The lamps were matched so that intensity was constant across the length and width of the bench. The bench was of sufficient size to allow the examination of photolysis reactions in 25 reactors at one time.

Barltrop and Coyle (1978) suggested that at least 10^{15} photons/second light energy be available for effective photolytic reactions to occur. The chemical actinometer system consisting of a tryptophanmethylene blue mixture was run repeatedly at varying distances from the lamps. By successive application of Equation 9,

$$\text{light energy} = \frac{\Delta CVN}{\phi_a t} \qquad (9)$$

where

C = change in tryptophan concentration (mole/liter)

V = volume of sample (liters)

ϕ_a = quantum yield of actinometer (mole/einstein)

t = reaction time (seconds)

N = 6.023×10^{23} (photons/einstein)

The light energy output in photons/second was determined for each trial distance. The base of the photobench was finally adjusted so that the test solutions were 14 cm from the lamps thereby receiving the suggested light energy input.

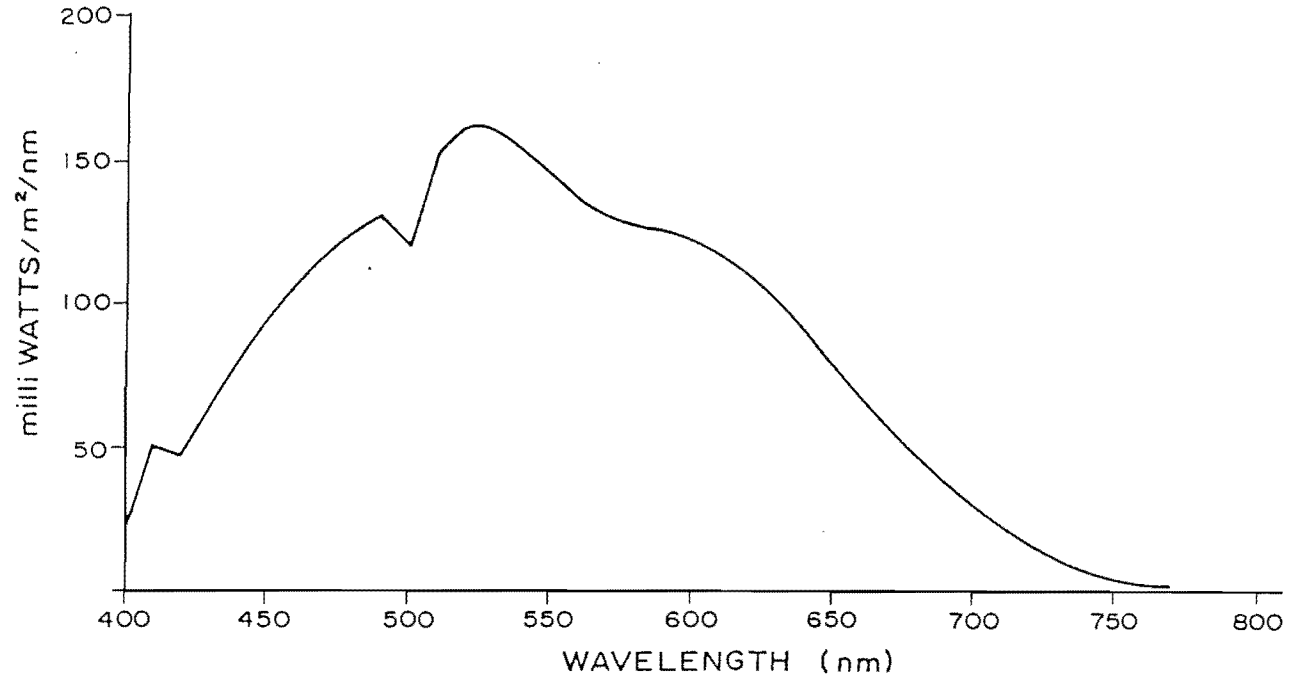

Figure 4. Radiation as a function of wavelength emitted from the DuroTest Vitalite lamps.

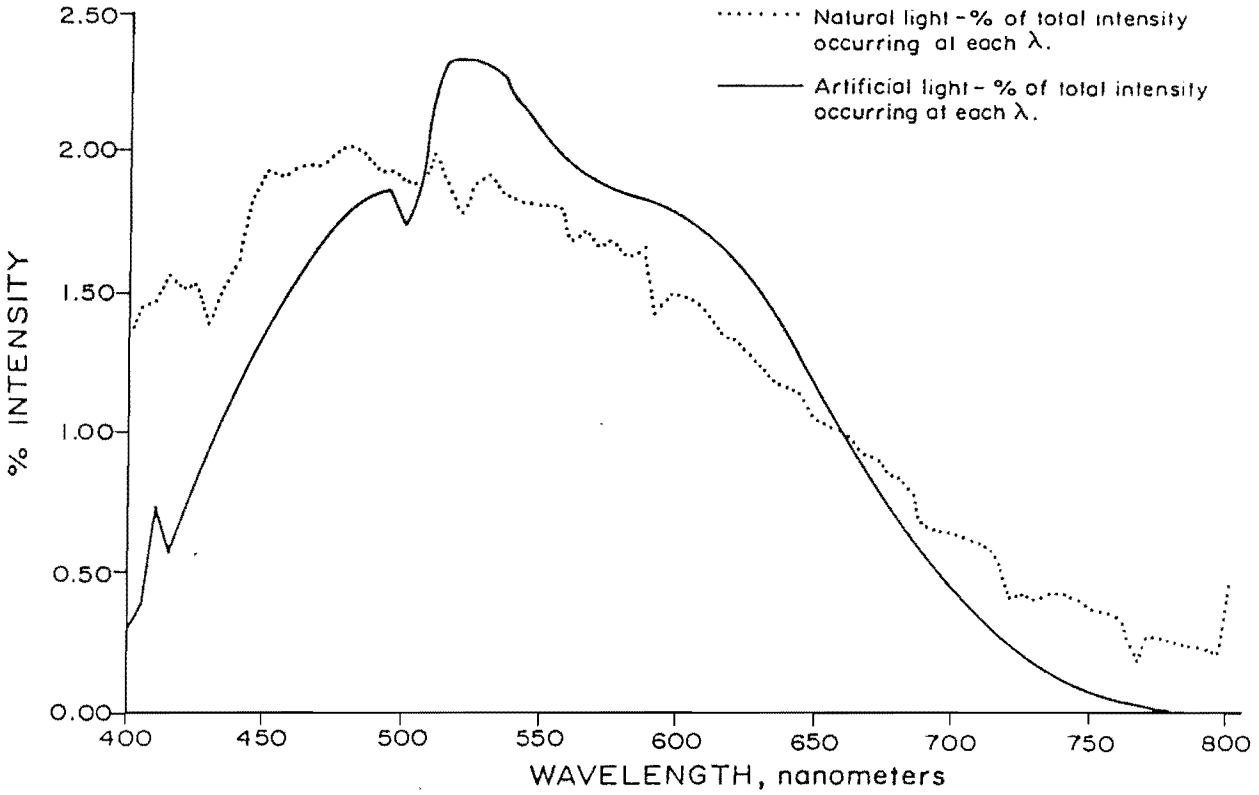

Figure 5. Percent of total light intensity occurring at each wavelength for natural sunlight and artificial light.

Reactors

Glass containers approximately 13 cm in diameter were used as photolysis reaction vessels. The average depth of the test solutions was approximately 2 cm. The reactors were prepared by washing with a 10 percent sulfuric acid solution followed by three rinses with distilled deionized water. A Milli-Q™ deionizing water system provided laboratory pure water for all washings and dilutions. Glass plates (7" x 7" x 1/4") were cut to fit over the reactors to minimize evaporation.

Photolysis

Two polynuclear aromatic hydrocarbons, anthracene and naphthalene, and their nitrogen heterocyclic analogs, acridine and quinoline, were selected as representative pollutants in retorting wastewater, and were used as photooxidation substrates. Optimum conditions for photodegradation were determined by varying the pH and sensitizing dye concentration.

Due to the low aqueous solubility of the four compounds used in this study, the use of a co-solvent was necessary. Acetonitrile was used as a 1 percent co-solvent due to its inert photochemical characteristics (Mabey et al. 1982). Reaction solutions were prepared from a stock solution of the chemical in HPLC Grade Acetonitrile at a concentration 100 times that used during photolysis. An aliquot of this solution was diluted with deionized water to yield a 1 percent acetonitrile in water solution, with final compound concentrations of 1.0 mg/l for anthracene and naphthalene and 5.0 mg/l for acridine and quinoline.

Optimum reaction conditions

The effect of pH on sensitized photooxidation rates was investigated over a pH range from 3 to 11 in 2 pH-unit intervals. Samples were buffered to prevent pH drift during experiments. Those samples buffered to pH 3, 5, and 7 were prepared using a citric acid-phosphate solution, while samples analyzed at pH 9 and 11 were buffered with a carbonate-bicarbonate solution. Buffer solution ingredients for each experimental pH condition are shown in Table 4.

Methylene blue was selected as the sensitizing dye for the experiment. The effect of dye concentration on the rate of photooxidation was examined using dilute dye solutions at concentrations of 10 mg/l or less. Blanks accounting for adsorption loss on containers and compound loss due to volatilization were analyzed for each compound by examining degradation rates in solutions containing no dye (direct photolysis) as well as in solutions with methylene blue maintained in the dark.

For each compound analyzed, an initial run was performed using a test solution containing 5 mg/l methylene blue. Table 5 represents an example of experimental set-up. Twenty-five 200 ml samples, comprising an experimental run, were divided into groups of five, with each group representing one sampling time interval. Within each group of five, the solutions were buffered to pH 3, 5, 7, 9, and 11. Samples were taken at five time intervals to allow determination of the rate law and rate constants governing the reactions. The time intervals were changed as necessary to suit the reactivity of the substrate.

Following the completion of triplicate analyses of the 5 mg/l sensitizer runs, a lower concentration of methylene blue, 2 mg/l, was investigated. The same experimental design was followed at this lower concentration. The third experimental methylene blue concentration was selected based upon the results of these first two runs. If the 2 mg/l methylene blue solutions were more successful in degrading the compound, then a lower concentration of dye, 1 mg/l was investigated. If, however, the 5 mg/l concentration of dye was more successful in

Table 4. Buffer solutions utilized for investigation of the effect of pH on the sensitized photolysis rates.

pH	Stock Buffer Solutions			
	A	B	C	D
3	844 ml	156 ml		
5	486 ml	514 ml		
7	130 ml	72 ml		
9			40 ml	460 ml
11			500 ml	20 ml

All solutions were diluted to 2 liters following the addition of the two stock solutions.

Solution A: 0.1 M Citric acid
B: 0.2 M dibasic sodium phosphate
C: 0.2 M sodium carbonate
D: 0.2 M sodium bicarbonate

Table 5. Experimental design configuration*.

Reactors Prepared	pH3 pH5 pH7 pH9 pH22	pH3 pH5 pH7 pH9 pH11	pH3 pH5 pH7 pH9 pH11	pH3 pH5 pH7 pH9 pH11	pH3 pH5 pH7 pH9 pH11
Methylene blue concentration	5 mg/l	5 mg/l	5 mg/l	5 mg/l	5 mg/l
Test compound	acridine	Acridine	Acridine	Acridine	acridine
Sample time (hrs)	0	4	12	24	48

*This procedure was repeated in triplicate for methylene blue concentrations of 2 mg/l, and either 10 mg/l or 1 mg/l.

photolysis, then a higher concentration of dye, 10 mg/l was used.

Due to the bleaching of the dye during lengthy photolysis runs, the concentration of methylene blue was monitored every 4 hours and adjusted as necessary.

At the end of a desired time interval, the five reactors used for that sampling time were removed from the photobench. To account for evaporation, the solutions were poured into 250 ml glass graduated cylinders and the volumes were adjusted to 200 ml. A 100 ml sample was then withdrawn and prepared for extraction and compound analysis.

Effect of substrate mixtures

To investigate the possibility of PNA compounds acting as sensitizers in photolysis reactions (Foote 1968), sample mixtures combining anthracene, acridine, and quinoline, buffered to pH 7, were examined both with dye (2 mg/l methylene blue) and without dye. Due to the volatility of naphthalene and the long photolysis time necessary when using a mixture of compounds, naphthalene was omitted.

Samples were prepared using a 1 percent acetonitrile co-solvent and the same chemical concentrations as in previous photolysis experiments: anthracene (1.0 mg/l), acridine and quinoline (5.0 mg/l).

Effect of initial substrate concentrations

The effect of initial substrate concentration on the rate of photolysis reactions was investigated using anthracene and acridine as the photosensitive substrates. The change in the rate of photodegradation was determined by analyzing the reaction rates of five initial substrate concentrations. The photooxidation of anthracene as a function of initial substrate concentration was analyzed using concentrations of 0.5, 1.0, 2.0, 5.0, and 10.0 mg/l, while the initial concentrations of acridine used were 1.0, 2.0, 5.0, 10.0, and 15.0 mg/l.

In this study phase, methylene blue concentration and pH conditions used were those determined to be optimal in initial experiments. Anthracene was examined using 2 mg/l methylene blue buffered to pH 7 and with no methylene blue present at pH 9. Acridine was subjected to photolysis conditions of 2 mg/l of methylene blue in a pH 5 solution.

Actinometry

Artificial light sources may fluctuate during operation and deteriorate with age making analysis of light output essential. A tryptophan-methylene blue actinometer was utilized to monitor light intensity at the maximum absorbing wavelengths of methylene blue (570 nm to 700 nm) (Figure 6). Methylene blue absorbs visible light energy, sensitizes the photodegradation of tryptophan, and produces a tryptophan decomposition rate directly proportional to the light intensity output of the lamps. The disappearance of tryptophan was measured on a Beckman DU UV Spectrophotometer at 280 nm.

The effective path length of light through the actinometer was adjusted by changing the depth of the actinometer solution, as well as the concentration of methylene blue in the reactor. This adjustment was made to ensure that all of the impinging light was absorbed through the entire solution depth so corrections for light transmitted and/or for the light reflected back from the bottom of the reactor were not necessary.

After initial tests, concentrations of 3 mg/l methylene blue and 20 mg/l tryptophan were chosen for actinometer conditions. A volume of 450 ml was

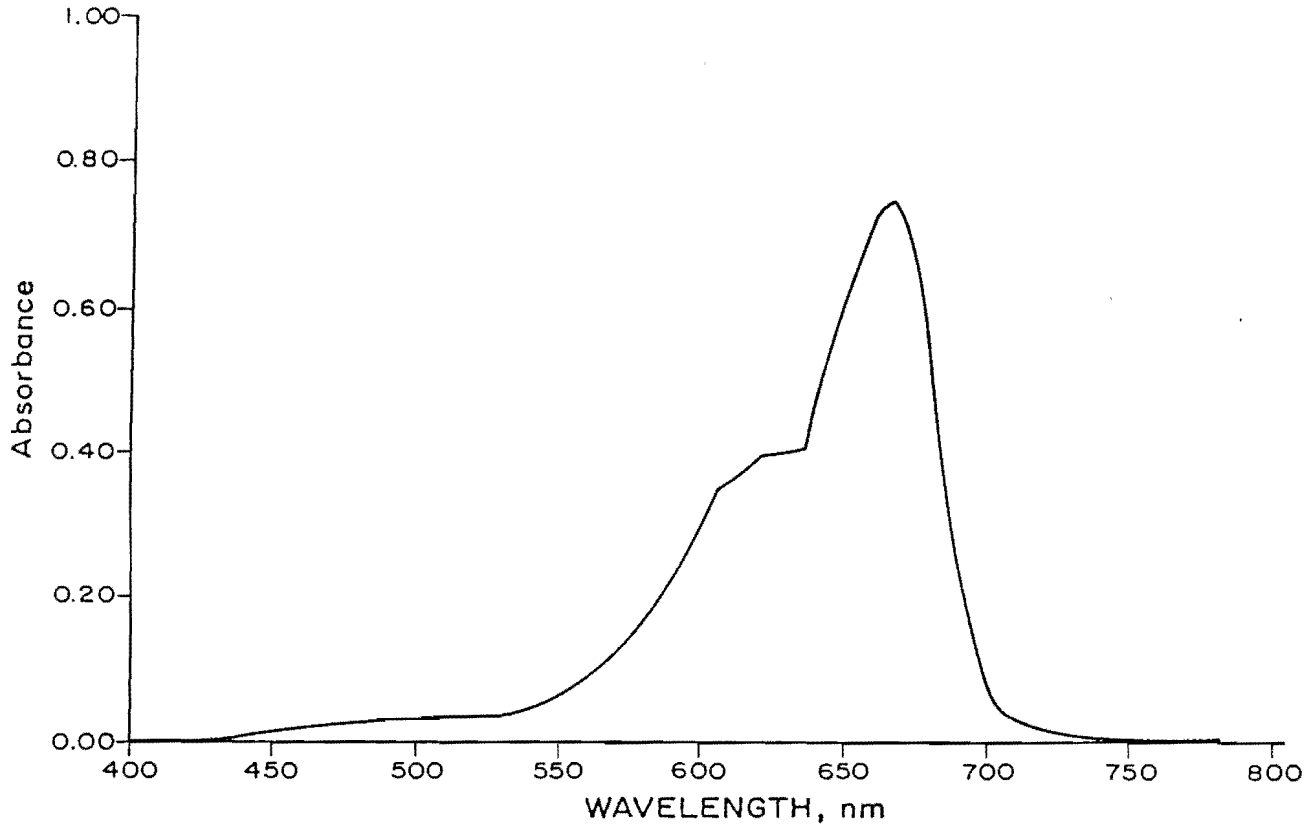

Figure 6. Absorbance spectrum for a 3 mg/1 methylene blue solution.

selected to provide a solution depth of 5 cm in the reaction beakers.

An actinometer was prepared prior to the start of each experimental analysis. A 20 mg/1 solution of tryptophan was buffered to pH 9 using a bicarbonate-carbonate buffer (Table 4). The solution (450 ml) was poured into a reaction beaker identical to the vessels used for the photolysis experiments. Methylene blue as added to a concentration of 3 mg/1. Before placing the actinometer under the photolamps, the initial absorbance of tryptophan was measured on the UV spectrophotometer. The absorbance was converted to initial concentration from a concentration/absorbance curve previously developed for varying concentrations of tryptophan in buffered 3 mg/1 methylene blue solutions.

A glass plate was placed over the reactor to simulate the same experimental conditions used in sample photolysis reactions. The reactor was placed under the lamps and the sensitized photooxidation reaction was allowed to proceed for 15 minutes. The reaction was then terminated since photo products formed began to interfere with absorbance readings. The reactor was removed from the lamps and the absorbance of tryptophan was measured. The number of moles of tryptophan photo degraded in 15 minutes is directly proportional to the intensity of the lamps at the maximum absorbing wavelengths of methylene blue. Lamp intensity was calculated using Equation 10.

$$I_o = \frac{\Delta CVNc}{\phi_a t A \lambda} \qquad (10)$$

where

I_o = incident light intensity, W/m^2

c = speed of light, 3 x 10^{10} cm/sec

λ = median wavelength, 6500 x 10^{-8} cm

A = surface area of solutions exposed to light, cm^2

Extractions Procedure

Extractions were performed using a 100 ml aliquot of sample from the 200 ml photolyzed sample. Federal Register, Method 610 (Federal Register 1979) was followed for the extraction procedure with all volumes decreased by a factor of 10 to accommodate a smaller sample size.

The 250 ml separatory funnels used in the extraction procedures were acid washed with a 10 percent sulfuric acid solution prior to each use. The 100 ml sample was poured from the sampling beaker into a separatory funnel, the beaker was rinsed with 6 ml of HPLC grade methylene chloride, and the rinsings were added to the contents of the funnel. The separatory funnel was shaken for 2 minutes and the solutions allowed to separate for 10 minutes. After solvent separation was complete, the methylene chloride layer was removed from the bottom of the funnel and collected in a 25 ml glass graduated cylinder. To prevent evaporation during the procedure, the cylinders were covered with aluminum foil.

After the extract was removed, another 6 ml of methylene chloride was added to the contents of the funnel and the extraction procedure was repeated twice. The volume of methylene chloride extract collected in the graduated cylinder was recorded to the nearest 0.5 ml. A concentration factor was calculated for each sample based on the volume of extract collected, e.g., 15 ml of extract from a 100 ml sample has been concentrated 6.67 times. Five ml glass sample vials, with teflon lined screw caps, were rinsed with the extract, filled, and labeled with the appropriate sample number. All samples were stored in the dark at -70°C until analyzed via gas chromatography.

Constituent Analysis

Disappearance of substrate was monitored using a Hewlett-Packard 5880A gas chromatograph with a Model 7672A automatic liquid sampler. A 6 ft x 2 mm (ID) glass column packed with 3 percent SP-2250 on 100/120 Supelcoport was used for compound separation. Chromatographic conditions for acridine, anthracene, and quinoline were as follows: injector port temperature 225°C, oven temperature 200°C (isothermal), detector temperature 250°C, and nitrogen carrier gas flow rate 30 ml/min. A flame ionization detector was used for compound identification.

Naphthalene was analyzed using the same isothermal chromatographic conditions except the oven temperature was lowered to 180°C to separate it from the solvent peak.

External standard calibration procedures were used for each compound. Standards were prepared in the same manner as the photolysis samples, using a 1 percent acetonitrile co-solvent. Standards were extracted using methylene chloride as per the extraction procedure previously described.

Toxicity Testing

Sunlight has been shown to increase the toxicity of water soluble components of refined petroleum products to fish (Scheier and Gominger 1976) and algae (Larson et al. 1979). To determine if the photoproducts from the oxidation of each compound were actually more toxic than the parent compound, each test mixture containing dye and PNA compound was analyzed for toxicity. Toxicity experiments were performed by a qualified laboratory technician utilizing a Beckman Microtox™ Toxicity Analysis system. In the Microtox™ system

lyophilized marine luminescent bacteria, a strain of Photobacterim phosphoreum, are re-hydrated and used as the test organisms for a rapid (5 to 30 minutes) determination of acute toxicity. Light output of phosphorescent bacteria exposed to a range of toxicant concentrations is used to develop an LC_{50} based on light output rather than mortality as the index of toxic response.

The primary advantages of the Microtox™ system as an acute toxicity test are its relatively short duration, as compared to 48 hours for Daphnia or fathead minnow standard EPA-approved tests, and the fact that the test organisms are cultured by one lab (Beckman) which, in theory, should reduce response variability.

Separate experimental runs were performed for the toxicity analysis. Two organic compounds, acridine in a solution of 2 mg/l methylene blue and pH 5, and anthracene without dye at pH 9 with 2 mg/l methylene blue at a pH of 7, were used as photooxidation substrates for toxicity experiments. For each toxicity experiment, the optimum photooxidation condition for individual compounds was used. Samples were taken prior to analysis, at one-half the run time, and after photolysis.

Statistical Analysis

Statistical analysis of the photolysis data was performed using analysis of variance (ANOVA) and Duncan's New Multiple Range Test. The analysis of variance test was performed to determine if a difference in treatment effectiveness existed between the rate constants and quantum yields obtained. The data were divided into two sets. The first set was used to examine the rate constants and quantum yield values from triplicate analyses at a constant methylene blue concentration to determine the rate constant and yield dependency on pH. The second set was used to analyze the rate constant and yield of each pH level, to determine the dependency of the photolysis rate and quantum yield on the concentration of methylene blue. The result of an ANOVA was a calculated F value which was applied to the homogeneity of variance analysis. The F value was compared with the tabulated critical value for F. If the calculated F from the ANOVA was greater than or equal to the critical value, then the variance of the samples was significantly different from each other indicating that a change in pH and/or dye condition did affect the rate of photodegradation.

The second statistical treatment of the data sets was performed using Duncan's New Multiple Range Test, a technique for identifying which rate constants and quantum yields were significantly different. This analysis was applied if a difference in the sample values had been identified using ANOVA analysis. Duncan's test identifies the statistical equality and difference between a set of mean values. It operates on the basis that the probability of equality decreases as the number of means under testing increases (Steel and Torrie 1980). Optimum pH and dye concentration conditions for the photodegradation of individual compounds were selected based on the results of Duncan's test.

EXAMPLE CALCULATIONS

The photolysis experiment involving anthracene in a solution containing 5 mg/l methylene blue and buffered to pH 9 was selected as an example to demonstrate the calculation methods and procedures used throughout this study. The photolysis data from this experiment is shown in Table 6. Table 7 contains pertinent information utilized in the analysis of both the actinometer and anthracene photolysis data.

Substrate Reaction Rate Constants

The first order reaction rate constant based on the disappearance of anthracene was determined to be 0.0973 $hour^{-1}$. The first order rate constant, k^c, was converted to an initial rate constant, K^c, for calculation of the overall quantum yield using Equation 11.

$$K^c = k^c(sec^{-1}) \times [An]\ (mole/liter) \times Volume\ (liters) \qquad (11)$$

Substituting values from Table 7 into Equation 11:

$$K^c = \frac{0.0973}{hour} \times \frac{1\ hour}{3600\ sec} \times 5.62 \times 10^{-6}\ \frac{mole}{liter} \times 0.20\ liter = 3.04 \times 10^{-11}\ \frac{mole}{sec} \qquad (12)$$

Actinometry

During the development of the tryptophan-methylene blue actinometer, sufficient photolysis time studies were performed to establish the photooxidation of tryptophan as a first order reaction, subsequently, only the initial and final tryptophan concentrations were recorded and used to determine the rate of reaction. The actinometer was run in conjunction with photolysis experiments to determine the amount of tryptophan degraded, which is the basis for calculations involving light intensity, light energy, and quantum yields.

Actinometer reaction rate constants

The first order reaction rate constant based on the disappearance of 2.5 mg/l tryptophan during 15 minutes of irradiation was 0.4741 $hour^{-1}$. Conversion of this rate, k^a, to an initial rate constant, K^a, was done using Equation 13.

$$K^a = k^a\ (sec^{-1}) \times [Trp]\ (mole/liter) \times Volume\ (liters) \qquad (13)$$

Substituting data from Table 7 into Equation 13:

$$K^a = \frac{0.4741}{hour} \times \frac{1\ hour}{3600\ sec} \times 9.79 \times 10^{-5}\ \frac{mole}{liter} \times 0.45\ liter = 5.80 \times 10^{-9}\ \frac{mole}{sec} \qquad (14)$$

Light energy

The light energy emitted from experimental lamps was calculated using Equation 9.

$$\text{Light energy} = \frac{\Delta CVN}{\phi_a t} \qquad (9)$$

Table 6. Photolysis data from the experiment involving anthracene with 5 mg/l methylene blue and buffered to pH 9; Run 2.

Time (hours)	Anthracene Concentration (mg/l)	In C/C_o
0	1.37	0.00
4	0.92	-0.40
8	0.65	-0.75
12	0.42	-1.18
24	0.00	

Table 7. Photolysis data representing experimental conditions and results for the example photolysis run.

ACTINOMETER	
Substrate photolyzed	Tryptophan
Methylene blue concentration	3 mg/l
Reaction pH	9
Initial substrate concentration	22.37 mg/l (9.79×10^{-5} mole/liter)
Final substrate concentration	19.87 mg/l (8.58×10^{-5} mole/liter)
Amount of Tryptophan degraded	2.5 mg/l (1.21×10^{-5} mole/liter)
First order rate equation	$y = -0.4741x + 0.00$
Solution volume	450 ml
Solution depth	5 cm
PHOTOLYSIS EXPERIMENT	
Substrate photolyzed	Anthracene
Methylene blue concentration	5 mg/l
Reaction pH	9
Initial substrate concentration	1.37 mg/l (5.62×10^{-6} mole liter)
First order rate equation	$y = -0.0973x + 0.001$
Solution volume	200 ml
Solution depth	2 cm

where the terms have previously been described.

Substituting the actinometer data from this run:

$$\text{Light energy} = 1.21 \times 10^{-5} \frac{\text{mole}}{\text{liter}} \times 0.45 \text{ liter} \times 6.023 \times 10^{23} \frac{\text{photons}}{\text{einstein}} \times \frac{1 \text{ einstein}}{\text{mole}} \times \frac{1}{900 \text{ sec}} = 3.64 \times 10^{15} \frac{\text{photons}}{\text{sec}} \quad (15)$$

Average incident light intensity

Incident light intensity was calculated using Equation 10.

$$I_o = \left(\frac{\Delta CVN}{\phi_a t}\right)\left(\frac{C}{A\lambda}\right) \quad (10)$$

Light intensity for this experimental run was found to be 0.084 $W/m^2/nm$ as shown in Equation 16.

$$I_o = \left(3.64 \times 10^{15} \frac{\text{photons}}{\text{secs}}\right) \times \left(\frac{3 \times 10^{10} \text{ cm/sec}}{133 \text{ cm}^2 \times 6500 \times 10^{-8} \text{ cm}}\right) \times 6.627 \times 10^{-27} \frac{\text{erg-sec}}{\text{photon}} \times \frac{1 \text{ Joule}}{10^7 \text{ erg}} \times \frac{10^2 \text{cm}^2}{\text{m}^2} \times \frac{1 \text{ Watt}}{1 \text{ Joule}} = 0.084 \text{ W/m}^2 \quad (16)$$

Actinometer correction factor

The sensitizer used for initiating photooxidation reactions in the actinometer was the same sensitizer used in the photolysis experiments. However, the actinometer and photolysis samples differed in volume and methylene blue concentration which affected the amount of light absorbed by each solution. To correct for the difference in absorbance, the percent of absorbed light, based on depth of solution and dye concentration, was calculated using the Beer-Lambert Law. Table 8 presents the absorbance and solution depth data utilized in calculating the percent of light absorbed by the photolyzed samples and actinometer.

A correction factor, C_a, was developed to normalize the absorbance of the photolysis samples to the actinometer. The anthracene example containing 5 mg/l methylene blue in a solution 2 cm deep absorbed 90 percent of incident light intensity. The actinometer contained 3 mg/l methylene blue in a solution 5 cm deep which absorbed 98 percent of the incident light intensity. The correction factor, C_a, for this example was 0.98/0.90 and was included in the calculations for quantum yield to normalize results to the actinometer.

Quantum yield

The overall reaction quantum yield was calculated using Equation 17.

$$\phi_{rxn} = \frac{K^c}{K^a} \phi_a C_a \quad (17)$$

Using data previously calculated:

$$\phi_{rxn} = \frac{3.04 \times 10^{-11} \text{ mole/sec}}{5.80 \times 10^{-9} \text{ mole/sec}} \left(\frac{1 \text{ mole}}{\text{einstein}}\right)\left(\frac{0.98}{0.90}\right) = 0.0057 \frac{\text{mole}}{\text{einstein}} \quad (18)$$

Table 8. Percent light absorbed in solutions of varying depth and methylene blue concentration.

Methylene Blue Concentration (mg/l)	Average Absorbance 1 cm cell 560 to 700 nm	Solution Depth cm	% Light Absorbed
1	0.096	2	36
2	0.194	2	59
3	0.346	5	98
5	0.499	2	90
10	0.980	2	100

RESULTS

This investigation, among others (Sargent and Sanks 1974, 1976 and Bulla and Edgerley 1968) has shown the reaction rates from sensitized photooxidations to be a function of several process parameters, i.e., pH, sensitizer concentration, light intensity and dissolved oxygen concentration. First order rate kinetics are commonly used, however, for reaction description under a given set of reaction conditions, as done in this analysis.

Kinetic reaction rate constants were calculated for each experiment based on the disappearance of the parent compound. The data were fitted to a first-order kinetics equation, i.e., natural logarithm of the fraction of substrate remaining as a function of time. Reaction rates were taken as the negative slope of the linear form of the first order equation.

The first order rate constants were used to compare results of various treatments studied in order to establish optimum conditions for photolysis, to evaluate the effect of initial substrate concentration and the effect of combining substrates on photolysis, and to calculate reaction quantum yields and half-lives of the organic compounds under investigation.

For aid in evaluating the effectiveness of a given treatment condition, the efficiency of a photochemical reaction, represented by the reaction quantum yield, ϕ_{rxn}, was calculated for each dye sensitized photooxidation experiment and is presented along with the observed first order reaction rate constants. The quantum yield, given as the number of moles of substrate reacted per mole of photons (einstein) absorbed, is a measure of the efficiency of utilization of the light energy absorbed by the system. The efficiency of the photooxidation reaction depends upon the rate of reaction relative to the rates of all processes leading to the deactivation of the excited state.

Triplicate analyses of each experiment were performed for statistical relevance. Chauvenet's Criterion (U.S. EPA 1978) was applied to the data to identify outliers. No data fit the criterion so all observed rate constants and reaction quantum yields were used in further statistical analyses. For clarity, the calculated means for the triplicate analyses are presented. The supporting data for the mean values of the rate constants and quantum yields are contained in Appendix A and B, respectively. For the statistical analyses see Appendix C of Naeger (1985).

Optimum Reaction Conditions

To determine optimum conditions for the photooxidation of each compound, the effects of pH and methylene blue concentration on observed reaction rates were examined. A comparison of treatment conditions was based on the magnitude of the first order reaction rate constant, i.e., the greater the rate constant, the more effective the treatment condition. The same comparison was performed with the obtained quantum yields as a means of supporting the selection of optimum treatment conditions for each compound.

Acridine

Sensitized photooxidation rate constants for acridine are shown in Table 9. Initial experiments were used

Table 9. First order kinetic decay constants (1/hour) for the photolysis of 5 mg/l aqueous solutions of acridine.

pH	Reaction Rate Constants (1/hour) Methylene Blue Concentrations, mg/l				
	10	5	2	1	0
3		0.0609 (±0.0343)*	0.0582 (±0.0297)	0.0233 (±0.0098)	0.0303 (±0.0703)
5		0.0824 (±0.1552)	0.1321 (±0.1009)	0.1293 (±0.0350)	0.0656 (±0.0539)
7	0.0174 (±0.0158)	0.0194 (±0.0087)	0.0157 (±0.0020)		0.0132 (±0.0116)
9	0.0032 (±0.0056)	0.0048 (±0.0039)	0.0030 (±0.0096)		0.0070 (±0.0011)
11	0.0087 (±0.0074)	0.0092 (±0.0105)	0.0037 (±0.0021)		0.0060 (±0.0122)

*Numbers in parentheses represent 95 percent confidence intervals.

to evaluate the photoosensitization of acridine with 2 and 5 mg/l methylene blue. In solutions buffered at pH 3 and pH 5, the rate of acridine decay was greater than in neutral and basic solutions. At a 95 percent confidence level, there was no significant difference in the degree of treatment in pH 3 solutions containing 2 or 5 mg/l methylene blue. There was, however, significantly better acridine removal, based on a greater reaction rate, using a lower dye concentration of 2 mg/l in pH 5 solutions. A lower dye concentration, 1 mg/l methylene blue, was analyzed in acidic solutions in further acridine tests. Since the rate of disappearance of acridine increased in pH 7, 9, and 11 solutions when the dye concentration increased from 2 to 5 mg/l, a higher concentration of methylene blue was investigated under basic conditions.

The photooxidation rate of acridine as a function of pH for each methylene blue concentration examined is shown in Figure 7. When 5 mg/l solutions of acridine were photolyzed, the rate of photolysis was dependent on reaction pH for each dye concentration examined. In solutions containing no dye, reaction rates were greatest when the solution was buffered to pH 5, while all other pH levels exhibited a statistically equal degree of acridine removal. When methylene blue was present as a sensitizer in concentrations of 1, 2, or 5 mg/l, pH 5 solutions produced the most effective removal of the substrate. The highest dye concentration used, 10 mg/l methylene blue, was applied only to pH 7, 9, and 11 solutions. The rate of acridine removal was statistically greater in solutions buffered to pH 7 than the other pH levels under these conditions.

Photooxidation rates as a function of methylene blue are shown in Figure 8 for each pH level analyzed. Unlike the dependency of rate constants on the pH for a given methylene blue concentration, the rate of removal of acridine was independent of methylene blue concentration, for samples photolyzed in solutions of pH 5, 7, 9, and 11, owing to the spread of the calculated rate constant values within the 95 percent confidence intervals. However, in solutions buffered to pH 3, a dependency on the concentration of methylene blue was shown. A greater treatment efficiency was exhibited in solutions containing 2 and 5 mg/l dye at pH 3 than solutions at the same reaction pH with 0 and 1 mg/l methylene blue.

Reaction quantum yields for the sensitized photolysis of acridine are shown in Table 10. The efficiency of the sensitized photochemical reaction based on quantum yields closely paralleled the magnitudes of the reaction rate constants in that the higher rate constants were observed in solutions with the most efficient utilization of absorbed light energy.

Reaction quantum yields as a function of pH obtained for the photolysis of acridine are shown in Figure 9. Similar to the dependency of the rate constants on reaction pH, the quantum yield was dependent on pH for all dye concentrations examined. At methylene blue concentrations of 1, 2, and 5 mg/l, pH 5 solutions achieved the highest quantum yield. In solutions containing 10 mg/l dye, solutions with a reaction pH of 7 were statistically more efficient at utilizing the absorbed light energy, at the 95 percent confidence level, than solutions buffered to pH 9 or 11.

The dependency of the reaction quantum yield on the concentration of methylene blue is shown in Figure 10. The quantum yields were independent of methylene blue concentration at all pH levels examined except pH 5 when the quantum yield observed in 1 mg/l dye solutions was significantly higher than the efficiency achieved in 2 mg/l solutions. At a 95 percent confidence level, solutions containing either 1 or 2 mg/l methylene blue achieved a higher quantum yield than solutions containing 5 mg/l.

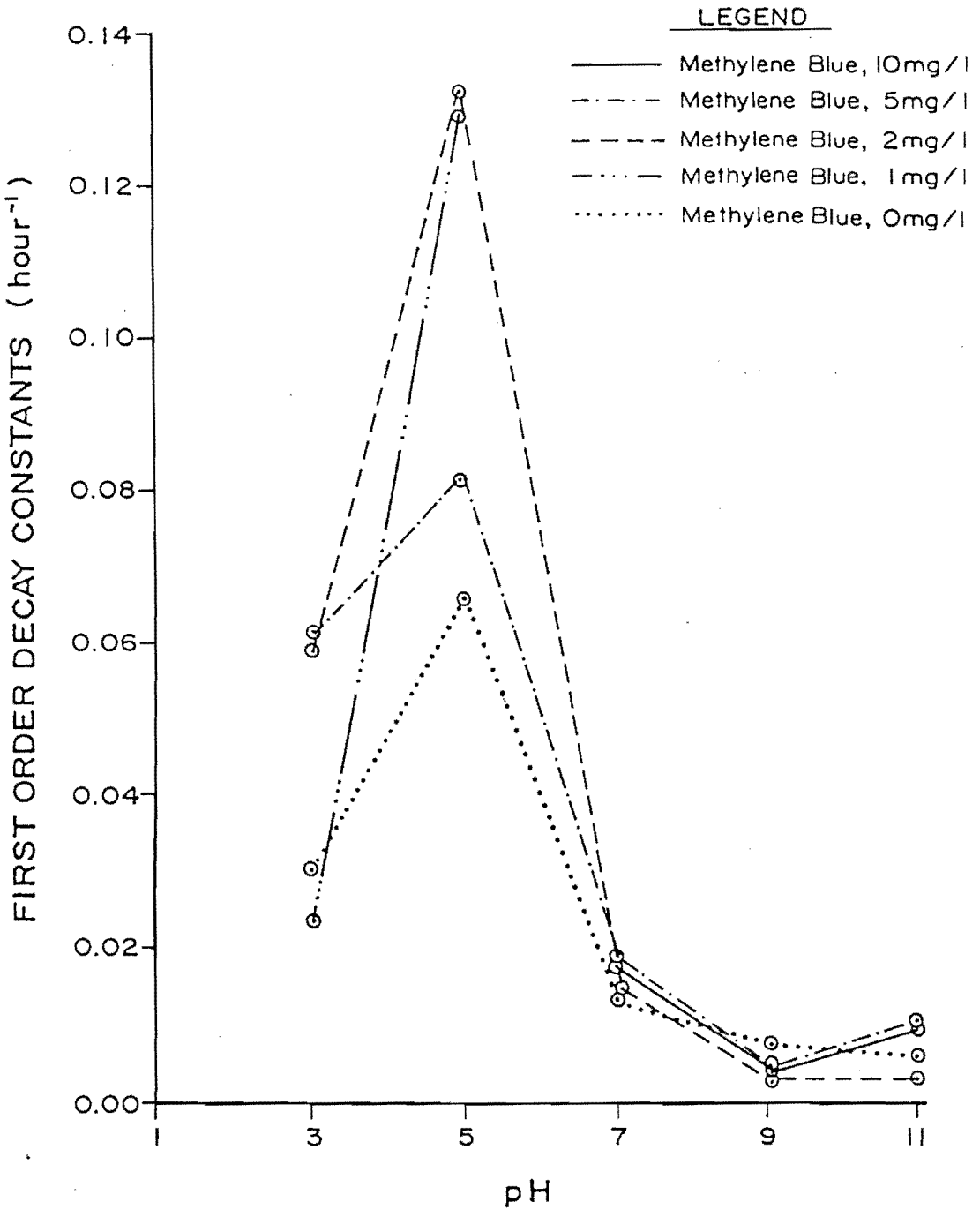

Figure 7. First order kinetic decay constants for the photolysis of 5 mg/l acridine solutions as a function of pH; comparison of methylene blue concentrations of 10, 5, 2, 1, and 0 mg/l.

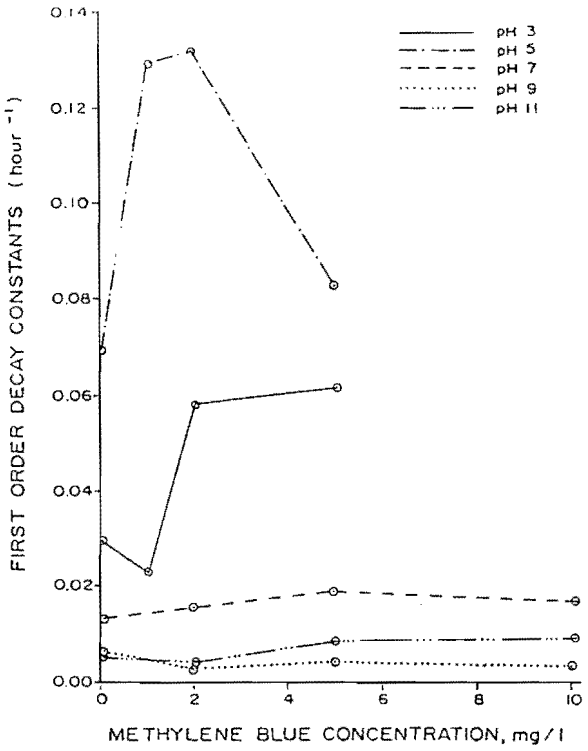

Figure 8. First order kinetic decay constants for the photolysis of 5 mg/l acridine solutions as a function of methylene blue concentration; comparison of pH 3, 5, 7, 9, and 11.

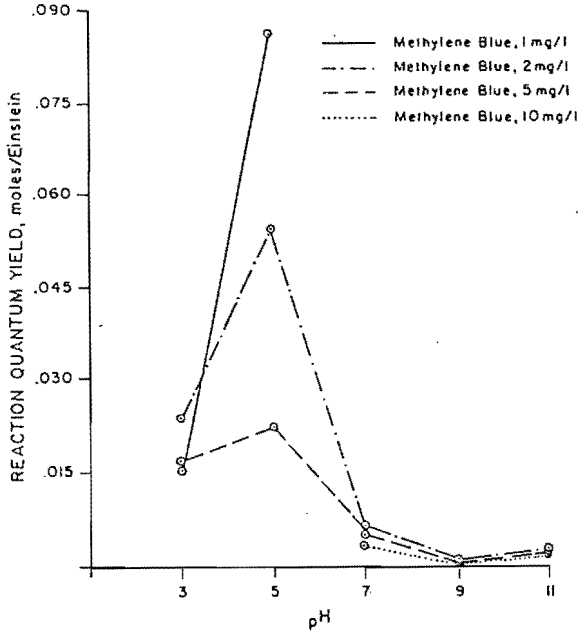

Figure 9. Reaction quantum yields for the photolysis of 5 mg/l acridine solutions as a function of pH; comparison of methylene blue concentrations of 10, 5, 2, and 1 mg/l.

Table 10. Reaction quantum yields (moles/einstein) for the photolysis of 5 mg/l aqueous solutions of acridine.

pH	Reaction Quantum Yields (moles/einstein) Methylene Blue Concentrations, mg/l			
	10	5	2	1
3		0.0165) (±0.0160)*	0.0241 (±0.0106)	0.0156 (±0.0101)
5		0.0221 (±0.0384)	0.0548 (±0.0400)	0.0866 (±0.0447)
7	0.0042 (±0.0043)	0.0051 (±0.0043)	0.0066 (±0.0014)	
9	0.0008 (±0.0015)	0.0013 (±0.0011)	0.0014 (±0.0038)	
11	0.0021 (±0.0021)	0.0025 (±0.0034)	0.0016 (±0.0010)	

*Numbers in parentheses represent 95 percent confidence intervals.

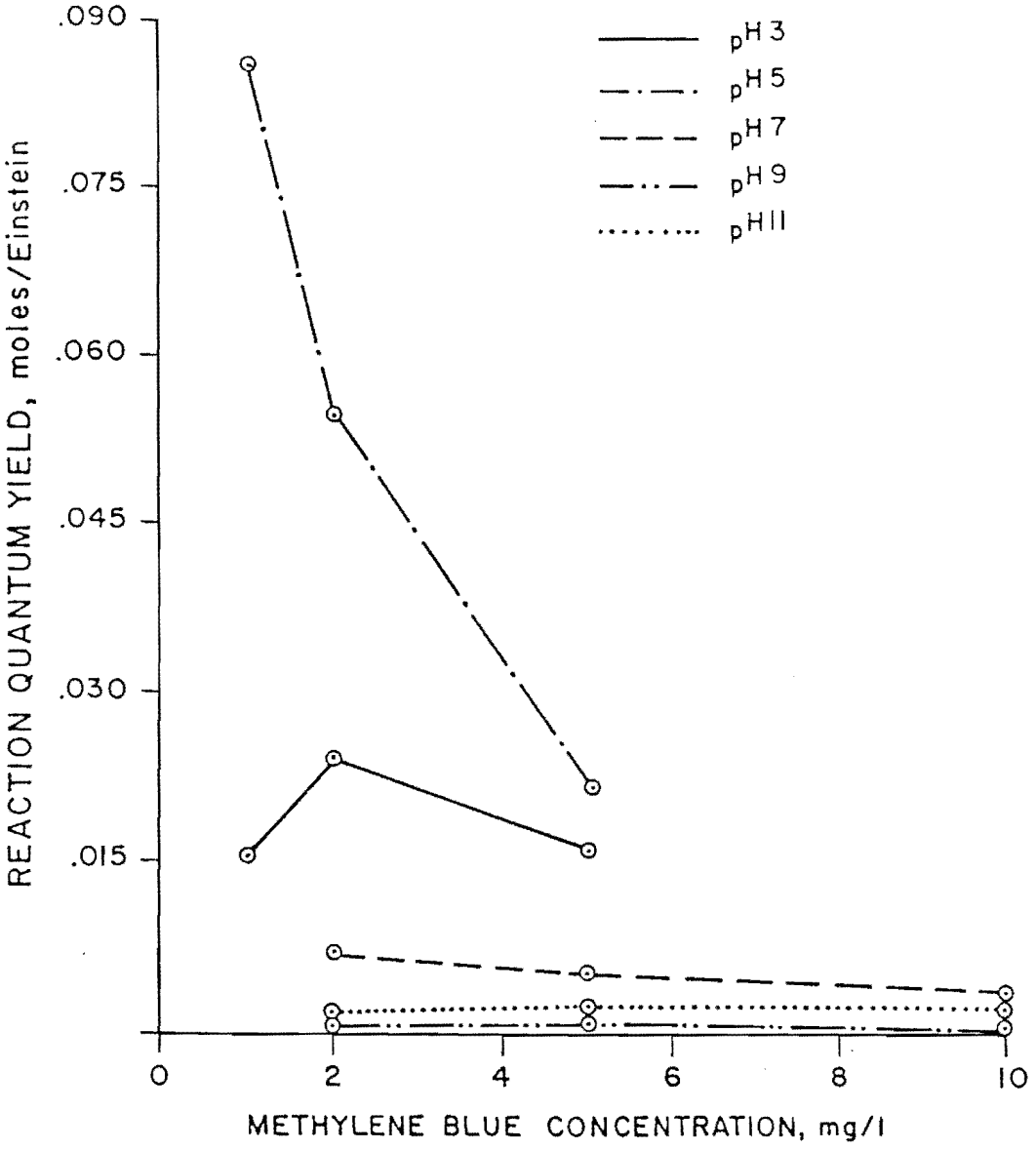

Figure 10. Reaction quantum yields for the photolysis of 5 mg/l acridine solutions as a function of methylene blue concentration; comparison of pH 3, 5, 7, 9, and 11.

Treatment efficiencies for the removal of acridine are shown in Table 11. The values represent the percent of acridine photooxidized in a 48-hour period. Optimum reaction conditions occurred in solutions buffered to pH 5 regardless of sensitizer concentration.

To identify the optimum conditions for acridine photodegradation, the entire data set was statistically evaluated using Duncan's New Multiple Range Test. The data divided into four groups, and examination of Figures 7 and 8 qualitatively confirm the results of this analysis. Table 12 is a representation of the statistical equality among reaction rate constants determined for the entire acridine data set. Rate constants contained within the same shaded areas were found to be statistically equal; the darker the shading, the more efficient the treatment.

Solutions at pH 5 with 1 and 2 mg/l methylene blue provided the optimum treatment conditions for the photodegradation of acridine. Samples treated with no dye and with 5 mg/l methylene blue, both at a pH of 5, were statistically equal to samples containing 2 or 5 mg/l methylene blue buffered to pH 3. The least efficient conditions were pH 3 samples with 1 mg/l methylene blue along with all samples buffered at pH 7, 9, and 11 at any dye concentration.

The same statistical comparison was made using the entire data set of reaction quantum yields observed for the photolysis of acridine. The results are shown in Table 13. Quantum yield values within the same shaded areas were found to be statistically equal; the darker the shading the more efficient the utilization of absorbed light energy, leading to a higher quantum yield. The entire data set of quantum yield values was examined since the term quantifies not only the rate of substrate decay but also the amount of light energy absorbed to achieve the given rate of decay. The quantum yield accurately represented the efficiency of each photochemical reaction which occurred, and supported the differences found among treatment conditions based on rate constants.

By including the quantum yields as a parameter for selecting optimum treatment conditions for acridine photooxidations, differences are more clearly defined. Based on reaction rate constants, the optimum process conditions for the removal of acridine occurred in solutions at pH 5 with either 2 or 1 mg/l methylene blue. Although there was no significant difference between two rate constants at the optimal level, there was a significant difference, at the 95 percent confidence level, between the reaction quantum yields. Solutions buffered to

Table 11. Comparison of treatment efficiencies (%) for the photooxidation of 5 mg/l solutions of acridine during a 48 hour photolysis period.

pH	Methylene Blue Concentration, mg/l				
	10	5	2	1	0
3		96.0	95.8	78.5	88.2
5		99.9	99.7	100.0	96.1
7	58.8	56.6	57.3		36.9
9	14.3	21.3	14.4		29.2
11	35.8	26.0	16.8		27.4

Table 12. Shaded representation of statistical equality among the observed reaction rate constants for the photolysis of acridine.

REACTION RATE CONSTANTS, 1/hour

pH	Methylene Blue Concentration, mg/l: 10	5	2	1	0
3		0.0609	0.0582	0.0233	0.0303
5		0.0824	0.1321	0.1293	0.0656
7	0.0174	0.0194	0.0157		0.0132
9	0.0032	0.0048	0.0030		0.0070
11	0.0087	0.0092	0.0037		0.0060

Table 13. Shaded representation of statistical equality among the observed reaction quantum yields for the sensitized photolysis of acridine.

REACTION QUANTUM YIELDS, moles/Einstein

pH	Methylene Blue Concentration, mg/l: 10	5	2	1
3		0.0165	0.0241	0.0156
5		0.0221	0.0548	0.0866
7	0.0042	0.0051	0.0066	
9	0.0008	0.0013	0.0014	
11	0.0021	0.0025	0.0016	

pH 5 and containing 1 mg/l methylene blue were significantly better at utilizing absorbed light energy than the solutions containing 2 mg/l methylene blue. Therefore, the optimum treatment condition for the removal of acridine would be in solutions at pH 5, which exhibited the highest photochemical efficiency.

Anthracene

First order kinetic decay rate constants for the photolysis of 1 mg/l solutions of anthracene are shown in Table 14. The samples containing no dye resulted in photolysis at least an order of magnitude higher than those samples containing dye.

Photolysis rates as a function of reaction pH for the degradation of anthracene are shown in Figure 11. Only at a methylene blue concentration of 2 mg/l was the resultant rate constant independent of reaction pH. At a dye concentration of 5 mg/l, the reaction rate was dependent on solution pH, with a reaction pH of 7 being significantly better at the 95 percent confidence level than other pH conditions at this dye concentration.

In the absence of methylene blue, the reaction rate was dependent on the reaction pH over the entire pH range studied, increasing as the pH increased to pH 9, after which the reaction rate decreased slightly.

Anthracene reaction rates as a function of methylene blue concentration are shown in Figure 12. The rate of anthracene photolysis was significantly better when no dye was present in the test solutions. In the sensitized photooxidation process, there was no significant difference in reaction rates

Table 14. First order kinetic decay constants (1/hour) for the photooxidation of 1 mg/l solutions of anthracene.

pH	Reaction Rate Constants (1/hour) Methylene Blue Concentrations, mg/l		
	5	2	0
3	0.0424 (±0.0673)*	0.0552 (±0.0220)	0.5207 (±0.3116)
5	0.0796 (±0.1109)	0.0661 (±0.0449)	1.0860 (±0.2197)
7	0.1595 (±0.1125)	0.0751 (±0.0474)	1.3486 (±1.1320)
9	0.0601 (±0.0392)	0.0558 (±0.0393)	3.571 (±1.8074)
11	0.0494 (±0.0149)	0.0513 (±0.0093)	2.404 (±0.4203)

*Numbers in parentheses represent 95 percent confidence intervals.

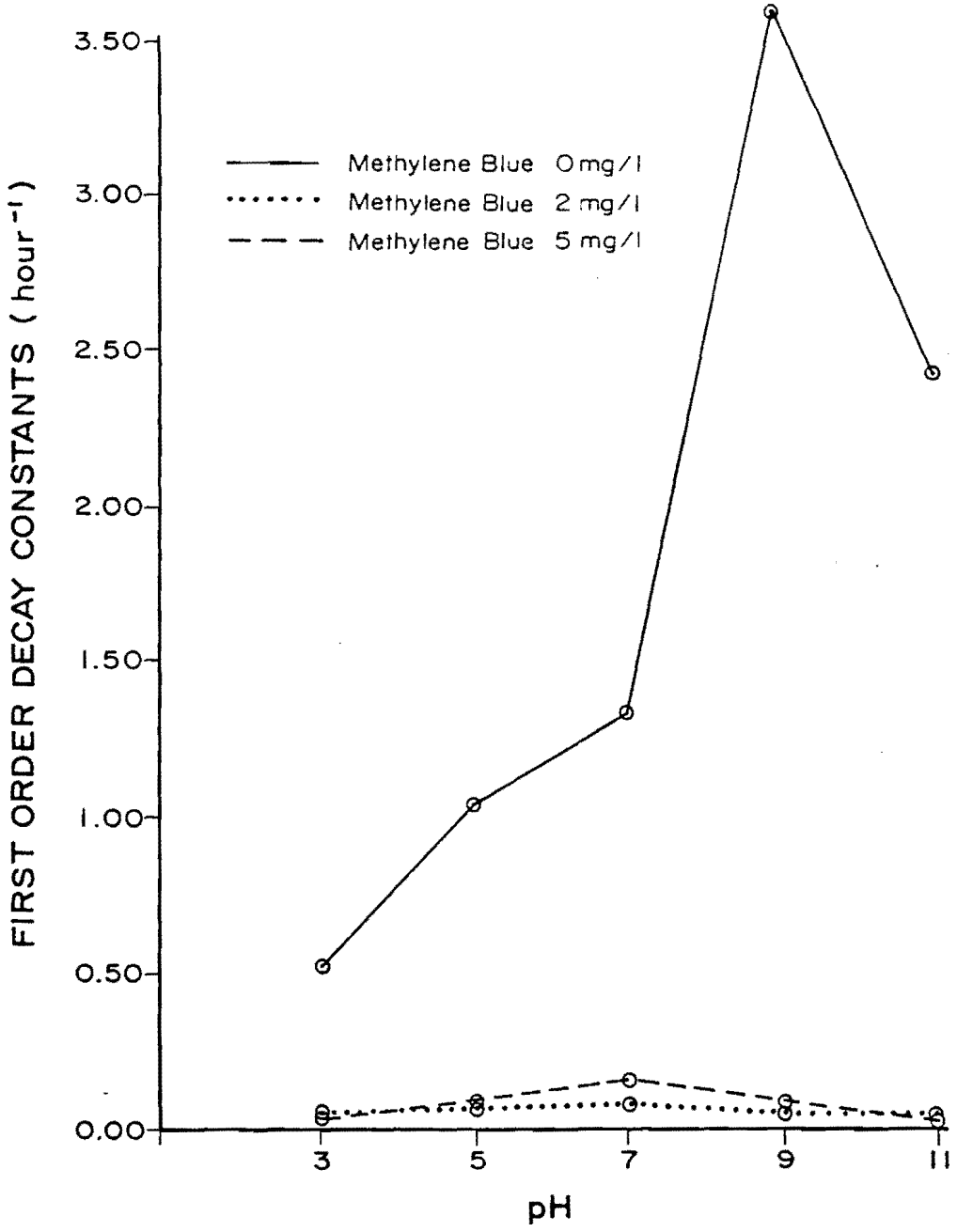

Figure 11. First order kinetic decay constants for the photolysis of 1 mg/l anthracene solutions as a function of pH; comparison of methylene blue concentrations of 5, 2, and 0 mg/l

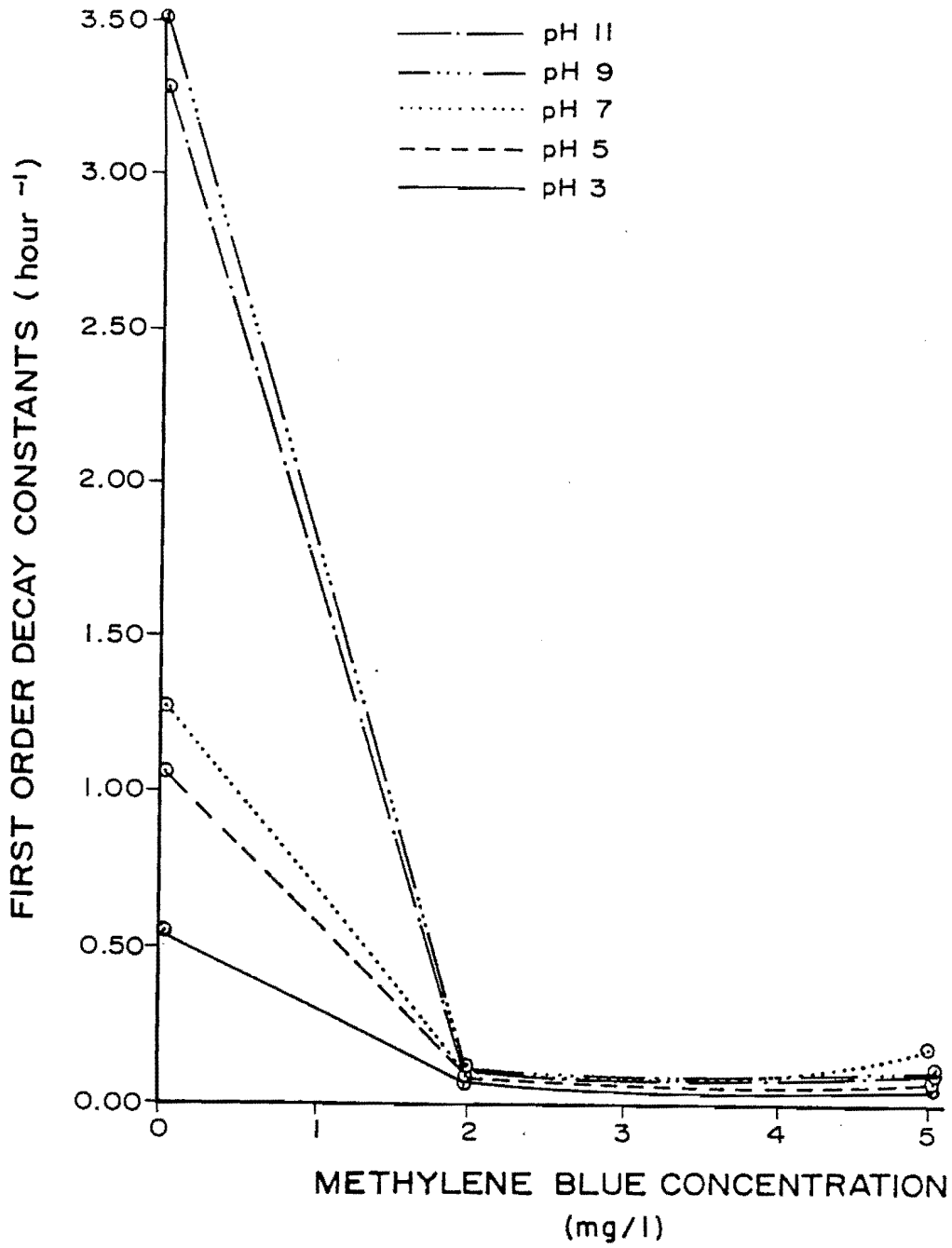

Figure 12. First order kinetic decay constants for the photolysis of 1 mg/l anthracene solutions as a function of methylene blue concentration; comparison of pH 3, 5, 7, 9, and 11.

between solutions containing 2 or 5 mg/l methylene blue, except in pH 7 solutions containing 5 mg/l methylene blue. Further analysis was suspended and research efforts were concentrated on exploring the mechanisms involved in the direct excitation and photodegradation of anthracene.

Treatment efficiencies for anthracene degradation are shown in Table 15. The percent of anthracene removal for sensitized photooxidations was achieved during a 24 hour irradiation period, while the percent removal for the direct photolysis represents a 50 minute irradiation period.

The reaction quantum yields for the sensitized photooxidation of anthracene are shown in Table 16. The optimal sensitized photooxidation conditions established for the degradation of anthracene based on first order reaction rates, and the largest overall quantum yields, occurred in solutions buffered to pH 7.

Figure 13 shows the reaction quantum yields as a function of pH for each dye concentration examined. Similar to the reaction rate analysis results, only at a methylene blue concentration of 2 mg/l was the reaction quantum yield independent of pH. At a dye concentration of 5 mg/l, the quantum yield was dependent on pH with solutions buffered to pH 7 achieving significantly higher quantum yield values at the 5 percent confidence level than other pH conditions.

Neutral pH conditions appeared to be optimal for the removal of anthracene via sensitized photooxidation based on statistical analysis of both reaction rate constants and quantum yields.

Quinoline

The first order kinetic decay constants for the photooxidation of 5 mg/l of quinoline with no dye and in the presence of 5 mg/l methylene blue are shown in Table 17. The standard t-test was applied to the rate constants observed for the photooxidation of quinoline to identify if rate constants were significantly different from zero. Solutions buffered to pH 5 and containing 0 or 5 mg/l methylene blue achieved reaction rates significantly greater than zero. In addition, rate constants observed for pH 3 solutions with no dye, and pH 7 solutions with 5 mg/l dye were significantly greater than zero. All other rate constants were statistically equal to zero, indicating that quinoline was relatively unreactive toward singlet oxygen.

The photodegradation of quinoline as a function of pH is shown in Figure 14. When no dye was present, reaction pH values of 3 and 5 were significantly better, at the 95 percent confidence level, than all other pH conditions tested. In the presence of a sensitizing dye, there was no significant difference in the effectiveness of compound removal at any pH level.

The photooxidation of quinoline was not improved through the use of methylene blue as a sensitizer. Due to the slow reaction rates compared to photolysis rates of acridine and anthracene, no further individual testing of the compound was performed.

The photolysis of 5 mg/l solutions of quinoline over a 72 hour period resulted in low treatment efficiencies (Table 18), compared to those achieved for acridine or anthracene.

In the presence of 5 mg/l methylene blue, there was no significant difference in the photodegradation of quinoline based on first order rates of reaction at any pH level. This same conclusion held true for the reaction quantum yields as shown in Figure 15 when the quantum yields are plotted as a function of pH. Only solutions buffered to pH 5 or 7 achieved quantum yields which were significantly greater than zero. Likewise, the sensitized reaction rates observed for pH 5 and 7 solutions

Table 15. Comparison of treatment efficiencies (%) for the photooxidation of 1 mg/l solutions of anthracene with dye for a 24 hour irradiation period and without dye for a 50 minute irradiation period.

pH	Percent Removal (%) Methylene Blue Concentrations, mg/l 5	2	0
	24 hour photolysis		50 minute photolysis
3	63.4	87.6	48.4
5	81.3	90.2	65.4
7	100.0	95.3	74.2
9	97.3	87.3	100.0
11	94.1	87.7	100.0

Table 16. Reaction quantum yields (moles/einstein) for the photooxidation of 1 mg/l aqueous solutions of anthracene.

pH	Reaction Quantum Yields (moles/einstein) Methylene Blue Concentrations, mg/l 5	2
3	0.0025 (±0.0037)*	0.0059 (±0.0036)
5	0.0053 (±0.0094)	0.0071 (±0.0062)
7	0.0102 (±0.0092)	0.0080 (±0.0062)
9	0.0050 (±0.0019)	0.0058 (±0.0031)
11	0.0031 (±0.0004)	0.0054 (±0.0003)

*Numbers in parentheses represent 95 percent confidence intervals.

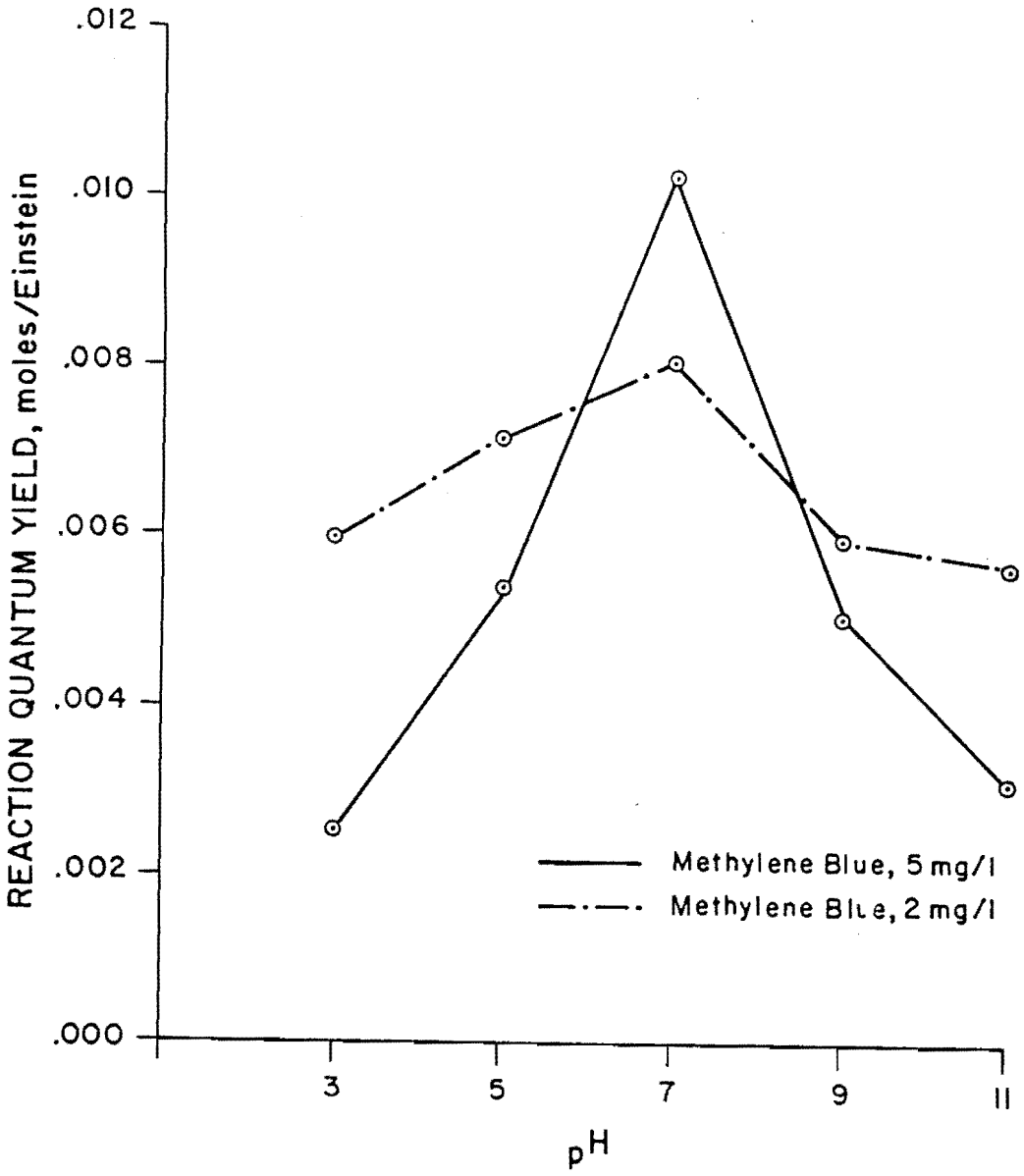

Figure 13. Reaction quantum yields for the photolysis of 1 mg/l anthracene solutions as a function of pH; comparison of methylene blue concentrations of 5 and 2 mg/l.

Table 17. First order kinetic decay constants (1/hour) for the photolysis of 5 mg/1 solutions of quinoline.

pH	Reaction Rate Constants (1/hour) Methylene Blue Concentrations, mg/1	
	5	0
3	0.0037 (±0.0071)*	0.0036 (±0.0016)
5	0.0026 (±0.0020)	0.0034 (±0.0007)
7	0.0022 (±0.0018)	0.0015 (±0.0029)
9	0.0030 (±0.0053)	0.0015 (±0.0030)
11	0.0008 (±0.0026)	0.0003 (±0.0009)

*Numbers in parentheses represent 95 percent confidence intervals.

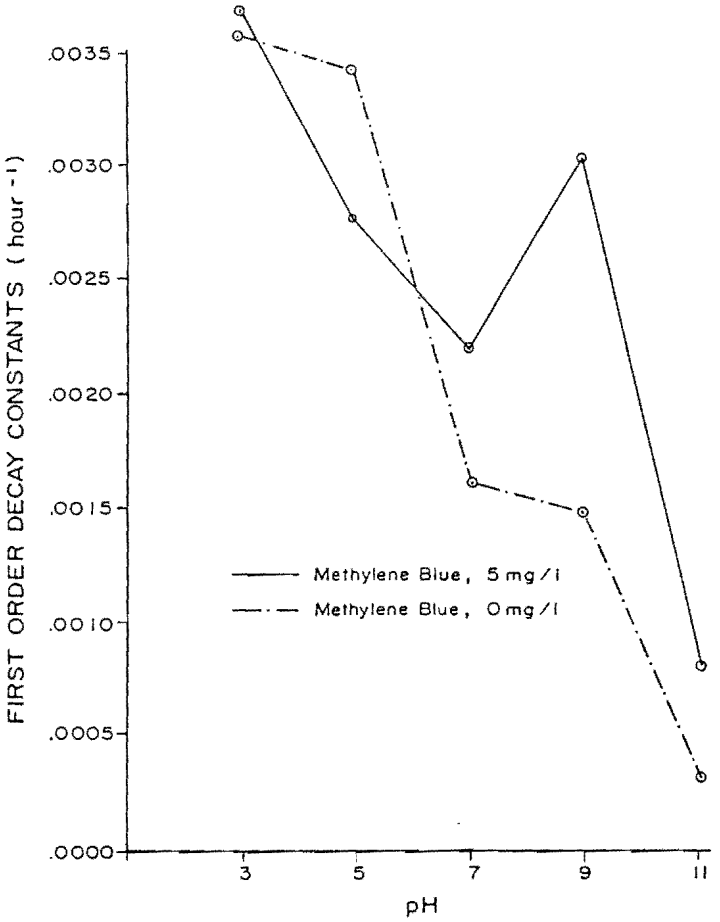

Figure 14. First order kinetic decay constants for the photolysis of 5 mg/1 quinoline solutions as a function of pH; comparison of methylene blue concentrations of 5 and 0 mg/1.

Table 18. Removal efficiencies (%) for the photolysis of 5 mg/l solutions of quinoline during a 72 hour photolysis period.

pH	Percent Removal Methylene Blue Concentrations, mg/l	
	5	0
3	23.5	26.3
5	15.4	23.9
7	16.4	9.6
9	24.4	13.0
11	8.0	9.1

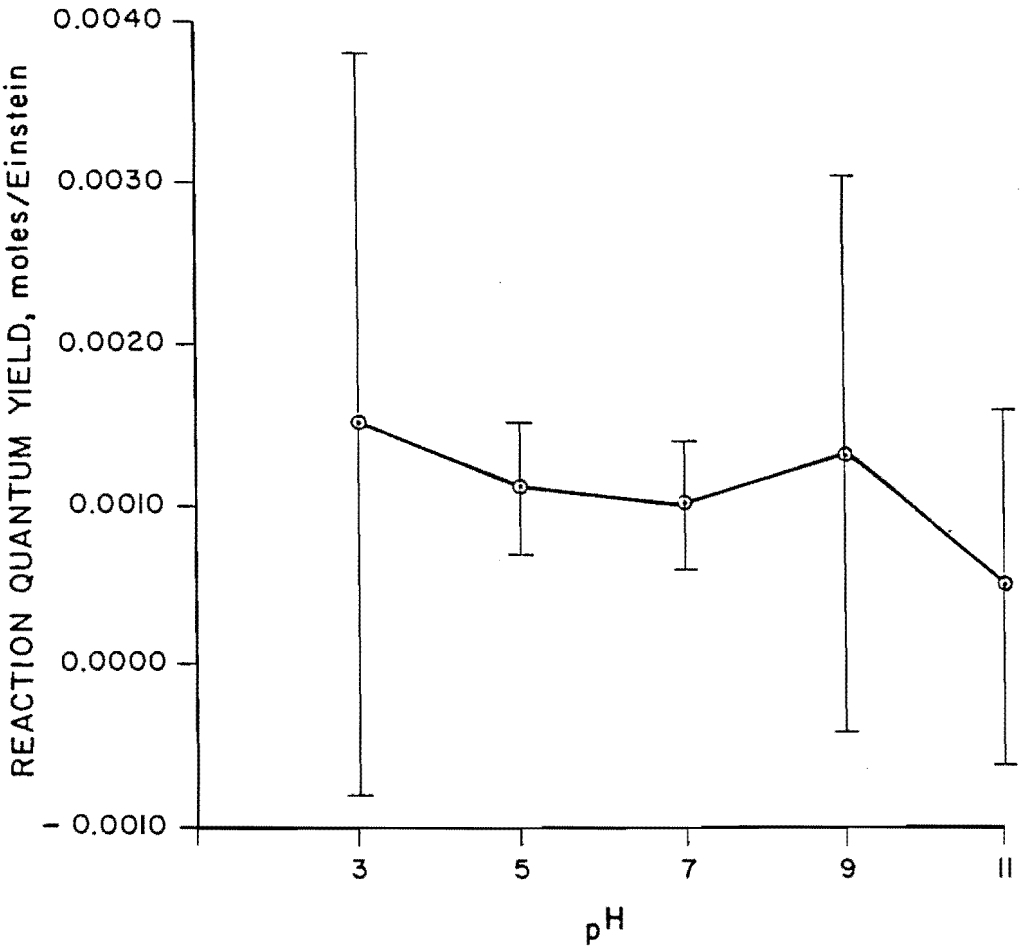

Figure 15. Reaction quantum yields for the phytolysis of 5 mg/l quinoline solutions as a function of pH in a 5 mg/l methylene blue solution (95 percent confidence limits shown for each data point).

were the only pH conditions which produced sensitized rates of reaction significantly greater than zero.

Naphthalene

Due to the characteristically volatile nature of naphthalene, photooxidation studies involving 1 mg/l solutions of naphthalene could not be performed until the rate of volatilization was established. Initial experiments indicated that a short reaction time would be necessary since an increasingly larger fraction of the compound was lost to volatilization as reaction time was lengthened (Table 19). The volatilization studies were conducted under the same experimental conditions used for photolysis studies. Solutions in the reactors were placed under photobench lamps, and glass plates used to minimize evaporation were placed over the reactors. Aluminum foil was then used to completely cover the reactors and eliminate the possibility of photolysis.

In order to minimize the effect of volatilization, all photolysis experiments were performed in less than 6 hours. For each experiment, an additional reactor was included to monitor the amount of naphthalene lost to correct for volatilization at each time interval sampled. The results of the sensitized and direct photooxidation of naphthalene are shown in Table 20. The sometimes uneven surfaces of the reactors on which the glass plates rested, resulted in inconsistent rates of volatilization. Because of the difficulty in monitoring volatilization and the seemingly unreactive nature of the substrate, no further testing of naphthalene was performed.

Initial Substrates Concentration

Optimum reaction treatment conditions for anthracene and acridine were chosen for the analysis of the effect of initial substrate concentration on photooxidation reaction rates. Both direct and sensitized photooxidation conditions were investigated for anthracene, choosing test solutions of 2 mg/l methylene blue buffered to pH 7 and pH 9 solutions without dye. Treatment conditions utilized as a function of substrate concentration were solutions buffered to pH 5 with 2 mg/l methylene blue.

Observed reaction rate constants from the examination of the effect of initial anthracene concentration are shown in Table 21, and these rates are plotted in Figure 16. The rate of direct photooxidation with 0 mg/l methylene blue increased initially with an increase in anthracene concentration from 0.5 to 1.0 mg/l. However, the rate dropped significantly as reactant concentration increased.

No significant difference in treatment effectiveness was found between initial anthracene concentrations with 2 mg/l methylene blue, indicating that the rate of sensitized photolysis is independent of initial concentration.

Figure 17 shows the sensitized photooxidation rate of acridine as a function of initial substrate concentration. No significant difference in reaction rates was observed, at the 95 percent confidence level, for five initial acridine concentrations, indicating that acridine photolysis was independent of initial concentration.

Table 19. Percent of naphthalene lost due to volatilization under photolysis reaction conditions with light eliminated; mean values from duplicate analyses.

Reaction Time (hours)	% Volatilized
0	--
6	22.6
18	43.0
30	61.3

Table 20. First order kinetic rate constants (1/hour) for the photolysis of 1 mg/l aqueous solutions of naphthalene.

	Reaction Rate Constants (1 hour) Methylene Blue Concentrations, mg/l			
	5		0	
pH	Uncorrected	Corrected	Uncorrected	Corrected
3	0.3215	-0.0021 (±0.0005)	0.0767	+0.0015 (±0.0041)
5	0.2691	-0.0001 (±0.0016)	0.1498	-0.0006 (±0.0058)
7	0.2773	-0.0001 (±0.0053)	0.0223	-0.0477 (±0.0049)
9	0.2440	+0.0011 (±0.0032)	0.1002	+0.0036 (±0.0005)
11	0.3290	+0.0026 (±0.0014)	0.1397	+0.0064 (±0.0020)

*Numbers in parentheses represent 95 percent confidence intervals.

Table 21. First order kinetic decay constants (1/hour) from the examination of the effect of initial anthracene concentration on the rate of photolysis.

Anthracene Concentration mg/l	Reaction Rate Constants (1/hour) Methylene Blue Concentration 2 mg/l pH 7	Methylene Blue Concentration 0 mg/l pH 9
0.5	0.0544 (±0.0955)*	1.2875 (±0.7233)
1.0	0.0597 (±0.0666)	3.6570 (±1.0910)
2.0	0.0302 (±0.0339)	0.5608 (±0.6171)
5.0	0.0302 (±0.0184)	0.6264 (±0.5796)
10.0	0.0238 (±0.0184)	0.4427 (±0.1594)

*Numbers in parentheses represent 95 percent confidence intervals.

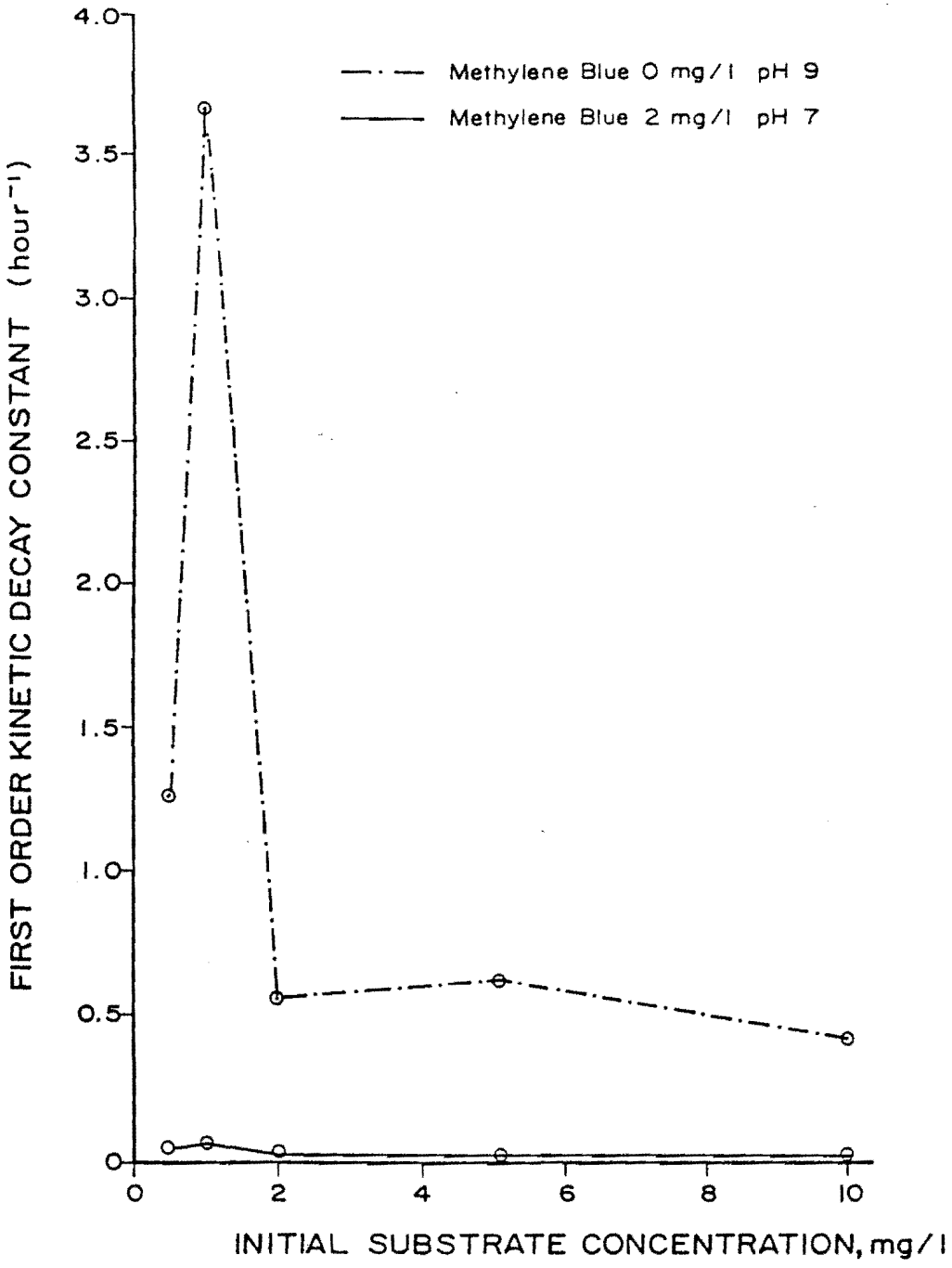

Figure 16. First order kinetic decay constants as a function of initial anthracene concentration; comparison of methylene blue concentrations of 2 and 0 mg/l.

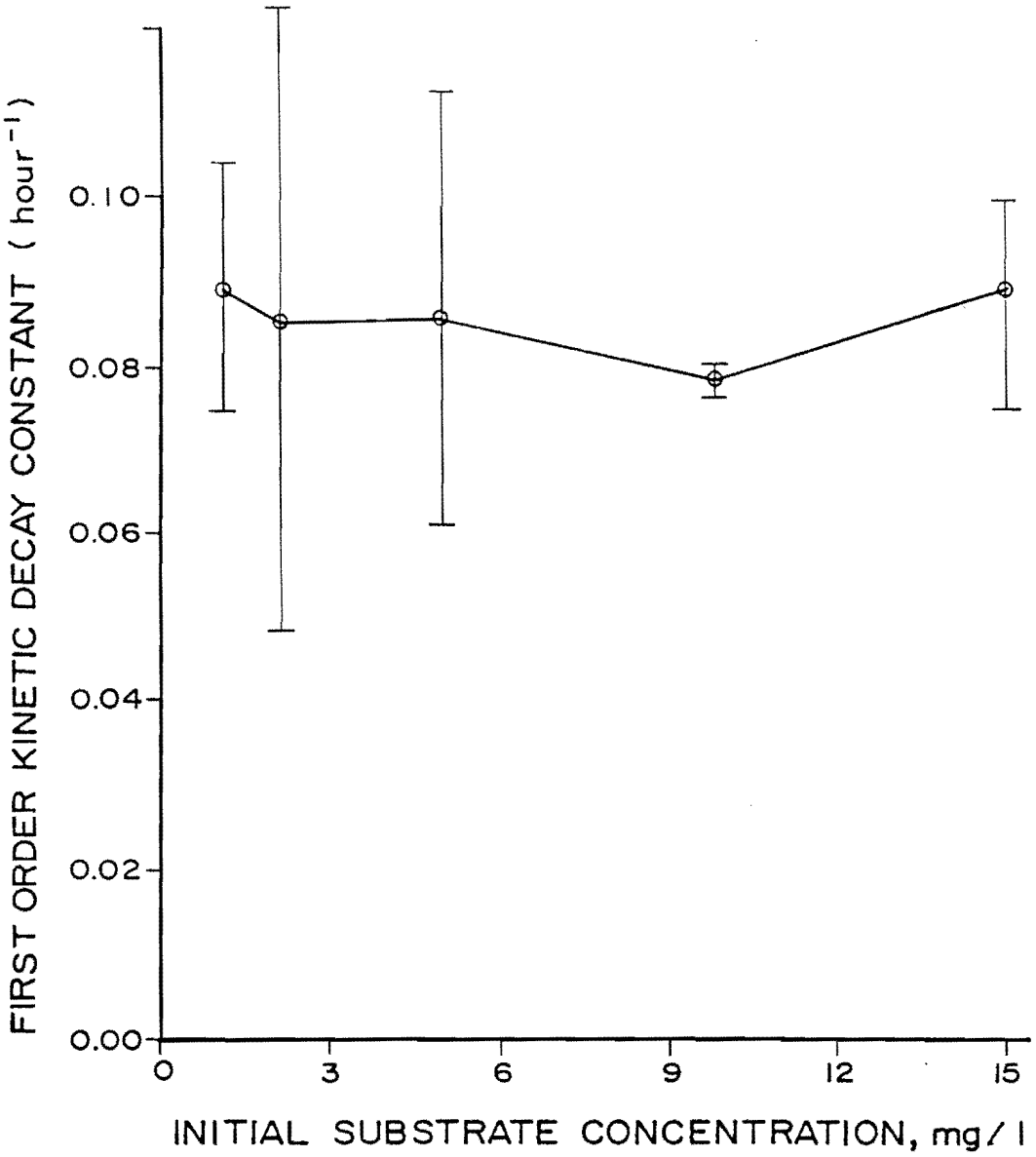

Figure 17. First order kinetic decay constants as a function of initial acridine concentration in a 2 mg/l methylene blue solution (95 percent confidence limits shown for each data point).

The dependency of reaction quantum yields on the initial concentration of acridine and anthracene in solution with dye was significantly different than the dependency of first order reaction rate constants on initial substrate concentration. The rate constants, k^c, observed for both compounds were independent of initial substrate concentration when photolyzed in solutions containing the sensitizing dye. In contrast, the quantum yields were dependent on the initial concentration of the compound. Figures 18 and 19 show the observed reaction quantum yields as a function of initial concentration for anthracene and acridine, respectively. The quantum yield increased with increasing substrate concentration due to the utilization of the initial rate constant, K^c, given as the number of moles of substrate reacted per second, in calculations involving quantum yield. The first order reaction rate constant, k^c, was independent of initial substrate concentration since the constant only represents the rate as a function of time, i.e., $hour^{-1}$.

The quantum yield values for sensitized photooxidations of both compounds increased with increasing concentration and although the reaction rates showed no change with concentration, the mass of compound photooxidized per second increased.

Substrate Mixtures

Foote (1968) found that some PNA compounds are capable of acting as sensitizers in photochemical experiments. This potential reaction was investigated by observing the effect of the combination of anthracene, quinoline and acridine on the rate of photolysis of each of the compounds. The results, shown in Table 22, compare the reaction rate of the compound when individually photolyzed with the rate of degradation observed in the compound mixture.

The reaction rate constant observed for quinoline and acridine when contained in the mixture of substrates with and without dye were statistically equal, based on the standard t-test, to the rate constants observed when the compounds were photolyzed individually. However, the reaction rate constants obtained for anthracene when contained in a mixture with and without dye were significantly less, at the 95 percent confidence level using the standard t-test, than the rate constants achieved when the compound was photolyzed individually.

Similar results were found when a comparison of observed quantum yields was made, as shown in Table 23. Quinoline and acridine achieved reaction quantum yields when in a mixture similar to those achieved when the compounds were individually photolyzed. Anthracene exhibited a significant decrease in quantum yield when the compound was photolyzed in the presence of acridine and quinoline.

Substrate Half-Lives

Determination of substrate half-lives is a useful means of predicting the persistence of chemicals in the environment. The calculated half-lives of organic substrates based on sensitized photolysis experiments represent a necessary parameter for the design of sensitized phototreatment lagoons. Half-lives of the substrates used in this study were calculated using Equation 19 and are presented in Tables 24, 25, and 26.

$$t_{1/2} = \frac{\ln 2}{k^c} \qquad (19)$$

where

$t_{1/2}$ = half-life of compound, days

k^c = first order reaction rate constant, 1/day

Half-lives ranged from 12 minutes (anthracene, direct photolysis, pH 9) to 96 days (quinoline, direct photolysis,

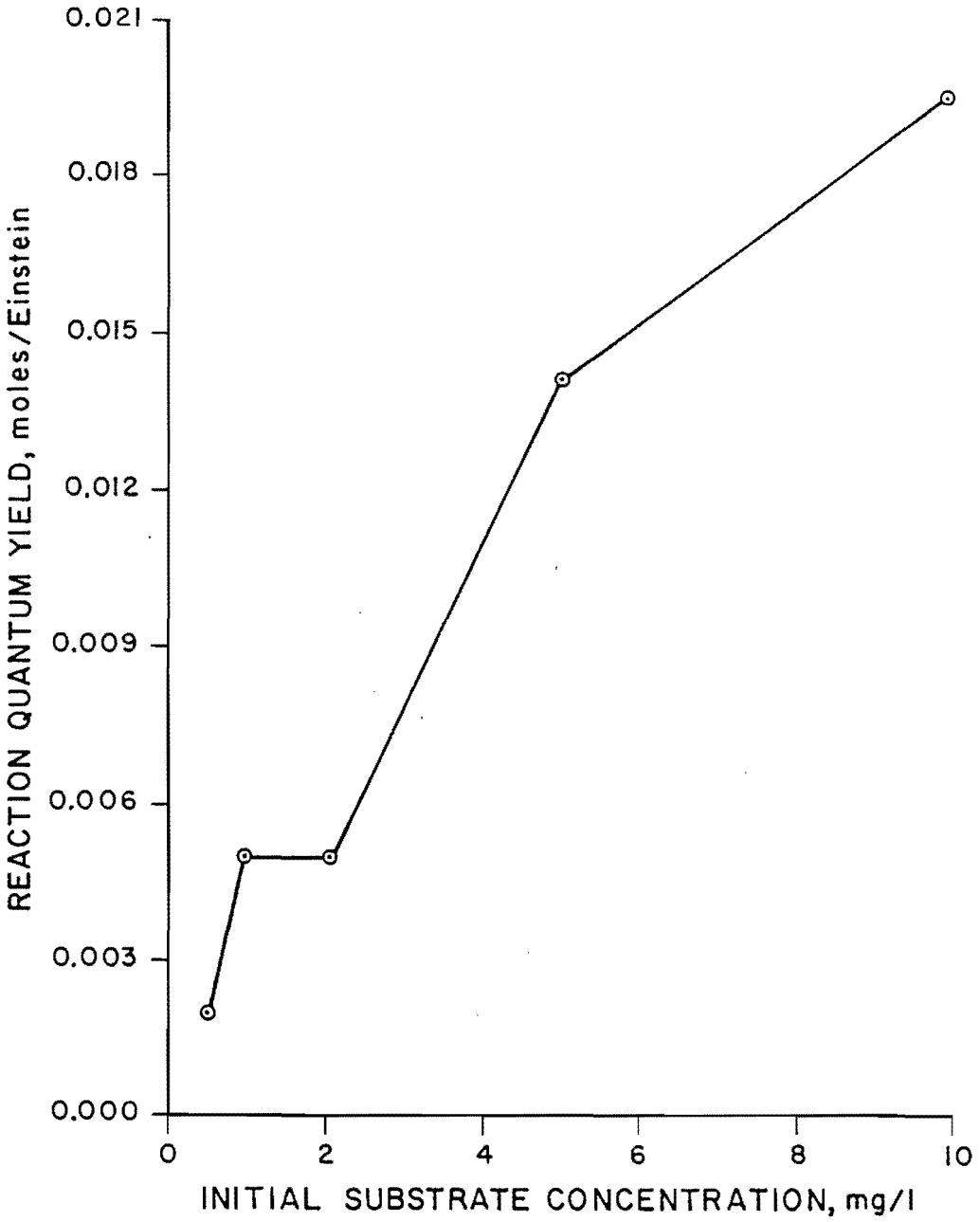

Figure 18. Reaction quantum yields as a function of initial anthracene concentration in a 2 mg/l methylene blue solution.

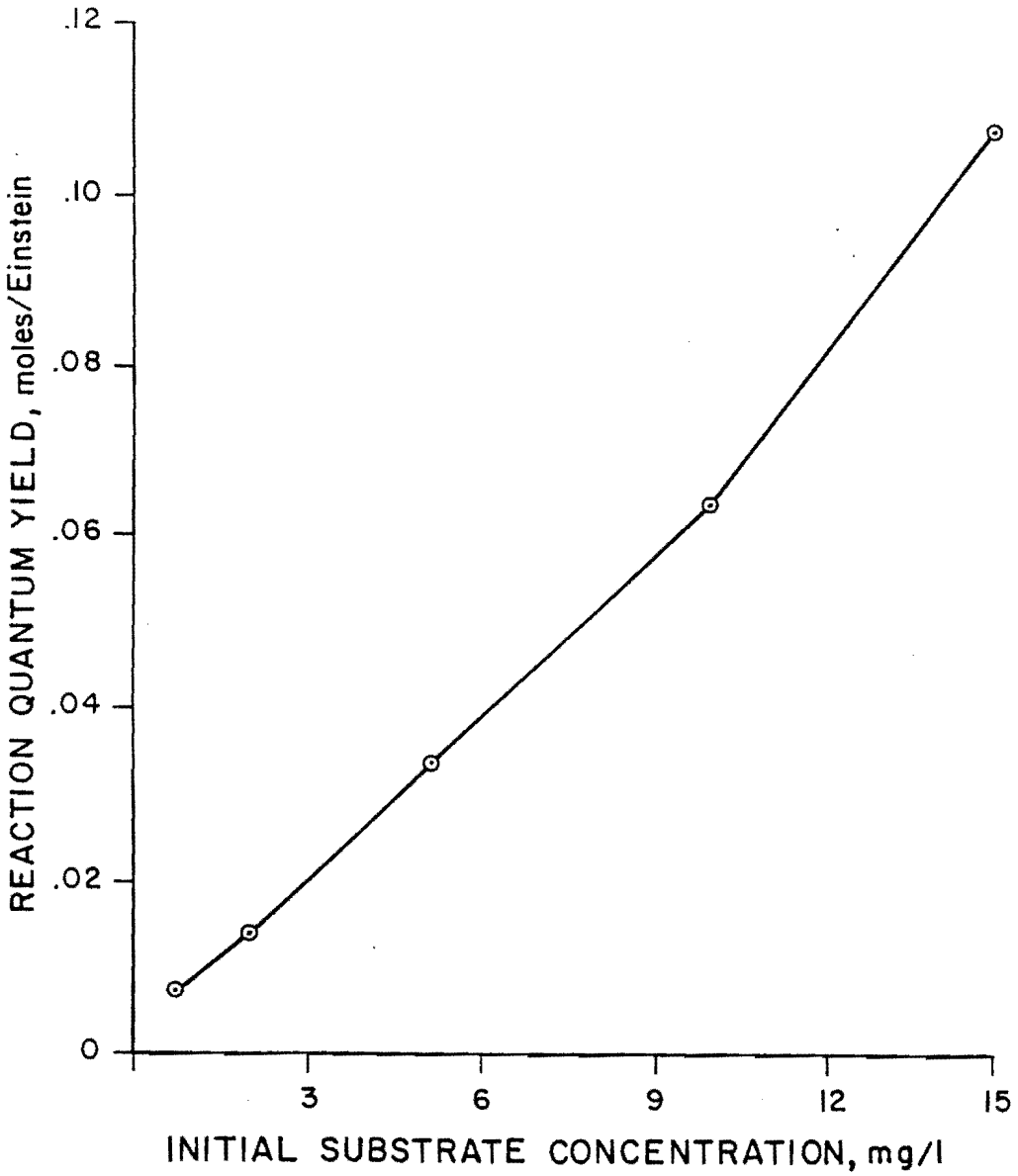

Figure 19. Reaction quantum yields as a function of initial acridine concentration in a 2 mg/l methylene blue solution.

Table 22. A comparison of the first order decay reaction rate constants (1/hour) for substrate mixture (acridine, 5 mg/1; anthracene, 1 mg/1; quinoline 5 mg/1) with the photolysis rates of each compound treated individually.

Compound	Methylene Blue Concentration mg/1	pH	Reaction Rate Constants (1/hour)	
			Mixture	Individually
Quinoline	2	7	0.0028	0.0022
Quinoline	0	7	0.0040	0.0015
Anthracene	2	7	0.0362	0.0751
Anthracene	0	7	0.0573	1.3486
Acridine	2	7	0.0150	0.0157
Acridine	0	7	0.0186	0.0132

Table 23. A comparison of quantum yields (moles/einstein) for substrate mixtures (anthracene, 1 mg/1, acridine and quinoline, 5 mg/1) with the quantum yields of each compound photolyzed individually.

Compound	Methylene Blue Concentration mg/1	pH	Reaction Quantum Yields (mole/einstein)	
			Mixture	Individually
Quinoline	2	7	0.0016	0.0010
Anthracene	2	7	0.0030	0.0080
Acridene	2	7	0.0061	0.0061

Table 24. Calculated half-lives for the photolysis of anthracene under different treatment conditions.

pH	Half-lives (days) Methylene Blue Concentrations, mg/1		
	5	2	0
3	0.68	0.52	0.055
5	0.36	0.44	0.027
7	0.18	0.38	0.021
9	0.48	0.52	0.008
11	0.58	0.56	0.012

Table 25. Calculated half-lives for the photolysis of acridine under different treatment conditions.

pH	Half-lives (days) Methylene Blue Concentrations, mg/l				
	10	5	2	1	0
3		0.47	0.50	1.24	0.95
5		0.35	0.22	0.22	0.44
7	1.66	1.49	1.84		2.19
9	8.94	6.02	9.53		4.13
11	3.33	3.14	7.74		4.81

Table 26. Calculated half-lives for the photolysis of quinoline under different treatment conditions.

pH	Half-lives (days) Methylene Blue Concentrations, mg/l	
	5	0
3	7.91	8.08
5	11.34	8.49
7	13.15	19.13
9	9.62	19.55
11	34.51	96.27

pH 11). The sensitized or direct photolysis of anthracene at any pH level resulted in half-lives of less than 1 day. Acridine photolysis was found to be extremely dependent on reaction pH and sensitizer concentration with half-lives ranging from 5 hours to 9 days. Quinoline has a much longer half-life than the other compounds studied and would be expected to be more persistent and difficult to treat.

Actinometry

Only the energy of the wavelengths absorbed by the sensitizing dye serves to generate the triplet sensitizer and in turn singlet oxygen. For efficient use of available light energy, the sensitizer should absorb as much of the light's emission spectrum as possible. The degree to which the light source emission spectrum and the sensitizer absorbance spectrum overlap is a measure of total energy absorbed. Figure 20 depicts the effectiveness of methylene blue as a sensitizer for the light emission source used. As shown, the light intensity output overlaps the entire absorbance spectra resulting in light energy being available at all absorbing wavelengths of methylene blue.

The actinometer system, incorporating a methylene blue sensitized

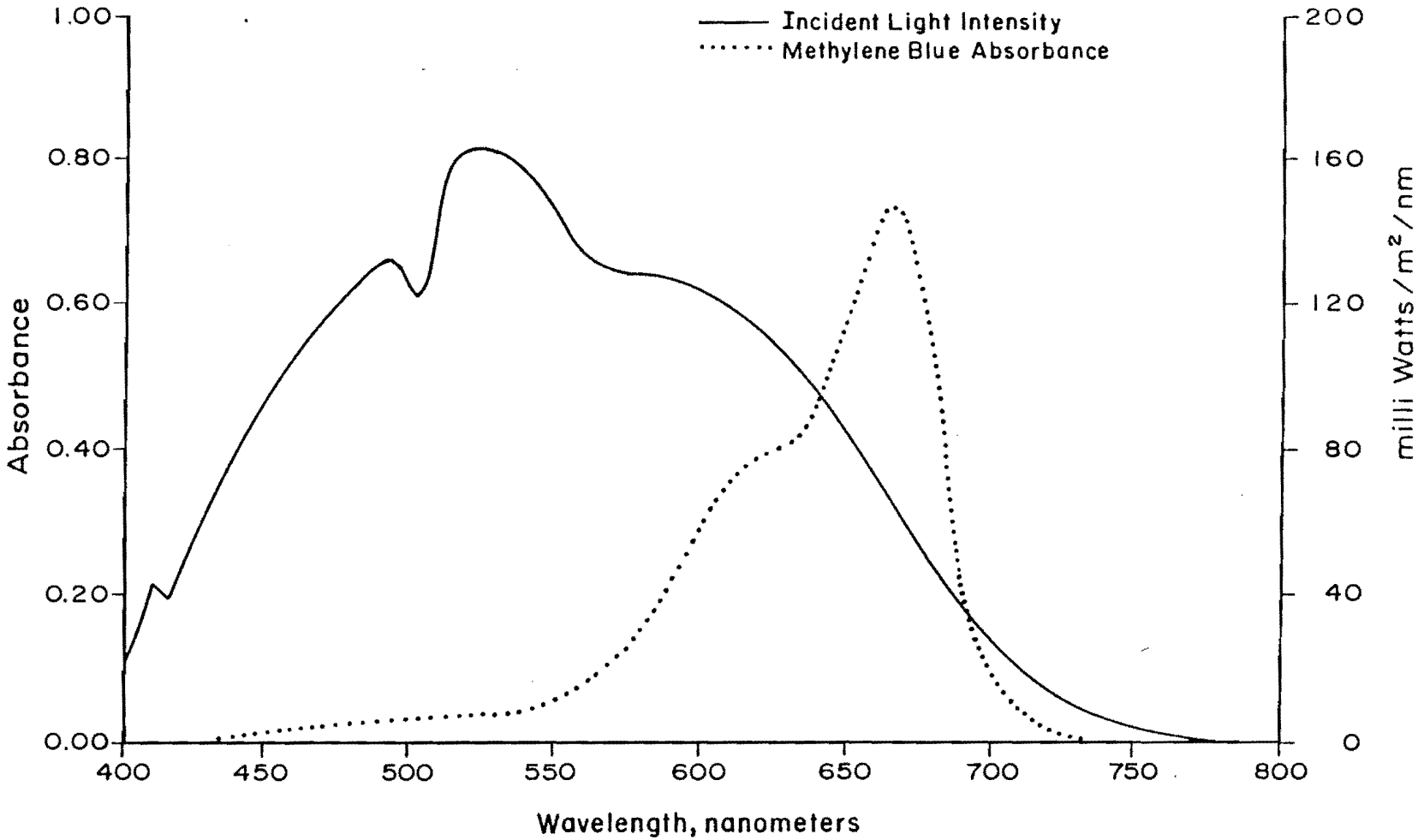

Figure 20. Methylene blue absorbance spectrum compared with the light source emission spectrum.

photoreaction, was used to monitor light intensity for the maximum absorbing wavelength of methylene blue (570 to 700 nm). By summing the light intensities emitted by the photobench lamps at wavelengths between 570 nm and 700 nm, as determined from the data obtained from the Optronics Spectroradiometer, an average light intensity of 0.095 $W/m^2/nm$ was established as the effective output of light per wavelength available for sensitized photoreactions.

The actinometer was run prior to the start of each experiment. The effective light intensity available per wavelength was calculated using 650 nm as the median wavelength in the methylene blue absorbance spectrum and by applying Equation 10:

$$I_o = \frac{\Delta CVN_c}{\phi_a A t \lambda} \qquad (10)$$

The intensity measurements as well as the reaction rate of the actinometer are contained in Appendix B.

Light emission for individual runs varied from 0.058 to 0.124 $W/m^2/nm$, however, a decrease in light intensity with time was not found, as the intensity readings appeared to vary randomly. An average light intensity for the entire experiment was 0.092 $W/m^2/nm$.

Including an actinometer in the experimental design allowed for not only the determination of incident light intensity, but also for the calculation of the overall quantum yields. This information provides support for the determination of the effectiveness of a given treatment condition.

Toxicity Testing

Samples of anthracene and acridine were analyzed for toxicity prior to photolysis, at half the reaction time and after photolysis, using the Beckman Microtox™ acute toxicity test. Optimum photooxidation conditions for each compound were used as the photolysis reaction conditions in the toxicity analysis. Table 27 shows the mean values from duplicate analyses using the Microtox™ acute toxicity test.

The numeric values assigned to the toxicity of a compound represent the percent of sample in a dilution which caused a 50 percent reduction in light output by the photoluminescent bacteria. The lower the reported toxicity value, on a scale of 100, the more toxic is the solution, since less sample is necessary to produce a toxic response from the bacteria, i.e., a 50 percent reduction in light output.

Anthracene was found to be nontoxic in all samples tested. Acridine, however, exhibited a toxic response prior to photolysis, and the degree of toxicity increased during photolysis indicating that the photoproducts produced were more toxic than the parent compound.

Table 27. Results of the toxicity analysis utilizing the Microtox acute toxicity test.

Compound	Methylene Blue Concentration (mg/l)	pH	Reaction Time (hours)	Toxicity*
Anthracene	2	7	0	NT
Anthracene	2	7	12	NT
Anthracene	2	7	24	NT
Anthracene	0	9	0	NT
Anthracene	0	9	0.33	NT
Anthracene	0	9	0.83	NT
Acridine	2	5	0	18.5
Acridine	2	5	24	13.1
Acridine	2	5	48	13.0

*NT = Non-toxic

DISCUSSION

Photochemical reactions are initiated by the absorption of light energy by a molecule and are terminated with the disappearance of that molecule, or with its return to ground state. In the course of a photochemical reaction, the excitation energy of the electron may be released in several ways, leading to chemical changes such as formation of excited molecules, intramolecular rearrangement or free radical formation. Essential to a discussion of photochemical reactions is an understanding of the pathways of excitation and deactivation possible for a light absorbing molecule. A Jablonski diagram (Figure 21) is a schematic representation of the redistribution of energy resulting from the absorbance of light energy by a molecule (S_o). The excited states initially produced by absorption of a photon (S_1, S_2) are almost always singlet states. A triplet state (T_1) is the result of an excitation to a singlet state accompanied by a reversal of the spin of the electron; its energy will be lower than that of the corresponding excited singlet state, since part of the energy has been used in reversing the electronic spin.

Although it was not the purpose of this study to concentrate on the energy redistribution mechanisms which occurred when the organic compounds of interest were photolyzed, the pathways represented in Jablonski's diagram are fundamental to the understanding of photochemical reactions. Explanation of the results required investigation into electronic transition pathways, particularly intersystem crossing, $S_1 \rightarrow T_1$, $T_1 \rightarrow S_o$, and internal conversion, $S_1 \rightarrow S_o$.

Optimum Reaction Conditions

Given that the quantum yield values observed for the sensitized photooxidation of each compound closely paralleled the results obtained for the analysis of reaction conditions using the observed kinetic rate constants, only the reaction rate constants will be used to discuss optimum reaction conditions.

The optimum reaction conditions for the photodecomposition of the organic substrates have been established based on the photooxidation conditions when a maximum reaction rate was achieved, accompanied by a maximum quantum yield value. The optimum reaction pH and sensitizer concentration for each compound are presented in Table 28. Optimum reaction conditions for each compound occurred at different pH values and with varying amounts of methylene blue present.

Anthracene photodimerization

The maximum reaction rates observed in this study occurred during the direct photolysis of anthracene and were at least several orders of magnitude greater than other photolysis conditions analyzed. The absorption spectrum for a 1 mg/l solution of anthracene is shown in Figure 22. Two significant absorbance peaks occurred at 375 nm and 398 nm. Murov (1973) and Turro (1978) reported that excitation of anthracene molecules to a singlet state can occur from the absorption of light of sufficient energy in the 375 nm range. In the excited state, anthracene can form a dimer with a ground state anthracene molecule (Neckers 1967, Cowan and Drisko 1976).

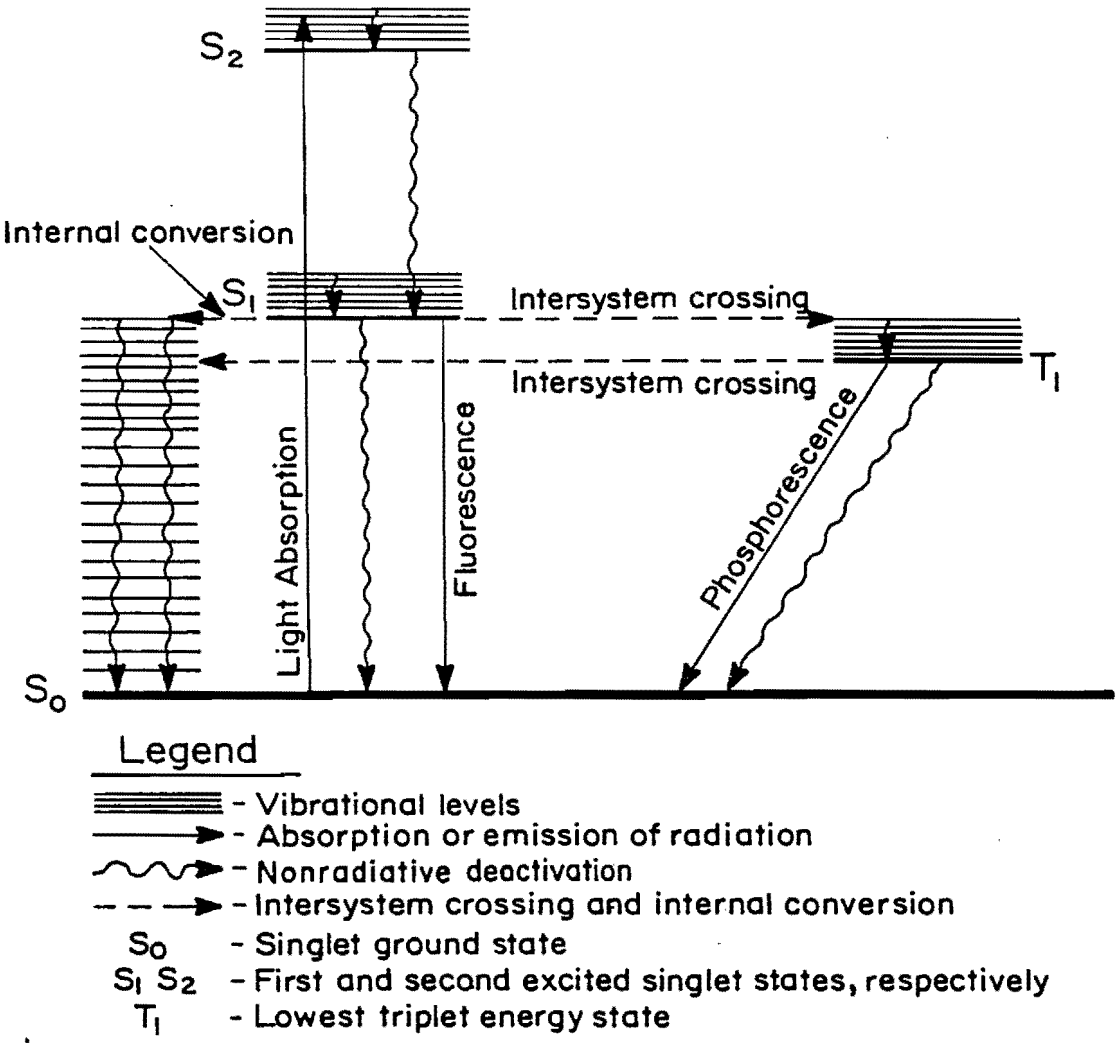

Figure 21. Jablonski's diagram.

Table 28. Optimum reaction conditions for the photodegradation of 5 mg/l solutions of acridine and quinoline and 1 mg/l solutions of anthracene.

Compound	Photolysis Process				
	Direct		Sensitized		
	pH	Rate	pH	Rate	Dye Concentration (mg/l)
Anthracene	9	3.57	0.1595	7	5
Acridine	5	0.0656	0.1293	5	1
Quinoline	5	0.0034	0.0025[a]	ND	5

[a]Represents an average rate for all pH levels
ND - No significant difference (= 0.05) in pH treatments

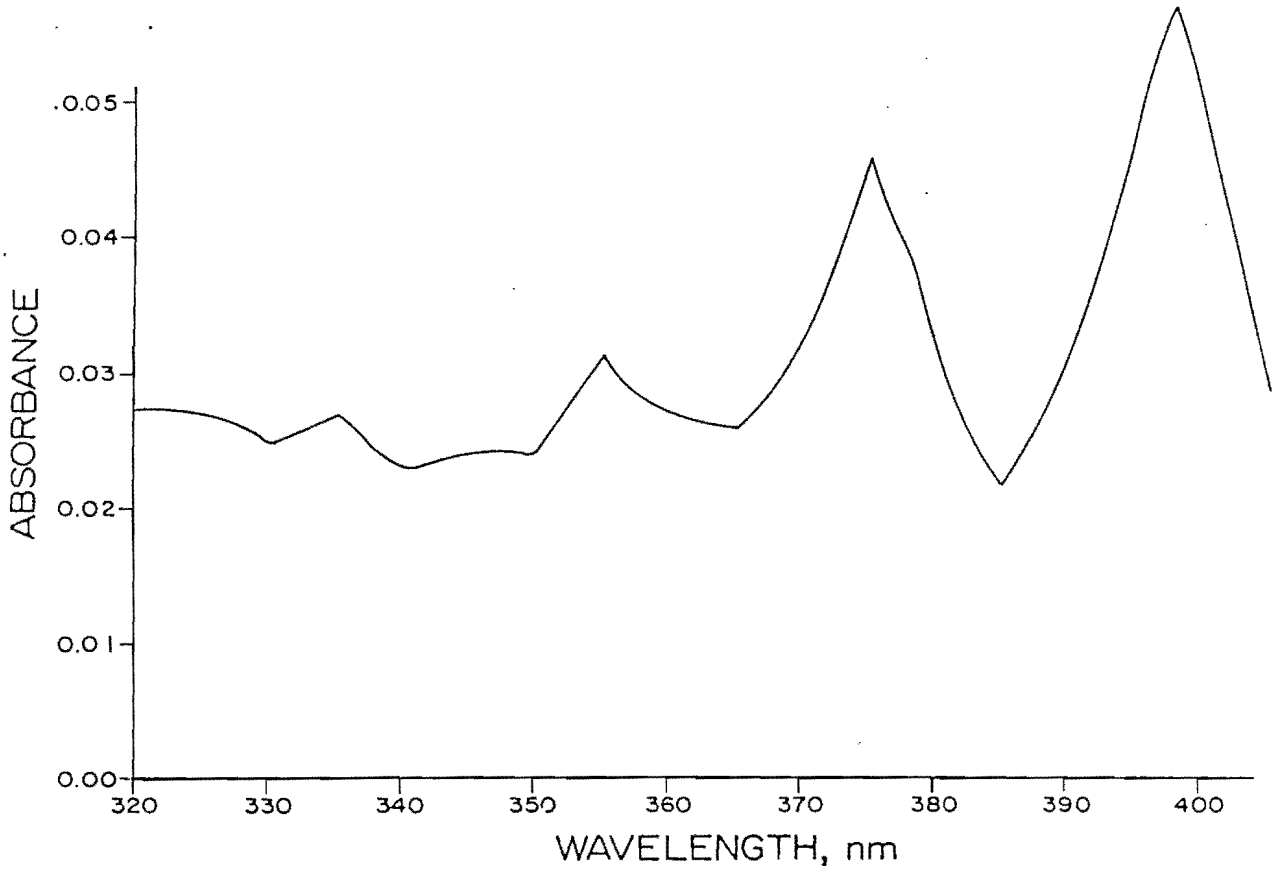

Figure 22. Absorbance spectrum for a 1 mg/l anthracene solution.

The photodimerization of anthracene was one of the first photochemical systems to be extensively investigated. The mechanism involves the following reaction steps:

$$An + hv \rightarrow An_1^* \quad (20)$$

$$An + An_1^* + hv \rightarrow \text{dimer} \quad (21)$$

$$An + An_1^* \rightarrow 2An \quad (22)$$

The excited singlet state, represented as An_1^*, is considered the reactive state for dimerization, rather than an excited triplet. The fact that as the concentration of anthracene in solution increases, the quantum yield of dimerization also increases, while the fluorescence efficiency ($S_1 \rightarrow S_o$) of excited anthracene decreases (Neckers 1967), is strong evidence supporting the singlet mechanism.

Dimerization occurs across the 9, 10 carbon atoms creating the structure shown in Figure 23.

To investigate whether the reaction rates observed for the direct photolysis of anthracene could be attributed to its dimerization, a glass filter was placed over a solution of anthracene that was then photolyzed. The filter effectively blocked the penetration of light below 420 nm, thereby inhibiting direct excitation of anthracene. The results, shown in Table 29, indicate that when the anthracene absorbing wavelengths of light were effectively blocked,

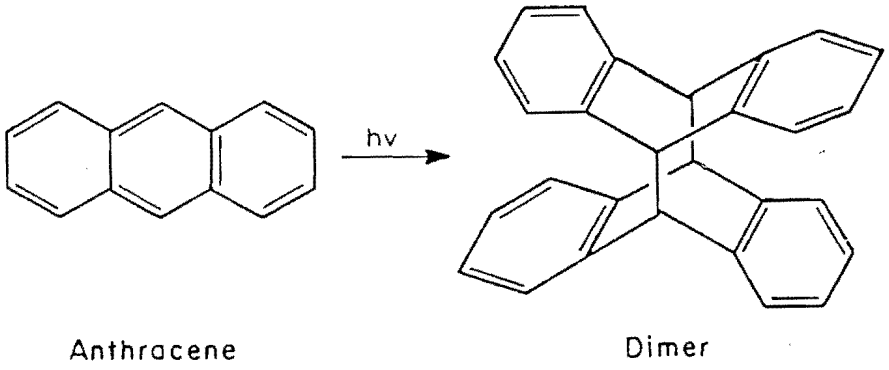

Figure 23. Photodimerization of anthracene.

Table 29. Change in the concentration of anthracene with time when photolyzed without a filter and with a 420 nm filter.

Time Hour	Concentration (mg/l) without filter	Time Hour	Concentration (mg/l) with 420 nm filter
0	1.08	0	1.30
0.167	0.80	0.25	1.30
0.333	0.45	0.50	1.26
0.500	0.20	1.00	1.16
0.833	0.00	2.00	1.30

essentially no reaction occurred, suggesting that reaction rates observed when the light was not filtered represented a direct absorbance of light by anthracene and excitation to a singlet state, initiating the photodimerization reaction.

Effect of sensitizing dye

The sensitizer involved in the photooxidation process reacts with molecular oxygen by transferring its energy from the triplet excited state. The mechanism proposed for the energy transfer is represented in the following equations:

$$\text{Sens} + h\nu \rightarrow \text{Sens}_1^* \quad (23)$$

$$\text{Sens}_1^* \rightarrow \text{Sens}_3^* \quad (24)$$

$$\text{Sens}_3^* + {}^3\Sigma g O_2 \rightarrow {}^1\Delta g O_2 + \text{Sens} \quad (25)$$

The sensitizer absorbs sufficient light energy to raise the molecule to its first excited singlet state, Sens_1^*. Intersystem crossing, which is a radiationless transition from an excited singlet state to a triplet state, proceeds by a coupling between the vibrationally nonexcited Sens_1^*, and the isoenergetic vibrational triplet state. This is followed by vibrational relaxation to vibrational sublevel zero

of the triplet state. Thus, intersystem crossing is an internal conversion with a change in the direction of spin (Mousseron-Canet and Mani 1972). Finally, the triplet sensitizer transfers its energy to molecular oxygen, forming a reactive singlet oxygen species, with the triplet sensitizer returning to ground state.

Anthracene reactions. Sensitized photochemical reaction rates involving anthracene were greatest when the highest dye concentration examined, 5 mg/l methylene blue, was utilized. This condition occurred in solutions buffered to an optimum pH of 7.

Since methylene blue does not absorb light effectively below 460 nm anthracene molecules were capable of absorbing light energy in the wavelength region where methylene blue was incapable of sensitizing a photoreaction. The excitation energy from the absorption of light from 350 to 420 nm was sufficient to elevate anthracene molecules to the singlet state from which dimerization could occur. Dimerization reactions occurred rapidly in the absence of dye. However, the rate of reaction was less in dye solutions than when no dye was present so another mechanism must have operated which competed with dimerization.

Quenching is a bimolecular process in which an excited state is converted to the ground state by transferring its energy to the quenching molecule, and it in turn is excited to a higher energy state. For quenching to occur, the quencher must possess a lower energy requirement for excitation than the energy of the excited molecule. Anthracene molecules possess 76 kcal and 42 kcal energy in their singlet and triplet states, respectively. Methylene blue requires 34 kcal energy to be raised to its excited state, and as such, is capable of accepting energy from the excited anthracene molecules in the system.

In this process, the excited singlet anthracene molecule could have been quenched by ground state methylene blue instead of reacting with ground state anthracene molecules to form a dimer. Anthracene would be returned to ground state and in turn, methylene blue would be excited to the more reactive triplet energy state.

The proposed mechanisms for energy transfers are given in the following equations:

$$An + h\nu \rightarrow An_1^* \qquad (20a)$$

$$An_1^* \rightarrow An_3^* \qquad (20b)$$

$$An_3^* + Sens \rightarrow Sens_1^* + An \qquad (26)$$

$$Sens + h\nu \rightarrow Sens_1^* \qquad (23)$$

$$Sens_1^* \rightarrow Sens_3^* \qquad (24)$$

$$Sens_3^* + {}^3\Sigma\, gO_2 \rightarrow {}^1\Delta\, gO_2 + Sens \qquad (25)$$

The greatest rate of photooxidation of anthracene would be achieved under conditions which give the greatest triplet sensitizer concentration thereby increasing the production of singlet oxygen. Quenching is a diffusion controlled process, and as such the rate of triplet sensitizer formed from the quenching of singlet anthracene would be expected to increase as the concentration of methylene blue was increased.

Acridine reactions. Sensitized photooxidation experiments involving acridine showed a strong dependence on methylene blue concentration in solutions buffered to optimum pH conditions of 3 or 5. Acridine solutions buffered at neutral and alkaline pH were nearly unreactive toward singlet oxygen and reaction rates were independent of methylene blue concentrations.

The maximum reaction rates for the sensitized photooxidation of acridine occurred when solutions contained the least amount of methylene blue. Acridine possesses photochemical

characteristics similar to those of anthracene in that it can absorb light energy in a wavelength region where methylene blue cannot. Its triplet energy is greater than the energy of methylene blue and the quenching mechanism proposed to occur in photooxidations involving anthracene, is photochemically allowed. Similar results were not obtained for optimum sensitizer concentration, however.

It is unclear what photochemical mechanism was involved when examining the results of the effect of dye concentration on the photolysis of acridine. It is suggested in the literature that many electron-rich heterocyclic organics, such as acridine, are capable of quenching singlet oxygen via a charge-transfer mechanism (Wasserman and Murray 1979). This reaction involves interaction of the electron-poor singlet oxygen molecule with electron donor molecules to give a charge-transfer complex, which can then dissociate to donor and ground state oxygen.

The reduced reaction rates in acridine solutions containing higher dye concentrations under optimum pH conditions could be attributed to a charge-transfer quenching of triplet methylene blue by ground state acridine similar to the quenching of singlet oxygen by a charge-transfer reaction. Methylene blue exists in solution as predominantly a cationic species capable of participation in the proposed charge-transfer reaction with acridine. This reaction is diffusion controlled and as such, the rate of quenching of triplet methylene blue would be expected to increase as the concentration of methylene blue was increased, leading to decreased reaction rates in solutions containing higher dye concentrations.

Quinoline reactions. The effect of sensitizer concentration on the rate of photooxidation of quinoline was insignificant since the rate of decomposition was not enhanced in the presence of methylene blue. At each pH level examined, there was no significant difference in the reaction rate constants between solutions containing a sensitizer and those without dye present.

Effect of pH

The effect of pH on the rate of photochemical reactions was examined over a pH range from 3 to 11 at 2-pH unit intervals. An optimum reaction pH was established for each compound tested and the results are shown in Table 28. The optimum reaction pH for dye sensitized and direct photolysis of acridine was pH 5. Quinoline also achieved maximum direct photolysis rates in low pH conditions of 3 and 5. In contrast, anthracene photochemically reacts at more rapid rates in solutions buffered to neutral and alkaline pH levels. Most reports in the literature (Sargent and Sanks 1976, Bellin and Yankus 1968, Bonneau et al. 1975) cite neutral to alkaline pH conditions as optimal for photochemical reactions, as was found in the photolysis of anthracene in this study.

The low pH conditions utilized when maximum reaction rates were observed for the photooxidation of quinoline and acridine were explained when a comparison was made of pKa values for these compounds with those compounds cited in literature. The pKa values for quinoline and acridine are 4.9 and 5.5, respectively. Bellin and Yankus (1968) reported that sensitized photooxidations of the amino acids tyrosine and histidine proceed more efficiently at alkaline pH and that photooxidation reactions are only rarely observable at acid pH. The pKa of tyrosine is 8.40 while that of histidine is 9.17. Bonneau et al. (1975) observed the rate of tryptophan photooxidation to be most efficient at a pH greater than 9 when sensitized with methylene blue. The pKa of tryptophan corresponds with the results of alkaline pH producing higher reaction rates reported to be 9.38. Finally, Sargent and Sanks (1976)

suggested alkaline pH conditions for the optimum rate of cresol or phenol photooxidation. Both compounds exist as 50 percent ionized species at pH levels of 10.1 for cresol and 9.89 for phenol.

It is unclear what causes the optimum pH for photooxidation to occur at exactly the pKa of the compound. It is apparent that compounds possessing high pKa value will achieve optimum rates of reactions in alkaline pH solutions and that a low pKa value will effect the optimum photoreaction for a compound in low pH solutions.

The pKa of the photochemical sensitizer also appears to govern the reactivity of the substrate. Bellin and Yankus (1968) found that the sensitizer, rose bengal, exists in solution as an anion due to its low pKa value of 4.3, and that rose bengal photosensitized the degradation of high pKa compounds, histidine and tryrosine, more efficiently than the high pKa dye, methylene blue. If the opposite condition is found to be true, in that a high pKa, cationic, dye sensitizes low pKa compounds more efficiently, then the choice of a sensitizer for photochemical experiments must include information regarding the pKa of the chemical substrates as well as the sensitizing dyes.

Although the choice of sensitizer, based on pKa values, effects the reactivity of the substrate, it does not appear to alter the fact that the optimum pH for reaction will occur at the pKa of the substrate. Photochemical experiments involving methylene blue (pKa 11.6) and high pKa compounds, attained maximum reaction rates in solutions buffered to the pKa of the photolyzed substrate (Bellin and Yankus 1968, Sargent and Sanks 1976). Maximum methylene blue sensitized photoreaction rates for low pKa compounds, acridine and quinoline, were also achieved in solutions buffered to the pKa of these compounds.

Initial Substrate Concentration

Anthracene and acridine were analyzed to determine the effect of initial substrate concentration on the rate of photooxidation. Figures 16 and 17 show the rate of substrate disappearance as a function of substrate concentration for anthracene and acridine, respectively.

Anthracene reaction

Anthracene was photolyzed utilizing the optimum conditions for both sensitized and direct photodegradation. The rate of reaction for the direct photolysis of anthracene increased as the initial concentration increased from 0.5 mg/l to 1.0 mg/l. The maximum rate constant was achieved at an anthracene concentration of 1.0 mg/l. As the anthracene concentration increased from the optimum, the rate constant decreased. This result was also reported by Sargent and Sanks (1976) with cresol, i.e., an initial increase in reaction rate as the cresol concentration increased up to an optimum concentration. As the cresol concentration increased from that optimum, the first-order reaction rate constant decreased, but the total weight of cresol oxidized increased. The theory given by these authors for the decrease in the rate of cresol oxidation beyond the optimum concentration was that cresol oxidation products became involved in secondary reactions that affected the reaction rate.

Due to the tendency for anthracene to dimerize, a self-interaction model, such as vertical stacking, best explains its decrease in reaction rate beyond the optimal concentration. The work of Ts'o and Chan (1964) has demonstrated that a number of different types of molecules form complexes of various degrees of self-association depending upon their total solution concentration. Gonzalez and Langerman (1977) studied the self-association of flavin mononucleotide molecules in solution and proposed a vertical stacking configuration of the

molecule upon dilution based on nuclear magnetic resonance data. Although verifiable evidence was not produced, vertical stacking of anthracene is supported by the anthracene quantum yield data collected.

The nature of the forces driving the association have been described as hydrophobic interaction and surface energy reactions (Kauzmann 1959). The hydrophobic interaction occurs since anthracene is a hydrophobic molecule which will tend to self-associate when in aqueous solutions. The surface energy model proposes that the important source of interaction energy is the surface energy required to form cavities around the molecule in the system. In an association reaction, the cavities around the two reactant species have a larger total surface area than the single cavity around the product, so that the tendency to minimize the surface energy literally squeezes the molecules together.

Gonzalez and Langerman (1977) reported that at concentrations of solute well below their solubility, monomers and dimers were the most prevalent forms of flavin mononucleotide in solution. At the lower concentrations of anthracene, 0.5 and 1.0 mg/l, the solution likely contained predominantly monomers and dimers. A concentration of 1 mg/l exhibited a significantly faster reaction rate than the observed rate for 0.5 mg/l solutions since the rate of dimerization is diffusion controlled, and the higher anthracene concentration will exhibit a higher rate of dimerization. As the initial concentration of anthracene increased from 1 mg/l, the tendency to self-associate increased due to the increase in the number of anthracene molecules present. The various reaction equilibria are characterized by the equations of the form:

$$An + An \rightarrow (An)_2 \quad (25)$$

$$An + (An)_2 \rightarrow (An)_3 \quad (26)$$

$$An + (An)_{n-1} \rightarrow (An)_n \quad (27)$$

Gonzalez and Langerman (1977) reported that at high solute concentrations, vertical stacking occurred and that configurations ranged from monomers up to polymers of 50 stacked molecules. At the higher anthracene concentrations, 2, 5, and 10 mg/l, self-interaction by vertical stacking is expected to have increased. The decrease in reaction rate observed at the higher concentrations is postulated to be due to the addition of the nonpolar extraction solvent, methylene chloride, to the photolyzed samples, thereby reducing the hydrophobic interactions responsible for the stacking of anthracene molecules. When the stacks broke apart, the monomers of anthracene were released into the extract solution, and were subsequently measured by gas chromatography.

The rapid rate of reaction in solutions which contained 0.5 and 1 mg/l anthracene was observed because the predominant reaction was the photochemical dimerization of anthracene. The bonded, photochemically formed dimer does not break apart when added to the nonpolar extraction solvent since the bonds of dimerization are not due to hydrophobic interaction as with the vertically stacked polymers of anthracene. The photochemical dimer was not detected under the gas chromatographic conditions utilized and thus resulted in apparent high rates of parent compound disappearance.

Not all of the anthracene molecules in the solutions of higher concentration without dye participated in the vertical stacking mechanism given that the reaction rate obtained at these concentrations were significantly higher than the rates for the sensitized photooxidation of anthracene. The data suggest that photochemically formed dimers were being produced as well as complexes formed by vertical stacking.

When the effect of initial anthracene concentration on the rate of sensitized

photooxidation was investigated, no significant difference was found between rates of reaction. In these solutions, the sensitized photooxidation process was the primary mechanism for the disappearance of anthracene, suggesting that the self-association by vertical stacking was inhibited by the presence of the charged, cationic sensitizing dye, and the interaction of this dye with singlet oxygen.

Acridine reactions

The sensitized photodegradation of acridine showed no significant difference in the rate of reaction at the various initial concentrations examined. Unlike anthracene, acridine did not exhibit a tendency to self-associate most likely due to the charge of the molecule at the nitrogen position. This result is supported by the work of Sarma et al. (1968) in that self-association of pyridine rings by vertical stacking did not occur due to the positive charge on the pyridine nitrogen.

Effect of Mixing Substrates

The effect of combining substrates on the rate of photolysis was investigated for solutions with sensitizing dye present and in the absence of a dye. Experiments without a dye present were performed to determine whether one or more of the organic compounds in the mixture was capable of acting as a photochemical sensitizer. The experiment was repeated with 2 mg/l methylene blue added to the solutions to investigate the possible competition among substrates and molecular oxygen for the energy from the triplet sensitizer, and to determine if singlet oxygen favors the oxidation of one compound over another.

In order for a compound to be an effective sensitizer when a sensitizing dye is not present, it must first be capable of absorbing visible light energy to initiate the photochemical reaction. Secondly, there must be a substance present with an energy requirement for excitation lower than the energy available from the sensitizer. The absorbance spectrum for each compound contained in the mixtures is shown in Figure 24. The wavelength region of interest in this experiment ranges from 350 nm, where the glass cover plates block light penetration, to 420 nm, where the most actively absorbing compounds in the mixture no longer effectively absorb visible light.

Quinoline cannot perform as a photochemical sensitizer since the compound does not absorb light in the wavelength region of interest. However, acridine and anthracene absorb light energy and could possibly act as sensitizers since the first criteria, the absorption of visible light, is satisfied.

The second criteria is that a substance be present whose first excited state lies below the energy level of the excited sensitizer so that energy transfer can occur. Anthracene receives sufficient energy from the absorption of light in the 375 to 400 nm wavelength range to be raised to an excited singlet (Turro 1978) requiring 76 kcal energy (Murov 1973). The efficiency of intersystem crossing from $S_1 \rightarrow T_1$ is 75 percent so the predominant excited species of anthracene will be T_1^* with 42 kcal of energy available. Since the energy of formation for the excited state of quinoline and acridine requires 62 kcal and 45 kcal, respectively, anthracene would be unable to transfer its excited energy to these compounds requiring more energy. Molecular oxygen would however, be capable of accepting energy from the excited anthracene molecule thus forming either $^1\Sigma g$ (37 kcal) or $^1\Delta g$ (22 kcal) singlet oxygen species.

Acridine, showing a strong absorbance peak in the wavelength region of interest, requires 45 kcal of energy to be raised to its excited state. An

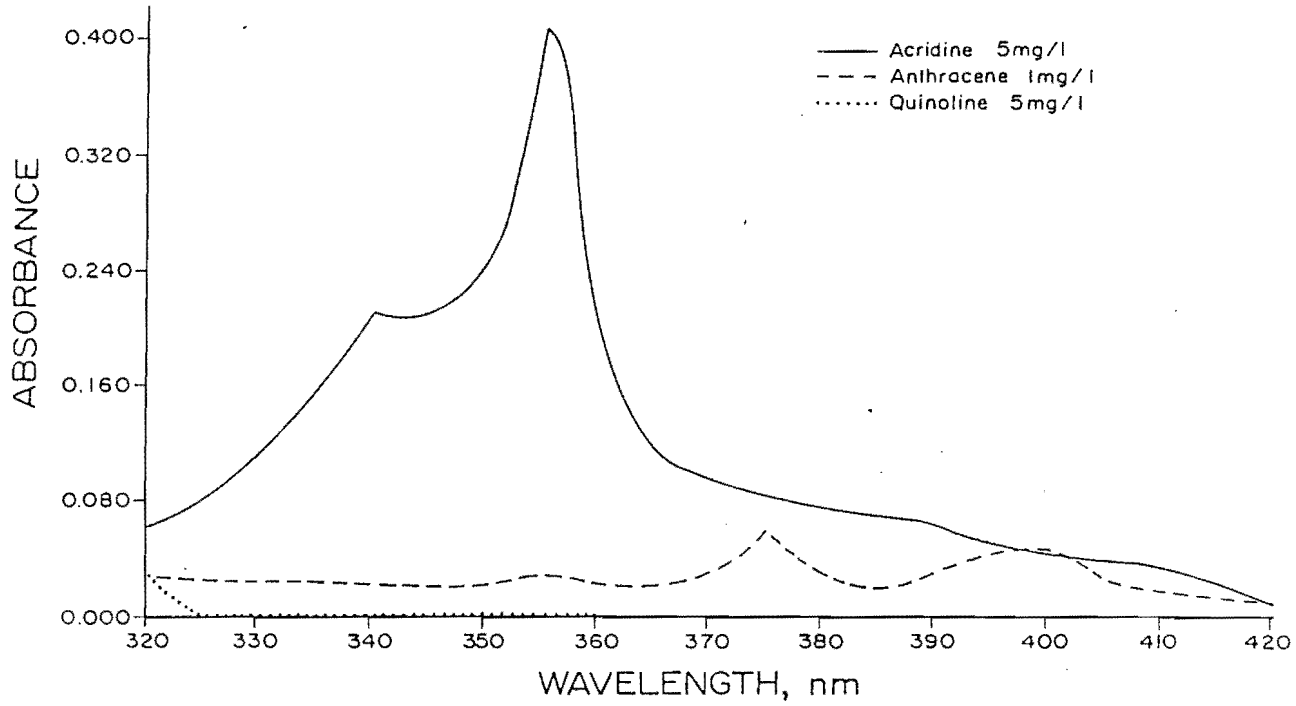

Figure 24. Absorbance spectrum for 5 mg/l acridine solutions, 5 mg/l quinoline solutions and 1 mg/l anthracene solutions.

excited acridine molecule could not transfer energy to a molecule of quinoline since quinoline requires more energy, 62 kcal, than acridine is capable of transferring. Anthracene and molecular oxygen would be capable of accepting the energy from acridine since the energy requirement for excitation for both compounds would be satisified with the energy received from an excited acridine molecule. Acridine could also be involved in a photochemical process termed energy migration (Barltrop and Coyle 1978) in which the donor and acceptor molecule are identical and is represented by Equation 30:

$$Ac^* + Ac \rightarrow Ac + Ac^* \qquad (28)$$

A comparison of observed reaction rates for the photolysis of a mixture of organic substrates with the reaction rates obtained when the organics were photolyzed individually is shown in Table 22. Rates of photoreaction for acridine and quinoline when in the mixture without dye were similar to the reaction rates observed when the compounds were photolyzed with the dye individually. If the photodegradation observed for each compound was due to oxidation via singlet oxygen, then it was likely that one of the compounds in the mixture without dye was able to sensitize the reaction and initiate the formation of singlet oxygen. Quinoline was not acting as the sensitizing molecule given that it cannot absorb visible light energy above 350 nm.

Acridine appeared to sensitize photochemical reactions as effectively as methylene blue as evidenced by the reaction rates observed for the

photolysis of quinoline. The rate of photodegradation of quinoline in a mixture without methylene blue, with acridine acting as the sensitizer, was statistically equal to the rate of decomposition achieved when quinoline was photolyzed individually in the presence of methylene blue. The same held true for the photolysis of acridine and anthracene as their reaction rates in a mixture without dye were equal to the rate of photooxidation achieved with methylene blue present when photolyzed individually.

Anthracene was the only compound which exhibited a decrease in the rate of reaction when combined with other organic substrates. When anthracene was photolyzed individually in the absence of methylene blue, dimerization occurred at a rapid rate leading to the high reaction rate. However, when acridine was included in the mixture, anthracene was unable to compete for the available visible light energy since acridine, at the experimental concentration of 5 mg/l, absorbs light more strongly (Figure 24).

The reaction rate for the photolysis of anthracene in a mixture without methylene blue was statistically greater, at the 95 percent confidence level, than the photolysis rate achieved when methylene blue was added to the mixture. In these mixtures without dye, the disappearance of anthracene was attributed to acridine-sensitized photooxidation in addition to photodimerization, although dimerization occurred at a much slower rate.

It was shown earlier that acridine was capable of sensitizing photochemical reactions with an efficiency equal to methylene blue. If the reaction rate of anthracene in a mixture without dye was greater than with dye, the difference would equal the rate of dimerization when anthracene was competing with acridine for the available light energy.

When anthracene was photolyzed in a mixture with methylene blue, the rate of reaction was significantly less than when photolyzed indivdually with methylene blue. The lower reaction rate was due to acridine absorbing light energy below 420 nm more effectively than anthracene. The primary photoreaction was consequently oxidation via singlet oxygen sensitized by methylene blue and acridine. When individually photolyzed with methylene blue, anthracene can absorb light where methylene blue cannot, and dimerization occurs, resulting in an increase of the overall reaction rate.

Analysis of Toxicity

Of the two organic compounds analyzed for toxicity, only acridine exhibited a toxic response when exposed to bacteria in the Microtox™ acute toxicity test. Anthracene was found to be non-toxic both prior to and following photolysis, in solution with methylene blue and in the absence of methylene blue.

The results of the analysis of toxicity are contained in Table 27. Acridine exhibited a toxic response when in solution prior to photolysis. The degree of toxicity increased when the solution was treated with light for 24 hours. After photolysis was completed, following 48 hours of irradiation, the degree of toxicity was not significantly changed from the 24 hour results.

The photoproducts formed during the photooxidation of acridine are more toxic than the parent compound. In addition, the stability of these compounds was suggested by the fact that the degree of toxicity did not decrease with continued irradiation. After 24 hours, 95 percent of the acridine had been photodegraded and following 48 hours of irradiation acridine was not detected in solution, yet the continued treatment with light was unable to reduce the toxicity by further degradation of the photoproducts.

Prediction of Reaction Rates

Establishing the reaction quantum yield based on laboratory kinetic data provides a means for estimating environmental photolysis rates. The reaction quantum yield of complex molecules in solution is usually independent of wavelength and light intensity (Turro 1978). Therefore, once the overall reaction quantum yield is determined for a specific compound, the reaction rate for the photolysis of the compound under different conditions may be predicted using Equation 8. Equation 8 is applicable for environmental photolysis if conditions of the actinometers of choice resemble the reaction conditions used for the photolysis of the organic compound.

From the results of this study, environmental photolysis rate predictions can be made for each of the compounds investigated, under any light conditions, by establishing the rate of reaction for the actinometer under the light conditions to which the compound will be subjected. The overall reaction quantum yield for the compound of interest is independent of light intensity and wavelength and will remain constant as will the quantum yield for the actinometer. If the compound is to undergo sensitized photolysis utilizing the same sensitizer as the actinometer, Equation 8 can be used to calculate the only unknown, the rate constant for the sensitized photooxidation of the specific compound. Correction for differences in volume and methylene blue concentration between actinometer and sample should be made if necessary as per the example calculation presented earlier.

If, however, the environmental photolysis rate prediction involves a complex mixture of organic compounds, the individual quantum yield data from this study could not be utilized. Quantum yield is not only a measure of photochemical efficiency, but also a measure of processes competing with photooxidation. Quantum yield values obtained when a compound is individually photolyzed will not necessarily equal the yield obtained when the compound is included in a mixture. Reaction pathways for degradation of the compound may differ when combined with other compounds due to competing processes involved in the excitation or deactivation of substrate molecules. One such process, capable of altering the rate of photodegradation and subsequently the quantum yield of a substrate when combined in a mixture, is the absorbance of light energy by compounds competing for light energy, for excitation and initiation of photochemical reactions.

In this study, anthracene achieved a quantum yield of 0.008 mole/ einstein when photolyzed individually with methylene blue. When the same concentration of anthracene was photolyzed in a mixture of substrates, the quantum yield decreased by over 60 percent. The decrease in yield was attributed to the absorbance of light energy by other compounds in the mixture in the same wavelength region at which anthracene could absorb light and sensitize a photoreaction. It therefore, becomes important to evaluate the absorbance characteristics of the waste prior to bench scale analysis.

Since photolysis data for individually treated compounds cannot be utilized if competing reactions within the mixture occur, bench scale analysis must be performed to determine the quantum yield for each component of the mixture. To do this, the sample must be characterized both qualitatively and quantitatively, so that the disappearance of each component due to photooxidation can be monitored with time.

An estimation of optimum pH conditions for utilization in bench scale analyses can be obtained through examination of pKa values for each waste component. Results from this study indicate that optimum reaction pH is

established at the pKa of the substrate being photolyzed.

Although the rate of reaction in sensitized photooxidation reactions was found to be independent of the initial substrate concentration, the quantum yield increased with increasing concentration. Since the quantum yield value is used in calculations for environmental rate predictions, this term must be quantified for several expected substrate concentrations during bench scale analyses.

The bench scale photooxidation analysis of the complex waste will provide the necessary data for calculating the overall reaction quantum yield for each waste component. An actinometer, utilizing the same dye as for sample photolysis will allow direct calculation of laboratory quantum yield using Equation 8.

With the laboratory data obtained for the photolysis of the complex waste, prediction of photolysis rates under natural sunlight, to be used for example, for a design of a sensitized photooxidation treatment lagoon, can be accomplished. Light intensity data are necessary for the area in which the waste will be photolyzed. If an actinometer can be run in this area, with the same sensitizer utilized in photolysis experimentation, then Equation 8 can again be used to predict the rate of photooxidation of each waste component using the reaction quantum yield calculated from lab data for each compound. Otherwise, Equation 6 should be utilized.

$$\phi_{rxn} = \frac{\Sigma I_\lambda \varepsilon_\lambda{}^a}{\Sigma I_\lambda \varepsilon_\lambda{}^c} \frac{K^c}{K^a} \phi_a \qquad (6)$$

Bench scale photolysis testing provides values for reaction quantum yield for each component of the waste. The term $\Sigma I_\lambda \varepsilon_\lambda{}^a$ can be calculated from light intensity data for laboratory lamps used in the bench scale analysis and by calculating the extinction coefficient for the actinometer over the useful wavelength range in the experiment. A relationship is established between the terms $\Sigma I_\lambda \varepsilon_\lambda{}^a$ and K^a based on laboratory data. This same relationship $\Sigma I_\lambda \varepsilon_\lambda{}^a / K^a$ will hold for any light conditions of either an artificial or natural source.

The term representing the light intensity to which the waste mixture will be exposed, $\Sigma I_\lambda \varepsilon_\lambda{}^c$, can be determined from spectroradiometer data of the light to be utilized. If spectroradiometer data are unavailable, Mabey et al. (1982) have presented values for solar radiation for latitudes of 20°N, 30°N, 40°N, and 50°N, from 296 nm to 825 nm, for each of the four seasons of the year. By choice of the appropriate intensity data from the tables presented by these authors, Equation 6 can be solved for the only unknown, the initial rate constant for each compound in the waste.

From the prediction of environmental photolysis rates, utilizing either Equations 6 or 8, a photo-sensitized treatment lagoon can be designed for anywhere in the world. Reaction rates of each component in the mixture can be obtained and the limiting rate constant used in design calculations.

ENGINEERING SIGNIFICANCE

The science of photochemistry has been studied for hundreds of years. It is only in the last decade that researchers have begun to apply the fundamental principles of photochemical reactions to the treatment of toxic and hazardous organic compounds. This research has demonstrated the utility of photooxidation for the successful treatment of hazardous waste constituents.

Sargent and Sanks (1974, 1976) and Watts (1983) provided the most engineering-oriented approach in the application of photooxidation to waste treatment by establishing optimum sensitized photooxidation conditions for several organic compounds. Reaction conditions and design parameters established by these authors are however, compound specific.

This report provides an analysis of photochemical reaction data that suggests trends in reactivity based on pKa values of both sensitizer and substrate, initial substrate concentration and light absorbance characteristics of the substrates. Estimates of photochemical reaction rates and optimum reaction conditions for a variety of compounds can now be made based on photochemical trends established in this research.

A chemical actinometer is essential in photochemical experiments and was included in this experimental design to monitor light intensity emitted by the photobench. The actinometer provides a means for calculating quantum yield values for each of the organic compounds studied, and with these quantum yield data, design of hazardous waste treatment systems using photooxidation reactions becomes possible. Since the quantum yield is independent of light intensity and wavelength, the yield values obtained for a specific compound can be utilized to predict the rate of photodegradation of that compound in a treatment lagoon under natural sunlight conditions. The following sensitized phototreatment lagoon design exemplifies the usefulness of these quantum yield data.

Design of a Sensitized Photooxidation Lagoon

Determination of flowrate

Oil shale retorting operations are expected to produce 50,000 barrels of oil per day, if and when commercialization begins (Yen 1978). Nowacki (1980) estimates that a modified in-situ retort will produce 0.52 barrels of wastewaters per barrel of oil produced. The following equation was used to determine the flow of wastewater requiring treatment for the removal of organics from a typical typical modified in-situ retort operation.

$$Q = 50{,}000 \frac{\text{bbl oil}}{\text{day}} \times 0.52 \frac{\text{bbl water}}{\text{bbl oil}} \times \frac{55 \text{ gal}}{\text{bbl}} \times \frac{3.785 \text{ liter}}{\text{gal}} \times \frac{1 \text{m}^3}{1000 \text{ liter}} = 5{,}413 \text{ m}^3/\text{day} \quad (31)$$

where

Q = wastewater flowrate, m^3/day

Design considerations

The design of a phototreatment lagoon must be based upon the rate-limiting substrate within the mixture of

compounds. The organic compounds utilized in this study were characterized as typical components of oil shale retort wastewater. The rate limiting compound in the mixture was quinoline, exhibiting the slowest reaction rate constant, 0.0028 $hour^{-1}$, and smallest quantum yield, 0.0016 mole/einstein.

Table 3 contains a chemical characterization of typical retort wastewater from the modified in-situ retort process. The pH of the waste stream is approximately 8 and since the alkalinity is extremely high, in excess of 92,000 mg/l, pH adjustment would be costly due to the alkalinity creating a high buffer capacity. Therefore, the pH of the waste stream will not be adjusted in the design presented.

The results of this study showed that the observed quantum yield and first order reaction rate constants from the photolysis of quinoline were independent of reaction pH. It was assumed for this design that the quantum yield for the photolysis of quinoline in a mixture at pH 8 would not be significantly different than the quantum yield observed when in a mixture buffered to pH 7. The quantum yield data utilized for the lagoon design would be 0.0016 mole/einstein, the value achieved in a 2 mg/l dye solution with acridine and anthracene, buffered to pH 7.

To maintain low cost of operation, the methylene blue concentration suggested is 2 mg/l. The lagoon would be designed to achieve 90 percent removal of quinoline. A plug flow reactor design would be utilized by applying the design equation (Metcalf and Eddy 1979).

$$V = \frac{Q}{k} (\ln C/C_o) \qquad (32)$$

where

V = volume, m^3

Q = flowrate, m^3/day

k = first order reaction rate constant, day^{-1}

C = effluent substrate concentration, mg/l

C_o = influent substrate concentration, mg/l

Watts (1983) has shown that a minimum of 1.0 mg/l dissolved oxygen was required to maintain photochemical reactions via singlet oxygen. Sufficient oxygen can be supplied from atmospheric oxygen to maintain the required oxygen concentration without the need for mechanical aeration.

Photooxidation reactions are independent of temperature from 5°C to 40°C (Bulla and Edgerley 1968, Watts 1983) and as such, the wastewater temperature entering the lagoon system would need no adjustment.

Actinometry

A methylene blue-tryptophan actinometer was run under natural light conditions so that an estimate of the rate of quinoline photooxidation in sunlight can be made and utilized in lagoon design.

The actinometer was run on a cloudy day so that the predicted rate of reaction for quinoline would be based on the lowest light intensity available. The rate of tryptophan decay in the actinometer was expected to be greater in natural sunlight than under laboratory lamps, so to insure that the rate was not limited, the tryptophan concentration was doubled. The actinometer contained 3 mg/l methylene blue in a 450 ml solution which was buffered to pH 9. Table 30 shows the results of the actinometer photolysis.

Determination of rate constants

The first order reaction rate constant, k^a, was 0.9491 $hour^{-1}$. This rate was converted to an initial rate constant using Equation 33:

Table 30. Results from tryptophan-methylene blue actinometer performed under natural light conditions on a cloudy day at 42°N latitude.

Time (Hours)	Tryptophan Concentration (mg/l)	$\ln C/C_o$
0	43.45	0
0.0833	40.47	-0.071
0.1667	36.91	-0.163
0.2500	34.42	-0.233

$$K^a = \frac{0.9491}{\text{hour}} \times \frac{1 \text{ hour}}{3600 \text{ sec}}$$

$$\times 2.13 \times 10^{-4} \frac{\text{mole}}{\text{liter}} \times 0.45 \text{ liter}$$

$$= 2.52 \times 10^{-8} \frac{\text{mole}}{\text{sec}} \qquad (33)$$

The predicted rate of quinoline photooxidation on a cloudy day can be determined using the quantum yield observed in the laboratory, 0.0016 mole/einstein, when quinoline was combined in a mixture and applying Equation 17.

$$\phi_{rxn} = \frac{K^c}{K^a} \phi_a C_a \qquad (17)$$

The correction factor, C_a, for a 2 mg/l methylene blue solution, normalized to a 3 mg/l methylene blue actinometer is 0.98/0.59 as taken from Table 8.

Solving for the only unknown, K^c,

$$0.0016 = \frac{K^c}{2.52 \times 10^{-8} \text{ mole/sec}}$$

$$\frac{1 \text{ mole}}{\text{einstein}} \frac{0.98}{0.59} \qquad (34)$$

The initial rate constant, K^c, is 2.43 x 10^{-11} mole/sec and is converted to the first order rate constant, k^c, using Equation 35.

$$k^c = 2.43 \times 10^{-11} \frac{\text{mole}}{\text{sec}} \times \frac{3600 \text{ sec}}{\text{hour}}$$

$$\times \frac{\text{liter}}{3.88 \times 10^{-5} \text{ mole}} \times \frac{1}{0.20 \text{ liter}}$$

$$= \frac{0.0113}{\text{hour}} = \frac{0.2706}{\text{day}} \qquad (35)$$

Design volume

Using the plug flow reactor design equation, and assuming a 90 percent reduction of substrate, the design volume is:

$$V = 5413 \frac{m^3}{\text{day}} \frac{\text{day}}{0.2703} \frac{\ln 0.5}{5.0}$$

$$= 46{,}111 \text{ m}^3 \qquad (36)$$

Design area

The area of the lagoon is calculated using Equation 37.

$$A = V/D \qquad (37)$$

where

A = area, acres

D = depth, cm

To determine minimum lagoon depth, the extinction coefficient for a 2 mg/l methylene blue solution is required, and is given as:

$$\varepsilon = \frac{A}{MB\,\ell} \qquad (38)$$

where

ε = extinction coefficient, $M^{-1}cm^{-1}$

A = average methylene blue absorbance from 570 to 700 nm

MB = molar concentration of methylene blue, mole/l

ℓ = path length, cm

For a 2 mg/l solution of methylene blue the extinction coefficient is calculated using Equation 39.

$$\varepsilon = \frac{0.194}{5.35 \times 10^{-6} \text{ mole/liter}} \times 1 \text{ cm}$$

$$= 36{,}268\ M^{-1}cm^{-1} \qquad (39)$$

The depth of the lagoon is determined by the depth of effective light penetration. Complete light absorbance occurs when the system reaches 2.0 absorbance units. The minimum depth is then calculated using Equation 40.

$$36{,}268\ M^{-1}cm^{-1} = \frac{2.0}{5.35 \times 10^{-6}\ M(1)} \qquad (40)$$

Solving for the depth, ℓ, achieves a minimum depth of 10.3 cm.

For a facultative lagoon system, depth can range from 2 to 5 feet (Metcalf and Eddy 1979). Sufficient mixing is expected from wind action, eddy diffusion and thermal mixing to occasionally bring wastewater from the deeper part of the lagoon to the surface. In addition, water loss due to evaporation will require a lagoon depth greater than 10 cm for the most efficient utilization of light.

A 2 foot (61 cm) lagoon depth was chosen for this design based on a minimum of 10 cm for effective light penetration and increasing depth to 61 cm, to account for evaporation, wind action, eddy diffusion and thermal mixing.

Solving Equation 41 results in the area of the lagoon:

$$A = 46{,}000\ m^3 \times \frac{1}{50\ cm} \times \frac{100\ cm}{1\ m} \times \frac{1\ ft^2}{0.0929\ m^2} \times \frac{1\ acre}{43{,}560\ ft^2}$$

$$= 18.6 \text{ acres} \qquad (41)$$

Based on the results of this research, a photooxidation treatment lagoon 61 cm deep, covering 19 acres with a retention time of 8.5 days would be sufficient to remove 90 percent of the most difficult to treat waste component. Lagoon design can be altered for light intensity changes or changes in waste composition.

Effluent concentrations

Effluent concentrations of acridine and anthracene can be predicted by estimating the initial rate constant of each compound using Equation 34 with the reaction quantum yield observed for each compound and the natural light actinometer data. The estimated initial rate constants for anthracene and acridine are 4.55×10^{-11} mole/sec and 9.25×10^{-11} mole/sec, respectively. Conversion of the initial rate constant to a first order reaction rate constant is performed by following Equation 35. Finally, the percent removal of acridine and anthracene under the lagoon design conditions is calculated using Equation 36. Substituting the design volume, flow rate values and the first order reaction rate constant, allows for the determination of the only unknown, the removal rate achieved for each compound.

Anthracene is expected to achieve 100 percent removal under the design

condition presented, while 99.9 percent of acridine would be removed.

Note that photoproducts from the photolysis of acridine exhibited greater toxicity than the parent compound as indicated by the results from this study. The proposed utilization of a phototreatment lagoon is as a pretreatment process prior to biological oxidation. The increase in toxicity attributed to the photoproducts of acridine would not affect the operation of a biological treatment process if the photoproducts are found to be more biodegradable than the refractory parent compound. If, however, the photoproducts are shown to be as recalcitrant as acridine, in addition to representing a higher degree of toxicity, an alternative pretreatment process would need to be implemented to remove acridine prior to photooxidation.

Chemical costs

Methylene blue costs for the given lagoon design are based on the estimate presented by Watts (1983) of $13.00/kg and adjusted to January 1985 prices (Chemical Engineering 1985) as $12.50/kg. The following equation was used to determine the annual chemical cost for the proposed lagoon.

$$2 \text{ mg/l} \times 1.43 \text{ mgd} \times \frac{8.34 \text{ lb}}{10^6 \text{ gal}} \times \frac{\$12.60}{\text{kg}} \times \frac{1 \text{ kg}}{2.2 \text{ lb}} = \$136.61/\text{day}$$

$$= \$49{,}862/\text{year}$$

SUMMARY AND CONCLUSIONS

Photooxidation studies were conducted to determine the sensitivity of four selected organic compounds to oxidation via singlet oxygen produced from the absorption of light energy. Kinetic rate studies involving the degradation of the substrates were performed and the observed first order reaction rate constants were used as a measure of the compounds' reactivity and susceptibility to photooxidation. Optimum photoreaction conditions for each compound were established based on sensitizer concentration and reaction pH.

The effect of initial substrate concentration on the rate of reaction was investigated using acridine and anthracene as photochemical substrates. Optimum reaction conditions determined in earlier experiments were used as the reaction conditions for this phase of testing.

Anthracene, acridine, and quinoline, were included in the analysis of the effect of combining substrates on the rate of reaction to determine whether these organic substrates could act as sensitizers in photochemical reactions.

Toxicity analyses were performed to determine if photoproducts from the oxidation of anthracene and acridine were actually more toxic than the parent compound.

An actinometer, utilizing tryptophan and methylene blue in a sensitized photoreaction, was run routinely throughout the experimentation. The actinometer results provided a means of determining the average incident light intensity for the absorbing wavelengths of methylene blue, as well as providing necessary data for the calculation of reaction quantum yields. Although not a measure of substrate reactivity, quantum yields were utilized as supporting data to the results obtained and conclusions drawn from comparisons of reaction rate constants. Quantum yield values were utilized in calculations for prediction of environmental reaction rate constants which are necessary for engineering design of photooxidation treatment lagoons.

From this research, the following conclusions can be drawn:

1. Optimum pH for sensitized photooxidation reactions can be predicted based on the pKa of the compound. Methylene blue-sensitized photooxidation of acridine and quinoline was most efficient at a reaction pH of 5, the pKa of each compound.

2. The optimum pH for anthracene photolysis, in the presence of methylene blue, occurred at pH 7. In the absence of methylene blue, photodimerization of anthracene was theorized from experimental evidence. Optimum reaction pH for photodimerization occurred at pH 9.

3. The rate of sensitized photooxidation of acridine and anthracene are independent of the initial substrate concentration. Although the first order rate of reaction does not change with an increase in substrate concentration, the mass of substrate oxidized per unit time increases with concentration.

4. The rate of direct photolysis of anthracene is dependent on the initial concentration of anthracene and will increase with increasing

concentration up to an optimum rate, after which increase in concentration tends to cause self-association by vertical stacking and a decrease in reaction rate.

5. Acridine, showing strong absorbance of light energy from 350 to 420 nm, is capable of sensitizing photoreactions involving anthracene and quinoline as efficiently as methylene blue.

6. Anthracene absorbs sufficient energy from light wavelengths of 350 to 420 nm to sensitize a self-associated photodimerization reaction, in addition to sensitizing photooxidation reactions via singlet oxygen. However, in the presence of compounds capable of successfully competing with anthracene for absorbance of light energy, the rate of photodimerization and photooxidation decreased significantly.

7. Absorbance spectra of compounds to be degraded by photooxidation become critically important to the understanding of overall reactions when substrates are capable of competitively absorbing visible light energy and sensitizing photooxidation reactions.

8. Acridine was toxic prior to and following photolysis, with the degree of toxicity increasing for photolyzed samples. Unidentified reaction products from the photooxidation of acridine appear to be more toxic than the parent compound as indicated by the Beckman Microtox Toxicity Analyzer. Anthracene was non-toxic both before and after photolysis.

RECOMMENDATIONS FOR FURTHER STUDY

Further research is necessary to expand the photochemical concepts and engineering applications developed in this study.

1. Prediction of optimum reaction pH based on the pKa of the substrate should be further verified by examining compounds with a wide range of pKa values.

2. The efficiency of the sensitized photooxidation process based on dye pKa values with respect to that of the substrate being photolyzed should be established.

3. An actinometer should be developed for use in calculating design parameters, such as quantum yield and reaction rate constants, for systems of substrate mixtures without sensitizing dyes present so that lagoon treatment systems can be designed without sensitizing dye.

4. Prediction of reaction rates and optimum photooxidation conditions based on a substrates' physical and chemical properties should be further investigated. An effort should be made to establish the correlations between ring structure, energy of triplet formation and sensitized photooxidation rates.

5. A correlation between the rate of photooxidation and the amount of available energy absorbed by a system per wavelength of light should be investigated.

6. The nature and biological recalcitrance of photooxidation products of selected compounds of environmental significance should be studied further.

REFERENCES

Acher, A. J., and I. Rosenthal. 1977. Dye-sensitized-photooxidation--a new approach to the treatment of organic matter in sewage effluents. Water Res. 11:557-562.

Altschuller, A. P., and J. J. Bufalini. 1971. Photochemical aspects of air pollution: A review. Environ. Sci. and Tech. 5:39-64.

Barltrop, J. A., and J. D. Coyle. 1978. Principles of photochemistry. John Wiley and Sons. Chichester, England. 213 p.

Bellin, J. S., and C. A. Yankus. 1968. Influence of dye binding on the sensitized photooxidation of amino acids. Archives of Biochem. and Biophysics 123:18-28.

Bonneau, R., R. Pottier, O. Bagno, and J. Joussot-Dubien. 1975. pH dependence of singlet oxygen production in aqueous solutions using thiazine dyes as photosensitizers. Photochem. Photobiol. 21:159-163.

Brauer, H. D., W. Drews, R. Schmidt, G. Gauglitz, and S. Hubig. 1982. Heterocoerdianthrone: A new actinometer for the visible (400-580 nm) range. J. of Photochem. 20:335-340.

Bulla, C. D., and E. Edgerley, Jr. 1968. Photochemical degradation of refractory organic compounds. JWPCF 40:546-556.

Calvert, J. G., and J. N. Pitts. 1966. Photochemistry. John Wiley & Sons, New York, New York. 899 p.

Coomes, R. M. 1979. Carcinogenic testing of oil shale materials. Twelfth Oil Shale Symp. Proc., Colorado School of Mines. pp. 311-320.

Cowan, D. O., and R. L. Drisko. 1976. Elements of organic photochemistry. Plenum Press, New York, New York. 586 p.

Crittenden, B. D., and R. Long. 1976. The mechanism of formation of polynuclear aromatic compounds in combustion systems. pp. 209-223. In: R. Freudenthal and P. W. Jones (eds.). Carcinogenesis-a comprehensive survey. Vol. 1. Polynuclear aromatic hydrocarbons-chemistry, metabolism, and carcinogenesis. Raven Press, New York, New York.

Dinneen, G. U. 1974. Oil shale and its potential utilization. Symposium Proceedings: Environmental Aspects of Fuel Conversion Technology. EPA-650/2-74-118. St. Louis, Missouri. pp. 341-352.

Dulin, D., and T. Mill. 1982. Development and evaluation of sunlight actinometers. Environ. Sci. and Tech. 16:815-820.

Federal Register. Guidelines establishing test procedures for the analysis of pollutants. U.S. Environmental Protection Agency. 44(233) December 3. pp. 69514-69516.

Foote, C. S. 1968. Mechanisms of photosensitized oxidation. Science 162:963-970.

Fox, J. P. 1980. Water related impacts of in-situ oil shale processing. LBL-6300. Lawrence Berkeley Laboratory, Berkeley, California.

Fox, J. P., D. E. Jackson, and R. H. Sakaji. 1980. Potential uses of spent shale in the treatment of oil shale retort waters. Thirteenth Oil Shale Symp. Proc., Colorado School of Mines. Golden, Colorado. pp. 311-320.

Fruchter, J. S., and C. L. Wilkerson. 1980. Characterization of oil shale effluents. Prepared for the U.S. Department of Energy, preliminary draft. PNL-SA-8816. Pacific Northwest Laboratory, Richland, Washington.

Gonzalez, M. J., and N. Langerman. 1977. A thermodynamic description of the self-association of flavin monomucleotide. Archives of Biochem. and Biophysics. 180:75-81.

Gurnani, S., M. Arifuddin, and K. T. Augusti. 1966. Effect of visible light on amino acids. I. - Tryptophan. Photochem. Photobiol. 5:495-505.

Harrison, R. M., R. Perry, and R. A. Welling. 1975. Review paper. Polynuclear aromatic hydrocarbons in raw, potable, and waste waters. Water Res. 9:331-346.

Hartstein, A. M., and B. M. Harney. 1981. The Department of Energy's oil shale RD & D program: An overview. pp. 1-12. In: H. C. Stauffer (ed.). Oil shale, tar sands and related materials. ACS Symposium Series 163. Washington, D.C.

Hatchard, C. G., and C. A. Parker. 1956. A new sensitive chemical actinometer. II. Potassium ferrioxalate as a standard chemical actinometer. Royal Soc. Proc. (London). Series A235:518-536.

Heelis, P. F., B. J. Parson, G. O. Phillips, and J. F. McKellar. 1981. The flavin sensitized photooxidation of ascorbic acid; A continuous and flash photolysis study. Photochem. Photobiol. 33:7-13.

Hicks, R. E., R. F. Probstein, I. Wei, D. S. Farrier, J. Lotwala, and T. E. Phillips. 1980. Wastewater treatment and management at oil plants. Thirteenth Oil Shale Symp. Proc., Colorado School of Mines. Golden, Colorado. pp. 321-334.

Houban-Herin, N., C. M. Calberg-Bacq, J. Piette, and A. Van de Vorst. 1982. Mechanisms for dye-mediated photodynamic action: Singlet oxygen production, deoxyguanosine oxidation and phage inactivating efficiencies. Photochem. Photobiol. 36:297-306.

Israelsen, C. E., V. D. Adams, J. C. Batty, D. B. George, T. C. Hughes, A. J. Seierstad, H. C. Wang, and H. P. Kuo. 1980. Use of saline water in energy development. Water Resources Planning Series. Utah Water Research Laboratory, UWRL/P-80/04. Utah State University, Logan, Utah. 128 p.

Jones, B. M., R. H. Sakaji, and C. G. Daughton. 1982. Physico-chemical treatment methods for oil shale wastewater: Evaluation as aids to biooxidation. Fifteenth Oil Shale Symp. Proc., Colorado School of Mines. Golden Colorado. pp. 581-597.

Kauzmann, W. 1959. Some factors in the interpolation of protein denaturation. pp. 1-64. In: C. B. Anfinsen and M. L. Anson (eds.). Advances in protein chemistry. Academic Press, New York, New York.

Kearns, D. R. 1971. Physical and chemical properties of singlet molecular oxygen. Chem Rev. 71:395-427.

Kearns, D. R., R. A. Hollins, A. U. Khan, R. W. Chambers, and P. Radlick. 1967a. Evidence for the participation of ^{1}g and ^{1}g oxygen in dyesensitized photooxidation reactions. I. Jour. Amer. Chem. Soc. 89:5455-5456.

Kearns, D. R., R. A. Hollins, A. U. Khan, and P. Radlick. 1967b. Evidence for the participation of ^{1}g and ^{1}g oxygen in dyesensitized photooxidation reactions. II. Jour. Amer. Chem. Soc. 89: 5456-5457.

Kingsbury, G. L., R. C. Sims, and J. B. White. 1979. Multimedia environmental goals for environmental assessment; Vol. IV. MEG charts and background information summaries (catagories 13-26). EPA-600/7-79-176b. Research Triangle Park, North Carolina. 494 p.

Klieve, J. R., G. D. Rawlings, and J. R. Hoeflein. 1981. Assessment of oil shale retort wastewater treatment and control technology: Phases I and II. EPA 600/7-81-081. Cincinnati, Ohio.

Kochevar, I. E., R. B. Armstrong, J. Einbinder, R. R. Walther, and L. C. Harber. 1982. Coal tar phototoxicity: Active compounds and action spectra. Photochem. Photobiol. 36:65-69.

Larson, R. A., T. L. Bott, L. L. Hunt, and K. Rogenmuser. 1979. Photooxidation products of a fuel oil and their antimicrobial activity. Environ. Sci. and Tech. 13:965-969.

Lee, M. L., and R. A. Hites. 1976. Characterization of sulfur-containing polycyclic aromatic compounds in carbon black. Anal. Chem. 48:1890-1893.

Lee, M. L., M. Novotny, and K. D. Bartle. 1976. Gas chromatography/ mass spectrometric and nuclear magnetic resonance spectrometric studies of carcinogenic polynuclear aromatic hydrocarbons in tobacco and marijuanna smoke condensates. Anal. Chem. 48:405-416.

Lee, M. L., M. V. Novotny, and K. D. Bartle. 1981. Analytical chemistry of polycyclic aromatic compounds. Academic Press, New York, New York. 462 p.

Leighton, P. A. 1961. Photochemistry of air pollution. Academic Press, New York, New York. 300 p.

McLaren, A. D., and D. Shugar. 1964. Photochemistry of proteins and nucleic acids. A Pergamon Press Book. MacMillan Company, New York, New York. 449 p.

Maase, D. L. 1980. An evaluation of polycyclic aromatic hydrocarbons from processed oil shales. PhD Dissertation, Utah State University, Logan, Utah.

Maase, D. L., and V. D. Adams. 1983. Polycyclic aromatic hydrocarbons - are they a problem in processed oil shales? UWRL/Q-83/07, Utah Water Research Laboratory, Utah State University, Logan, Utah.

Mabey, W. R., T. Mill, and D. G. Hendry. 1982. Photolysis in water. pp. 49-102. In: Laboratory protocols for evaluating the fate of organic chemicals in air and water. EPA-600/3-82-022. Athens, Georgia.

Malaney, G. W., P. A. Lutin, J. J. Cibulka, and L. H. Hickerson. 1967. Resistance of carcinogenic compounds to oxidation by activated sludge. JWPCF 39:2020-2029.

Mercer, B. W. 1980. Environmental control technology for oil shale wastewater. Battelle, Pacific Northwest Laboratory. Report to DOE. DOE/EV-0081.

Metcalf and Eddy, Inc. 1979. Wastewater engineering: treatment, disposal, reuse. McGraw Hill, New York, New York. 920 p.

Mousseron-Canet, M., and J. C. Mani. 1972. Photochemistry and molecular reactions. Israel Program for Scientific Translations. Jerusalem, Israel. 268 p.

Murov, S. L. 1973. Handbook of photochemistry. Marcel Dekker, Inc., New York, New York. 272 p.

Naeger, Betty-Ann. 1985. Engineering treatment of hazardous wastewaters utilizing dye-sensitized photooxidation. M.S. thesis, Utah State University, Logan, Utah. 201 p.

Neckers, D. C. 1967. Mechanistic organic photochemistry. Reinhold Publishing Corporation, New York, New York. 320 p.

Neff, J. M. 1979. Polycyclic aromatic hydrocarbons in the environment: Sources, fates and biological effects. Applied Science Publishers, LTD. Essex, England. 262 p.

Nowacki, P. (ed.). 1980. Health hazards and pollution control in synthetic liquid fuel conversion. Noyes Data Corporation. Park Ridge, New Jersey. 511 p.

Nowacki, P. (ed.). 1981. Oil shale technical data handbook. Noyes Data Corporation. Park Ridge, New Jersey. 309 p.

Pelroy, R. A., and M. R. Petersen. 1979. Use of Ames Test in evaluation of shale oil fractions. Environ. Health Perspect. 30:191-203.

Pfeffer, F. M. 1974. Pollutional problems and research needs for an oil shale industry. EPA-600/2-74-067. Ada, Oklahoma. 86 p.

Pitts, J. N., F. Wilkinson, G. S. Hammond. 1963. The vocabulary of photochemistry. pp. 1-21. In: J. N. Pitts, W. A. Noyes, and G. S. Hammond (eds.). Advances in photochemistry. Vol. 1. John Wiley and Sons, Inc. New York, New York. 484 p.

Plimmer, J. R. 1971. Principles of photodecomposition of pesticides. pp. 279-289. In: Degradation of synthetic organic molecules in the biosphere. National Academy of Science, Washington D. C.

Porter, G., and F. Wilkinson. 1961. Energy transfer from the triplet state. Royal Soc. Proc. (London). Series A264:1-18.

Rao, T. K., J. L. Eppler, M. R. Guerin, J. J. Schmidt-Collerus, and L. Leffler. 1979. Biological monitoring of oil shale products and effluents using short-term genetic analysis. In: Oil Shale Symposium: Sampling, analysis and quality assurance. EPA-600/9-80-022. Philadelphia, Pennsylvania.

Rao, T. K., R. W. Larimer, C. E. Nix, and J. L. Eppler. 1981. Mutagenicity testing of aqueous materials from alternate fuel production. L. P. Jackson, and C. C. Wright, (eds.). Amer. Soc. for Testing Materials. Special Technical Publication 720. Philadelphia, Pennsylvania.

Raphaelian, L. A., and W. Harrison. 1981. Organic constituents in process water from the in-situ retorting of oil from oil shale kerogen. Argonne National Laboratory. AN/PAG-5. Argonne, Illinois.

Redente, E. F., W. J. Ruzzo, C. W. Cook, and W. A. Berg. 1981. Retorted oil shale characteristics and reclamation. pp. 128-138. In: K. K. Peterson (ed.). Oil shale, the environmental challenges. Colorado School of Mines Press, Golden, Colorado.

Santodonato, J., and P. H. Howard. 1981. Azaarenes: sources, distribution, environmental impact and health effects. Hazard assessment of chemicals. Current developments, Vol. 1. 1:421-440. Academic Press, New York, New York.

Sargent, J. W., and R. L. Sanks. 1974. Light energized oxidation of organic wastes. JWPCF 46:2547-2554.

Sargent, J. W., and R. L. Sanks. 1976. Dye-catalyzed oxidation of industrial wastes. Jour. Environ. Engin. Div., Am. Soc. Civil Eng. 102:879-895.

Sarma, R. H., P. Dannies, and N. O. Kaplan. 1968. Investigations of inter- and intramolecular interactions in flavin-adenine and dinucleotide by proton magnetic resonance. Biochemistry. 7:4359-4367.

Scheier, A., and D. Gominger. 1976. A preliminary study of the toxic effects of irradiated vs. non-irradiated water soluble fractions of No. 2 fuel oil. Bull. Environ. Contam. and Toxicol 16:595-603.

Schmeltz, I., and D. Hoffmann. 1976. Formation of polynuclear aromatic hydrocarbons from combustion of organic matter. pp. 225-239. In: R. Freudenthal and P. W. Jones (eds.). Carcinogenesis--a comprehensive survey. Vol. 1. Polynuclear aromatic hydrocarbons-chemistry, metabolism, and carcinogenesis. Raven Press, New York, New York.

Smith, E. J. 1971. Apparatus for photochemical experimentation. pp. 3-42. In: J. M. Fitzgerald (ed.). Analytical photochemistry and photochemical analysis-solids, solutions, and polymers. Marcel Dekker, Inc., New York, New York.

Snipes, W., G. Keller, J. Woog, T. Vickray, R. Deering, and A. Keith. 1979. Inactivation of lipid-containing viruses by hydrophobic photosensitizers and near-ultraviolet radiation. Photochem. Photobiol. 29:785-790.

Spikes, J. D., and R. Straight. 1967. Sensitized photochemical processes in biological systems. Ann. Rev. Phys. Chem. 18:409-440.

Steel, R. G., and J. H. Torrie. 1980. Principles and procedures of statistics. A biometrical approach. McGraw-Hill Book Company, New York, New York. 633 p.

Tabek, H. H., S. A. Quave, C. I. Mashni, and E. F. Barth. 1981. Biodegradability studies with organic priority pollutant compounds. JWPCF 53:1503-1518.

Ts'o, P. O. P., and S. I. Chan. 1964. Interaction and association of bases and nucleosides in aqueous solutions. II. Association of 6-methylpurine and 5-bromouridine and treatment of multiple equilibria. Amer. Chem. Soc. 86:4176-4180.

Turro, N. J. 1978. Modern molecular photochemistry. The Benjamin/Cummings Publishing Co., Inc. Menlo Park, California. 628 p.

U. S. Department of the Interior. 1973. Final environmental statement for the prototype oil shale leasing program. Vol. I: Regional impacts of oil shale development. No. 2400-00785. Washington, D.C.

U. S. Environmental Protection Agency. 1976. Rationale for recommended list of priority pollutants. Memo to director of Effluent Guidelines Division. November 19. Washington, D.C.

U. S. Environmental Protection Agency. 1978. Introduction to environmental statistics-self-instruction course. SI473. #8. Research Triangle Park, North Carolina. 4 p.

Wagner, S., W. D. Taylor, A. Keith, and W. Snipes. 1980. Effect of acridine plus near ultraviolet light on escherichia coli membranes and DNA in vivo. Photochem. Photobiol. 32:771-779.

Wasserman, H. H., and R. W. Murray. 1979. Singlet oxygen. Academic Press, New York, New York. 684 p.

Watts, R. J. 1983. The development of design criteria for the construction of sensitized photooxidation lagoons for the treatment of toxic and biologically recalcitrant industrial wastes. PhD Dissertation, Utah State University, Logan, Utah.

Yen, T. F. 1978. Oil shale of the United States-a review. pp. 1-17. In: T. F. Yen (ed.). Science and technology of oil shale. Ann Arbor Science. Ann Arbor, Michigan.

Young, R. H., K. Wehrly, and R. L. Marten. 1971. Solvent effects in dye-sensitized photooxidation reactions. Jour. Am. Chem. Soc. 93:5774-5779.

Zepp, R. G., and D. M. Cline. 1977. Rates of direct photolysis in aquatic environment. Environ. Sci. and Tech. 11:359-366.

Zepp, R. G., N. L. Wolfe, G. L. Baughman, and R. C. Hollis. 1977. Singlet oxygen in natural water. Nature 267:421-423.

Appendix A

Supporting Data Reaction Rate Constants

Table 31. Results from triplicate analyses of 5 mg/l acridine solutions; reaction rate constants from sensitized and direct photooxidations.

	Methylene Blue Concentration, mg/l								
	10			5			2		
pH	Run 1	Run 2	Run 3	Run 1	Run 2	Run 3	Run 1	Run 2	Run 3
3				-0.0702	-0.0674	-0.0450	-0.0443	-0.0650	-0.0650
5				-0.0808	-0.0207	-0.1456	-0.0979	-0.1770	-0.1214
7	-0.0138	-0.0247	-0.0136	-0.0219	-0.0202	-0.0152	-0.0166	-0.0150	-0.0156
9	-0.0058	-0.0023	-0.0016	-0.0049	-0.0063	-0.0032	-0.0072	+0.0004	-0.0023
11	-0.0072	-0.0121	-0.0067	-0.0112	-0.0121	-0.0044	-0.0045	-0.0028	-0.0039

Table 31. Continued.

	Methylene Blue Concentration, mg/l					
	1			0		
pH	Run 1	Run 2	Run 3	Run 1	Run 2	Run 3
3	-0.0278	-0.0218	-0.0204	-0.0252	-0.0049	-0.0608
5	-0.1419	-0.1319	-0.1141	-0.0409	-0.0815	-0.0744
7				-0.0151	-0.0079	-0.0167
9				-0.0067	-0.0075	-0.0068
11				-0.0043	-0.0115	-0.0021

Table 32. Results from triplicate analyses of 1 mg/l anthracene solutions; reaction rate constants from sensitized and direct photooxidations.

	Methylene Blue Concentration, mg/l								
	5			2			0		
pH	Run 1	Run 2	Run 3	Run 1	Run 2	Run 3	Run 1	Run 2	Run 3
3	-0.0372	-0.0717	-0.0183	-0.0536	-0.0647	-0.0472	-0.5849	-0.3762	-0.6011
5	-0.0341	-0.0814	-0.1233	-0.0655	-0.0844	-0.0483	-1.1790	-1.0760	-1.0030
7	-0.1095	-0.1977	-0.1713	-0.0841	-0.0880	-0.0532	-1.1819	-1.8641	-0.9997
9	-0.0768	-0.0973	-0.0663	-0.0539	-0.0410	-0.0725	-3.64	-4.26	-2.81
11	-0.0536	-0.0520	-0.0425	-0.0541	-0.0470	-0.0527	-2.28	-2.597	-2.336

Table 33. Results from triplicate analyses of 5 mg/l quinoline solution; reaction rate constants from sensitized and direct photooxidations.

	Methylene Blue Concentration, mg/l					
	5			0		
pH	Run 1	Run 2	Run 3	Run 1	Run 2	Run 3
3	-0.0069	-0.0015	-0.0026	-0.0042	-0.0036	-0.0029
5	-0.0031	-0.0016	-0.0029	-0.0037	-0.0032	-0.0033
7	-0.0030	-0.0017	-0.0019	-0.0027	-0.0003	-0.0015
9	-0.0054	-0.0013	-0.0023	-0.0027	-0.0003	-0.0014
11	+0.0003	-0.0017	-0.0011	+0.00006	-0.0003	-0.0007

Table 34. Observed reaction rate constants from the photolysis of a mixture containing anthracene, acridine and quinoline.

Compound	pH	Methylene Blue Concentration mg/l	Run 1	Run 2	Run 3
Anthracene	7	2	-0.0310	-0.0371	-0.0404
Anthracene	7	0	-0.0680	-0.0460	-0.0519
Acridine	7	2	-0.0146	-0.0191	-0.0113
Acridine	7	0	-0.0260	-0.0183	-0.0115
Quinoline	7	2	-0.0035	-0.0028	-0.0022
Quinoline	7	0	-0.0073	-0.0026	-0.0020

Table 35. Observed reaction rate constants from experiments investigating tne effect of initial anthracene concentration on the rate of photolysis.

Initial Substrate Concentration mg/l	Methylene Blue Concentration 2 mg/l pH 7			Methylene Blue Concentration 0 mg/l pH 9		
	Run 1	Run 2	Run 3	Run 1	Run 2	Run 3
0.5	-0.0938	-0.0170	-0.0524	-1.572	-1.3003	-0.9901
1.0	-0.0510	-0.0384	-0.0898	-3.826	-4.029	-3.116
2.0	-0.0271	-0.0256	-0.0378	-0.3116	-0.8084	-0.5624
5.0	-0.0500	-0.0282	-0.0249	-0.4143	-0.5887	-0.8763
10.0	-0.0153	-0.0290	-0.0270	-0.3976	-0.4144	-0.5162

Table 36. Observed reaction rate constants from experiments investigating the effect of initial acridine concentration on the rate of photolysis.

Initial Substrate Concentration mg/l	Methylene Blue Concentration 2 mg/l pH 5				
	Run 1	Run 2	Run 3	Mean	Conf. Limit (95%)
1.0	-0.0951	-0.0835	-0.0883	-0.0890	±0.0145
2.0	-0.0101	-0.0723	-0.0826	-0.0856	±0.0372
5.0	-0.0783	-0.0968	-0.0808	-0.0853	±0.0249
10.0	-0.0787	-0.0788	-0.0790	-0.0788	±0.0004
15.0	-0.0834	-0.0911	-0.0909	-0.0885	±0.0109

Appendix B

Supporting Data Reaction Quantum Yields

Table 37. Summary table from triplicate analyses of the photolysis of 5 mg/l acridine solutions; average incident light intensity, reaction rate constants from actinometry, reaction rate constants from photolysis, absorbance correction factor, and reaction quantum yields.

pH	Methylene Blue Concentration mg/l	Run #	Average Incident Light Intensity $W/m^2/nm$	K^a mole/sec	K^c mole/sec	Absorbance Correction Factor	Reaction Quantum Yield mole/einstein
3	1	1	0.085	5.88×10^{-9}	4.31×10^{-11}	.98/.36	0.0200
3	1	2	0.089	6.12×10^{-9}	3.38×10^{-11}	.98/.36	0.0151
3	1	3	0.105	7.22×10^{-9}	3.17×10^{-11}	.98/.36	0.0119
5	1	1	0.085	5.88×10^{-9}	2.20×10^{-10}	.98/.36	0.1019
5	1	2	0.089	6.12×10^{-9}	2.05×10^{-10}	.98/.36	0.0911
5	1	3	0.105	7.22×10^{-9}	1.77×10^{-10}	.98/.36	0.0668
3	2	1	0.086	5.96×10^{-9}	6.88×10^{-11}	.98/.59	0.0192
3	2	2	0.091	6.26×10^{-9}	1.01×10^{-10}	.98/.59	0.0268
3	2	3	0.093	6.39×10^{-9}	1.01×10^{-10}	.98/.59	0.0262
5	2	1	0.086	5.96×10^{-9}	1.52×10^{-10}	.98/.59	0.0424
5	2	2	0.091	6.26×10^{-9}	2.75×10^{-10}	.98/.59	0.0729
5	2	3	0.093	6.39×10^{-9}	1.88×10^{-10}	.98/.59	0.0490
7	2	1	0.086	5.96×10^{-9}	2.58×10^{-11}	.98/.59	0.0072
7	2	2	0.091	6.26×10^{-9}	2.33×10^{-11}	.98/.59	0.0062
7	2	3	0.093	6.39×10^{-9}	2.42×10^{-11}	.98/.59	0.0063

Table 38. Summary table from triplicate analyses of the photolysis of 5 mg/l acridine solutions; average incident light intensity, reaction rate constants from actinometry, reaction rate constants from photolysis, absorbance correction factor, and reaction quantum yields.

pH	Methylene Blue Concentration mg/l	Run #	Average Incident Light Intensity $W/m^2/nm$	K^a mole/sec	K^c mole/sec	Absorbance Correction Factor	Reaction Quantum Yield mole/einstein
9	2	1	0.086	5.96×10^{-9}	1.12×10^{-11}	.98/.59	0.0031
9	2	2	0.091	6.26×10^{-9}	6.21×10^{-13}	.98/.59	0.0002
9	2	3	0.093	6.39×10^{-9}	3.57×10^{-12}	.98/.59	0.0009
11	2	1	0.086	5.96×10^{-9}	6.98×10^{-12}	.98/.59	0.0019
11	2	2	0.091	6.26×10^{-9}	4.35×10^{-12}	.98/.59	0.0012
11	2	3	0.093	6.39×10^{-9}	6.05×10^{-12}	.98/.59	0.0016
3	5	1	0.073	5.06×10^{-9}	1.09×10^{-10}	.98/.90	0.0234
3	5	2	0.107	7.34×10^{-9}	1.05×10^{-10}	.98/.90	0.0155
3	5	3	0.104	7.14×10^{-9}	6.98×10^{-11}	.98/.90	0.0107
5	5	1	0.073	5.06×10^{-9}	1.25×10^{-10}	.98/.90	0.0270
5	5	2	0.107	7.34×10^{-9}	3.21×10^{-11}	.98/.90	0.0048
5	5	3	0.104	7.14×10^{-9}	2.26×10^{-10}	.98/.90	0.0345
7	5	1	0.073	5.06×10^{-9}	3.24×10^{-11}	.98/.90	0.0070
7	5	2	0.107	7.34×10^{-9}	3.14×10^{-11}	.98/.90	0.0047
7	5	3	0.104	7.14×10^{-9}	2.36×10^{-11}	.98/.90	0.0036

Table 39. Summary table from triplicate analyses of the photolysis of 5 mg/l acridine solutions; average incident light intensity, reaction rate constants from actinometry, reaction rate constants from photolysis, absorbance correction factor, and reaction quantum yields.

pH	Methylene Blue Concentration mg/l	Run #	Average Incident Light Intensity $W/m^2/nm$	K^a mole/sec	K^c mole/sec	Absorbance Correction Factor	Reaction Quantum Yield mole/einstein
9	5	1	0.073	5.06×10^{-9}	7.60×10^{-12}	.98/.90	0.0016
9	5	2	0.107	7.34×10^{-9}	9.78×10^{-12}	.98/.90	0.0015
9	5	3	0.104	7.14×10^{-9}	4.97×10^{-12}	.98/.90	0.0008
11	5	1	0.073	5.06×10^{-9}	1.74×10^{-11}	.98/.90	0.0038
11	5	2	0.107	7.34×10^{-9}	1.88×10^{-11}	.98/.90	0.0028
11	5	3	0.104	7.14×10^{-9}	6.83×10^{-12}	.98/.90	0.0011
7	10	1	0.085	5.88×10^{-9}	2.14×10^{-11}	.98/1.00	0.0036
7	10	2	0.089	6.12×10^{-9}	3.83×10^{-11}	.98/1.00	0.0061
7	10	3	0.105	7.22×10^{-9}	2.11×10^{-11}	.98/1.00	0.0029
9	10	1	0.085	5.88×10^{-9}	9.00×10^{-12}	.98/1.00	0.0015
9	10	2	0.089	6.12×10^{-9}	3.57×10^{-12}	.98/1.00	0.0006
9	10	3	0.105	7.22×10^{-9}	2.48×10^{-12}	.98/1.00	0.0003
11	10	1	0.085	5.88×10^{-9}	1.12×10^{-11}	.98/1.00	0.0019
11	10	2	0.089	6.12×10^{-9}	1.88×10^{-11}	.98/1.00	0.0030
11	10	3	0.105	7.22×10^{-9}	1.04×10^{-11}	.98/1.00	0.0014

Table 40. Summary table from triplicate analyses of the photolysis of 1 mg/l anthracene solutions; average incident light intensity, reaction rate constants from actinometry, reaction rate constants from photolysis, absorbance correction factor, and reaction quantum yields.

pH	Methylene Blue Concentration mg/l	Run #	Average Incident Light Intensity $W/m^2/nm$	K^a mole/sec	K^c mole/sec	Absorbance Correction Factor	Reaction Quantum Yield mole/einstein
3	2	1	0.122	8.39×10^{-9}	1.67×10^{-11}	.98/.59	0.0054
3	2	2	0.107	7.36×10^{-9}	2.02×10^{-11}	.98/.59	0.0075
3	2	3	0.124	8.56×10^{-9}	1.47×10^{-11}	.98/.59	0.0047
5	2	1	0.122	8.39×10^{-9}	2.04×10^{-11}	.98/.59	0.0066
5	2	2	0.107	7.36×10^{-9}	2.63×10^{-11}	.98/.59	0.0098
5	2	3	0.124	8.56×10^{-9}	1.51×10^{-11}	.98/.59	0.0048
7	2	1	0.122	8.39×10^{-9}	2.63×10^{-11}	.98/.59	0.0085
7	2	2	0.107	7.36×10^{-9}	2.75×10^{-11}	.98/.59	0.0102
7	2	3	0.124	8.56×10^{-9}	1.66×10^{-11}	.98/.59	0.0053
9	2	1	0.122	8.39×10^{-9}	1.68×10^{-11}	.98/.59	0.0055
9	2	2	0.107	7.36×10^{-9}	1.28×10^{-11}	.98/.59	0.0047
9	2	3	0.124	8.56×10^{-9}	2.26×10^{-11}	.98/.59	0.0072
11	2	1	0.122	8.39×10^{-9}	1.69×10^{-11}	.98/.59	0.0055
11	2	2	0.107	7.36×10^{-9}	1.47×10^{-11}	.98/.59	0.0054
11	2	3	0.124	8.56×10^{-9}	1.65×10^{-11}	.98/.59	0.0052

Table 41. Summary table from triplicate analyses of the photolysis of 1 mg/l anthracene solutions; average incident light intensity, reaction rate constants from actinometry, reaction rate constants from photolysis, absorbance correction factor, and reaction quantum yields.

pH	Methylene Blue Concentration mg/l	Run #	Average Incident Light Intensity $W/m^2/nm$	K^a mole/sec	K^c mole/sec	Absorbance Correction Factor	Reaction Quantum Yield mole/einstein
3	5	1	0.090	6.20×10^{-9}	1.61×10^{-11}	.98/.90	0.0020
3	5	2	0.084	5.80×10^{-9}	2.24×10^{-11}	.98/.90	0.0042
3	5	3	0.065	4.48×10^{-9}	5.72×10^{-12}	.98/.90	0.0014
5	5	1	0.090	6.20×10^{-9}	1.06×10^{-11}	.98/.90	0.0019
5	5	2	0.084	5.80×10^{-9}	2.54×10^{-11}	.98/.90	0.0048
5	5	3	0.065	4.48×10^{-9}	3.85×10^{-11}	.98/.90	0.0094
7	5	1	0.090	6.20×10^{-9}	3.42×10^{-11}	.98/.90	0.0060
7	5	2	0.084	5.80×10^{-9}	6.17×10^{-11}	.98/.90	0.0116
7	5	3	0.065	4.48×10^{-9}	5.35×10^{-11}	.98/.90	0.0130
9	5	1	0.090	6.20×10^{-9}	2.40×10^{-11}	.98/.90	0.0042
9	5	2	0.084	5.80×10^{-9}	3.04×10^{-11}	.98/.90	0.0057
9	5	3	0.065	4.48×10^{-9}	2.07×10^{-11}	.98/.90	0.0050
11	5	1	0.090	6.20×10^{-9}	1.67×10^{-11}	.98/.90	0.0029
11	5	2	0.084	5.80×10^{-9}	1.62×10^{-11}	.98/.90	0.0031
11	5	3	0.065	4.48×10^{-9}	1.33×10^{-11}	.98/.90	0.0032

Table 42. Summary table from triplicate analyses of the photolysis of 5 mg/l quinoline solutions; average incident light intensity, reaction rate constants from actinometry, reaction rate constants from photolysis, absorbance correction factor, and reaction quantum yields.

pH	Methylene Blue Concentration mg/l	Run #	Average Incident Light Intensity $W/m^2/nm$	K^a mole/sec	K^c mole/sec	Absorbance Correction Factor	Reaction Quantum Yield mole/einstein
3	5	1	0.090	6.22×10^{-9}	1.49×10^{-11}	.98/.90	0.0026
3	5	2	0.058	4.01×10^{-9}	3.23×10^{-12}	.98/.90	0.0009
3	5	3	0.079	5.45×10^{-9}	5.60×10^{-12}	.98/.90	0.0011
5	5	1	0.090	6.22×10^{-9}	6.68×10^{-12}	.98/.90	0.0012
5	5	2	0.058	4.01×10^{-9}	3.45×10^{-12}	.98/.90	0.0009
5	5	3	0.079	5.45×10^{-9}	6.25×10^{-12}	.98/.90	0.0013
7	5	1	0.090	6.22×10^{-9}	6.46×10^{-12}	.98/.90	0.0011
7	5	2	0.058	4.01×10^{-9}	3.66×10^{-12}	.98/.90	0.0010
7	5	3	0.079	5.45×10^{-9}	4.09×10^{-12}	.98/.90	0.0008
9	5	1	0.090	6.22×10^{-9}	1.16×10^{-11}	.98/.90	0.0020
9	5	2	0.058	4.01×10^{-9}	2.80×10^{-12}	.98/.90	0.0008
9	5	3	0.079	5.45×10^{-9}	4.95×10^{-12}	.98/.90	0.0010
11	5	1	0.090	6.22×10^{-9}	6.46×10^{-13}	.98/.90	0.0001
11	5	2	0.058	4.01×10^{-9}	3.66×10^{-12}	.98/.90	0.0010
11	5	3	0.079	5.45×10^{-9}	2.37×10^{-12}	.98/.90	0.0005

Table 43. Summary table from triplicate analyses examining the effect of combining substrates on the yields and reaction rates; mixtures were photolyzed in 2mg/l methylene blue solutions and buffered to a pH of 7.

Substrate	Substrate Concentration mg/l	Run #	Average Incident Light Intensity $W/m^2/nm$	K^a mole/sec	K^c mole/sec	Absorbance Correction Factor	Reaction Quantum Yield mole/einstein
Acridine	5.0	1	0.092	6.34×10^{-9}	2.67×10^{-11}	.98/.59	0.0059
Acridine	5.0	2	0.092	6.34×10^{-9}	2.96×10^{-11}	.98/.59	0.0078
Acridine	5.0	3	0.092	6.34×10^{-9}	1.75×10^{-11}	.98/.59	0.0046
Anthracene	1.0	1	0.092	6.34×10^{-9}	9.68×10^{-12}	.98/.59	0.0025
Anthracene	1.0	2	0.092	6.34×10^{-9}	1.16×10^{-11}	.98/.59	0.0030
Anthracene	1.0	3	0.092	6.34×10^{-9}	1.26×10^{-11}	.98/.59	0.0033
Quinoline	5.0	1	0.092	6.34×10^{-9}	7.45×10^{-12}	.98/.59	0.0020
Quinoline	5.0	2	0.092	6.34×10^{-9}	6.12×10^{-12}	.98/.59	0.0016
Quinoline	5.0	3	0.092	6.34×10^{-9}	4.76×10^{-12}	.98/.59	0.0013

Table 44. Summary table from triplicate analyses examining the effect of initial anthracene concentration on the reaction rates and yields; average incident light intensity, reaction rate constants from actinometry, reaction rate constants from photolysis, absorbance correction factor, and reaction quantum yields in 2 mg/l methylene blue solutions.

pH	Anthracene Concentration mg/l	Run #	Average Incident Light Intensity $W/m^2/nm$	K^a mole/sec	K^c mole/sec	Absorbance Correction Factor	Reaction Quantum Yield mole/einstein
7	0.5	1	0.092	$6.34x10^{-9}$	$1.46x10^{-11}$	.98/.59	0.0038
7	0.5	2	0.092	$6.34x10^{-9}$	$2.65x10^{-12}$	.98/.59	0.0007
7	0.5	3	0.092	$6.34x10^{-9}$	$8.18x10^{-12}$	.98/.59	0.0021
7	1.0	1	0.092	$6.34x10^{-9}$	$1.59x10^{-11}$	.98/.59	0.0042
7	1.0	2	0.092	$6.34x10^{-9}$	$1.20x10^{-11}$	.98/.59	0.0031
7	1.0	3	0.092	$6.34x10^{-9}$	$2.80x10^{-11}$	.98/.59	0.0073
7	2.0	1	0.092	$6.34x10^{-9}$	$1.69x10^{-11}$	.98/.59	0.0044
7	2.0	2	0.092	$6.34x10^{-9}$	$1.60x10^{-11}$	.98/.59	0.0042
7	2.0	3	0.092	$6.34x10^{-9}$	$2.36x10^{-11}$	.98/.59	0.0062
7	5.0	1	0.092	$6.34x10^{-9}$	$7.80x10^{-11}$	.98/.59	0.0205
7	5.0	2	0.092	$6.34x10^{-9}$	$4.40x10^{-11}$	.98/.59	0.0115
7	5.0	3	0.092	$6.34x10^{-9}$	$3.89x10^{-11}$	.98/.59	0.0102
7	10.0	1	0.092	$6.34x10^{-9}$	$4.78x10^{-11}$	.98/.59	0.0125
7	10.0	2	0.092	$6.34x10^{-9}$	$9.05x10^{-11}$	.98/.59	0.0237
7	10.0	3	0.092	$6.34x10^{-9}$	$8.43x10^{-11}$	.98/.59	0.0221

Table 45. Summary table from triplicate analyses examining the effect of initial acridine concentration on the reaction rates and yields; average incident light intensity, reaction rate constants from actinometry, reaction rate constants from photolysis, absorbance correction factor, and reaction quantum yields in 2 mg/l methylene blue solutions

pH	Acridine Concentration mg/l	Run #	Average Incident Light Intensity $W/m^2/nm$	K^a mole/sec	K^c mole/sec	Absorbance Correction Factor	Reaction Quantum Yield mole/einstein
5	1.0	1	0.092	6.34×10^{-9}	2.95×10^{-11}	.98/.59	0.0077
5	1.0	2	0.092	6.34×10^{-9}	2.59×10^{-11}	.98/.59	0.0068
5	1.0	3	0.092	6.34×10^{-9}	2.74×10^{-11}	.98/.59	0.0072
5	2.0	1	0.092	6.34×10^{-9}	6.32×10^{-11}	.98/.59	0.0166
5	2.0	2	0.092	6.34×10^{-9}	4.49×10^{-11}	.98/.59	0.0118
5	2.0	3	0.092	6.34×10^{-9}	5.13×10^{-11}	.98/.59	0.0134
5	5.0	1	0.092	6.34×10^{-9}	1.22×10^{-10}	.98/.59	0.0318
5	5.0	2	0.092	6.34×10^{-9}	1.50×10^{-10}	.98/.59	0.0394
5	5.0	3	0.092	6.34×10^{-9}	1.25×10^{-10}	.98/.59	0.0329
5	10.0	1	0.092	6.34×10^{-9}	2.44×10^{-10}	.98/.59	0.0640
5	10.0	2	0.092	6.34×10^{-9}	2.45×10^{-10}	.98/.59	0.0640
5	10.0	3	0.092	6.34×10^{-9}	2.45×10^{-10}	.98/.59	0.0643
5	15.0	1	0.092	6.34×10^{-9}	3.88×10^{-10}	.98/.59	0.1018
5	15.0	2	0.092	6.34×10^{-9}	4.24×10^{-10}	.98/.59	0.1111
5	15.0	3	0.092	6.34×10^{-9}	4.23×10^{-10}	.98/.59	0.1109